

1 of 2

PNL-6117
UC-520

FULL-LENGTH HIGH-TEMPERATURE
SEVERE FUEL DAMAGE TEST #5
FINAL SAFETY ANALYSIS

D. D. Lanning
N. J. Lombardo
F. E. Panisko

April 1987 - Completed
September 1993 - Published

Prepared for
U.S. Nuclear Regulatory Commission
Under U. S. Department of Energy
Contract DE-AC06-76RLO 1830

Pacific Northwest Laboratory
Richland, Washington 99352

MASTER

DISTRIBUTION OF THIS DOCUMENT IS UNLIMITED

fp

ABSTRACT

This report presents the final safety analysis for the preparation, conduct, and post-test discharge operation for the Full-Length High Temperature Experiment-5 (FLHT-5) to be conducted in the L-24 position of the National Research Universal (NRU) Reactor at Chalk River Nuclear Laboratories (CRNL), Ontario, Canada. The test is sponsored by an international group organized by the U.S. Nuclear Regulatory Commission. The test is designed and conducted by staff from Pacific Northwest Laboratory with CRNL staff support. The test will study the consequences of loss-of-coolant and the progression of severe fuel damage.

An array of full-length LWR fuel rods will be subjected to conditions that simulate loss-of-coolant flow at decay-heat power level. The 12-position array includes one pre-irradiated PWR rod, 10 fresh fuel rods, and one instrument thimble containing a dummy steel rod. The boilaway of the coolant will permit heatup of the rods to the point of rapid cladding oxidation with concomitant cladding melting, partial fuel liquefaction, fuel oxidation, hydrogen generation, and fission product release. The hydrogen generation (from the oxidation reaction), the bundle temperatures, the liquid level, and the fission product release will be monitored during the test. The melt progression will be assessed using post test visual and metallographic examination results.

Experience from similar FLHT tests is combined with analysis results to show that: 1) high-temperature material will be contained within the shroud that surrounds the rod array, precluding damage to the NRU loop pressure tube; 2) the released fission products and hydrogen will be contained and disposed of by the effluent control system in a manner that poses no unresolved safety hazard to operating personnel or to the public; and 3) the radiation exposure to operating personnel and to the public will remain below approved control limits.

ACKNOWLEDGMENTS

The authors wish to thank the following Pacific Northwest Laboratory staff for contributions to this report and their review:

- H. D. Cummings
- D. E. Hurley
- D. E. Fitzsimmons
- U. P. Jenquin
- L. L. King

We also wish to recognize the contributions of Chalk River Nuclear Laboratories staff, in particular Mr. I. C. Martin, in reviewing the safety analyses presented herein. Finally, we thank the staff of the Fuel Behavior Research Branch of the United States Nuclear Regulatory Commission (in particular R. Van Houten) for support and encouragement of the overall project.

CONTENTS

ABSTRACT	iii
ACKNOWLEDGMENTS	v
ACRONYMS AND ABBREVIATIONS	xiii
1.0 INTRODUCTION	1.1
2.0 EXPERIMENT HARDWARE	2.1
2.1 TEST TRAIN ASSEMBLY	2.1
2.1.1 Closure Region	2.1
2.1.2 Plenum Region	2.5
2.1.3 Fuel Rod Region	2.6
2.1.4 Inlet Region	2.13
2.2 EFFLUENT CONTROL MODULE	2.13
2.3 REACTOR/LOOPS	2.16
2.4 INSTRUMENTATION	2.17
2.5 DATA ACQUISITION AND CONTROL SYSTEM	2.21
3.0 EXPERIMENT PROCEDURES, CONDITIONS, AND CONTROLS	3.1
3.1 TEST HARDWARE PREPARATION AND INSTALLATION	3.1
3.1.1 Bundle and Shroud Assembly and Connections	3.1
3.1.2 Test Train Installation	3.2
3.2 PRECONDITIONING OPERATION	3.2
3.3 TEST PHASE SEQUENCE AND CONDITIONS	3.3
3.4 POST-TEST DISCONNECTION AND DISASSEMBLY	3.5
3.4.1 Deposition Rod Removal	3.7
3.4.2 Crimping and Cutting Effluent and Connector Lines	3.7
3.5 CONTROLS AND PROCEDURES TO MAINTAIN SAFETY	3.7

4.0	SAFETY CONCERNS DURING NORMAL OPERATION	4.1
4.1	RADIOACTIVE FISSION PRODUCTS	4.1
4.1.1	Radiation Fields Resulting From Fission Product Release	4.3
4.1.2	Stack Releases of Radioactive Fission Products	4.7
4.2	REACTIVITY EFFECTS	4.8
4.3	HYDROGEN GENERATION	4.9
4.4	MATERIALS AT HIGH TEMPERATURE	4.10
4.4.1	Heat Flux Through Inner and Outer Rounds	4.10
4.4.2	Consequence of Loss of Shroud Insulation	4.13
4.5	ANALYSIS OF STEAM EXPLOSION AND STEAM PRESSURE PULSES	4.16
4.6	UNCERTAINTIES ASSOCIATED WITH NORMAL EXPERIMENT OPERATION	4.17
5.0	SAFETY CONCERNS DURING ACCIDENTS	5.1
5.1	LOSS OF BYPASS COOLANT FLOW	5.1
5.2	LOSS OF BUNDLE PRESSURE	5.2
5.3	ECM PIPING RUPTURE	5.3
5.4	LOSS OF ALL POWER	5.4
6.0	REFERENCES	6.1
APPENDIX A	- IN-HOUSE CODE AND SCDAP CODE POST-TEST CALCULATIONS FOR FLHT-4 AND PRETEST CALCULATIONS FOR FLHT-5	A.1
APPENDIX B	- CORSOR FISSION PRODUCT RELEASE CALCULATIONS	B.1
APPENDIX C	- UPDATED STEAM EXPLOSION AND PRESSURE SPIKE ANALYSIS FOR FLHT-5	C.1

FIGURES

2.1	FLHT-5 Hardware Arrangement	2.2
2.2	FLHT-5 Test Train Assembly	2.3
2.3	FLHT-5 Closure Schematic	2.4
2.4	Closure Region Feed-Throughs for FLHT-5	2.5
2.5	Axial Cross Section of the FLHT-5 Insulated Closure and Heated/Insulated Plenum	2.7
2.6	Transverse Cross Section of the Insulated Plenum for FLHT-5 Showing Nominal Dimensions	2.8
2.7	Deposition Rod for FLHT-5	2.8
2.8	Axial Schematic of FLHT-5 Fuel Rod Region	2.9
2.9	Cross Section of FLHT-5 Test Assembly Core Region	2.10
2.10	FLHT-5 Shroud	2.11
2.11	Flow Paths in the Effluent Control Module	2.15
2.12	Electrical Connections for the DACS, LCS, ECM, Test Train, and Data Stations	2.23
2.13	Sample Floor Plan of the Data Acquisition and Control System	2.24
4.1	Maximum Predicted Post-Test Dose Rates on West Exterior Surface of the ECM	4.5
4.2	Maximum Predicted Post-Test Dose Rates Three Feet from the West Side of the ECM	4.5
4.3	Maximum Predicted Post-Test Dose Rates on the North Side Cave Exterior	4.6
A.1	FLHT-4 Hydrogen Generation Rate Data Compared with SCDAP and In-House Code Calculations	A.6
A.2	Calculated Bundle Oxidation Heat Generation Rate for FLHT-4, Compared to Values Derived from Hydrogen Flow Measurements	A.7
A.3	Typical Cladding thermocouple Readings from FLHT-4	A.8
A.4	Saddle Thermocouple Readings During FLHT-4	A.9

A.5	SCDAP Nodal Cladding Temperatures Calculated for FLHT-4	A.10
A.6	In-House Code Nodal Temperatures Calculated for FLHT-4	A.11
A.7	SCDAP and In-House Code Mid-Plane Peak Cladding Temperatures Versus Data for FLHT-4	A.12
A.8	Hydrogen Production Rates Predicted for FLHT-5	A.13
A.9	Bundle Oxidation Heat Generation Rates Predicted for FLHT-5	A.14
A.10	SCDAP Nodal Temperatures Calculated for FLHT-5	A.15
A.11	In-House Code Nodal Temperatures Calculated for FLHT-5	A.16
A.12	SCDAP and In-House Code Calculated Mid-plane Peak Cladding Temperatures for FLHT-5	A.17
A.13	In-House Code Nodal Saddle Temperatures Calculated for FLHT-5	A.18
A.14	In-House Code Nodal Radial Heat Loss Calculated for FLHT-5	A.19
A.15	Total Bundle Radial Heat Loss to Bypass as Predicted by the In-House Code for FLHT-5	A.20

TABLES

1.1	CBDP Program Test Matrix Features	1.2
2.1	Fuel Bundle Instrumentation Summary	2.18
2.2	Shroud Instrumentation Summary	2.19
2.3	Plenum/Steam Line Instrumentation Summary	2.20
3.1	FLHT-5 Preconditioning Operating Conditions	3.4
3.2	FLHT-5 Test Phase Operating Conditions	3.6
3.3	FLHT-5 Experiment Safety Trip Functions	3.8
4.1	Predicted FLHT-5 Curie Inventories and Release Fractions	4.4
4.2	Bypass Coolant Margins	4.12
4.3	Margins for Local Boiling and Dryout on Bypass at 48 kW Radial Heat Flow	4.13
A.1	Code/Data Comparisons of Bundle Oxidation for FLHT-4	A.3
A.2	Predicted Bundle Oxidation and Hydrogen Production for FLHT-5	A.5
B.1	CORSOR Calculated Release Fractions for FLHT-5	B.2

ACRONYMS AND ABBREVIATIONS

ACRR - Annular Core Research Reactor
AECL - Atomic Energy of Canada Limited
BWR - boiling-water reactor
CBDP - coolant boilaway and damage progression
CRNL - Chalk River Nuclear Laboratories
DACS - data acquisition and control system
DG - Data General
ECM - effluent control module
EOP - experiment operations plan
FLHT - full-length, high-temperature
HEPA - high-efficiency particulate air (filter)
LCS - loop control system
LOCA - loss-of-coolant accident
LWR - light-water reactor
MMPD - molten metal penetration detector
NRC - U.S. Nuclear Regulatory Commission
NRU - National Research Universal
NTP - normal temperature and pressure (70°F and 14.7 psia)
PBF - Power Burst Facility
PNL - Pacific Northwest Laboratory
PWR - pressurized-water reactor
SFD - severe fuel damage
ST - source term
STP - standard temperature and pressure (32°F and 14.7 psia)
TC - thermocouple
TD - theoretical density
TDR - time domain reflectometer (used to measure coolant level)

1.0 INTRODUCTION

The Coolant Boilaway and Damage Progression (CBDP) Program is conducted by Pacific Northwest Laboratory (PNL)^(a) as part of the U.S. Nuclear Regulatory Commission (NRC) Severe Fuel Damage/Source Term (SFD/ST) Program.^(b) The CBDP Program consists of in-reactor experiments using full-length light-water reactor (LWR) fuel rods to determine fuel bundle behavior and fission product release during simulated small-break loss-of-coolant accidents (LOCA) that result in a partially uncovered reactor core. As the coolant boils away and the fuel rods become uncovered, the temperature of the rods increases above design limits. As the temperature increases, the rods become damaged, potentially dangerous radioactive fission products are released from the fuel, and large quantities of hydrogen are produced.

The CBDP Program to date consists of six tests designed to investigate fuel bundle damage behavior from 820 to 2500°C (1508 to 4500°F) in a series of progressively more severe tests at prototypic power densities, thermal gradients, and steam mass fluxes. Five tests have been completed (Table 1.1). Three of these tests have provided data on fuel bundle behavior during coolant boilaway conditions that resulted in peak temperatures as high as 2300°C (4200°F). The experiments use full-length LWR fuel rod bundle test assemblies and are being performed in the National Research Universal (NRU) Reactor at Chalk River Nuclear Laboratories (CRNL) at Chalk River, Ontario. Coolant boilaway is achieved using low-level fission heat to simulate decay heat levels. Highlights of the test conditions are given in Table 1.1.

-
- (a) Operated for the U.S. Department of Energy (DOE) by Battelle Memorial Institute under Contract DE-AC06-76RLO 1830.
 - (b) Partners in this program with NRC include nuclear organizations from the following countries: Belgium, Canada, England, Federal Republic of Germany, Italy, Japan, The Netherlands, Republic of China (Taiwan), Republic of Korea, Spain, and Sweden.

TABLE 1.1. CBDP Program Test Matrix Features

<u>Test</u>	<u>Goal Peak Temperature, °C</u>	<u>Hydrogen Measurement</u>	<u>Preirradiated Rods</u>	<u>Test Date</u>
MT-6A	820	No	0	6/84
MT-6B	1280			
FLHT-1	1880 (2200 achieved)	Yes	0	3/85
FLHT-2	2200 (2150 achieved)	Enhanced ^(a)	0	12/85
FLHT-4	2200-2500 (2300 achieved)	Enhanced ^(b)	1	8/86
FLHT-5	2200-2500	Enhanced ^(b)	1	5/87

(a) Included mass spectrometry and thermal conductivity meter for hydrogen measurement.

(b) Two or three independent devices for measuring hydrogen production included.

The following data will be obtained from the CBDP tests and will be used to confirm the validity of results obtained from separate effects tests that are being sponsored by the NRC at PNL and other laboratories:

- coolant boilaway progression
- axial temperature distribution for full-length fuel bundles as a function of liquid level
- hydrogen evolution
- fuel bundle damage progression (core degradation) behavior
- cladding melt progression
- core debris and grid spacer interaction
- debris bed formation and coolability
- flow channel blockage behavior
- fission product release and transport

These data provide a basis for developing accident mitigation strategies, for evaluating postulated coolant boilaway accidents, for developing concepts for accident prevention and quantifying safety margins, and for developing, benchmarking, and validating computer codes such as SCDAP, MELPROG, and MELCOR.

The CBDP experiments utilize the following advantages of the NRU Reactor: 1) the capability to test highly instrumented, multirod 12-ft-long fuel bundles under thermal-hydraulic conditions representative of contemporary LWRs; 2) the ability to achieve power densities and axial power distributions typical of small break loss-of-coolant accident (LOCA) conditions, using preirradiated fuel rods with commercial enrichment; and 3) the ability to provide prototypic coolant mass fluxes at the fluid/vapor interface typical of LOCA boildown conditions. These unique capabilities will reduce uncertainties associated with length and power distribution scaling factors and the interpretation of the experimental results from small-scale separate effects tests.

The CBDP tests are the only known full-length in-reactor pressurized water reactor (PWR) and boiling water reactor (BWR) multirod boilaway tests being performed. The deformation, rupture, fission product release, and debris bed data can be used to help quantify the safety limits used in the nuclear industry.

In order to obtain approval to conduct a full-length high-temperature (FLHT) experiment, PNL performs preliminary and final safety analyses of the proposed test and submits them to the safety engineers at CRNL. CRNL safety engineers review the PNL analytical results and then prepare and submit corresponding preliminary and final safety technical notes to the Canadian Nuclear Safety Advisory Committee (NSAC) for review and approval. CRNL test engineers review and approve not only the safety analysis but also the Experiment Operating Plan (EOP) and expected test conditions. This report is the final safety analysis for the FLHT-5 experiment.

In brief, the FLHT-5 experiment deviates from its predecessor (FLHT-4) in the following major ways:

- The calibrated bundle nuclear heating rate will be 30 kW (in the water-filled bundle) as compared with 23 kW in the previous tests.

- The predicted maximum cladding temperature is 2600°C (4700°F) compared to about 2300°C (4200°F) attained in FLHT-4. This increased temperature is expected because the greater nuclear heating will cause faster cladding heatup after dryout, resulting in accelerated oxidation earlier in the boildown, when steaming rates are higher, and the resultant oxidation heat generation is proportionately higher.
- The nuclear operation of the assembly (past the time of achievement of maximal temperatures) will be approximately 1 h, as compared with 30 min in FLHT-4.
- The test assembly will be subjected to a preconditioning period of up to 10 h at up to 800 kW assembly power prior to the transient phase, as compared with 1 h at ~700 kW in FLHT-4.

This safety analysis report includes a description of the FLHT-5 experiment hardware and test conditions.

2.0 EXPERIMENT HARDWARE

The experiment hardware consists of the test train assembly, the effluent control module (ECM), the NRU reactor coolant system, instrumentation, and the data acquisition and control system (DACS). The hardware arrangement is depicted in Figure 2.1. The figure illustrates the test train suspended inside one of the reactor pressure tubes. The ECM is located on the top of the reactor near the test train. Individual (separate and independent) coolant supply systems are connected to the test train and the reactor pressure tube. The test train assembly consists of the approximately 4-m-long test fuel assembly and its surrounding shroud, above which is a 4-m-long insulated plenum containing the effluent steam tube from the fuel assembly, and electrical heaters to prevent heat loss and steam condensation. The DACS is located in a room about 30 m from the test train. Electrical cables connect the test train assembly and the ECM to the DACS, allowing control of the test assembly and the effluent conditions. The experiment components are highly instrumented, especially the test train assembly. The instruments measure mainly pressure, temperature, and flow rates.

2.1 TEST TRAIN ASSEMBLY

The approximately 8-m-long test train assembly that hangs inside the reactor pressure tube consists of four sections that occupy different regions of the reactor: the closure, plenum, fuel rod, and inlet regions (Figure 2.2).

2.1.1 Closure Region

The closure hardware is located at the top of the test assembly and contains the components that support the rest of the assembly and seal it to the reactor pressure tube. The closure hardware consists of the closure plug, seal ring, gaskets, two bolting rings, and feed-through plugs. The closure plug is sealed to the reactor pressure tube using two metallic gaskets, the seal ring, and the two bolting rings (Figure 2.3).

Pressure boundary penetrations are made through the closure plug for instrument lines, pressurization tubes, three coolant supply lines, a flush line, and the bundle effluent line. The closure region penetrations are illustrated in Figure 2.4.

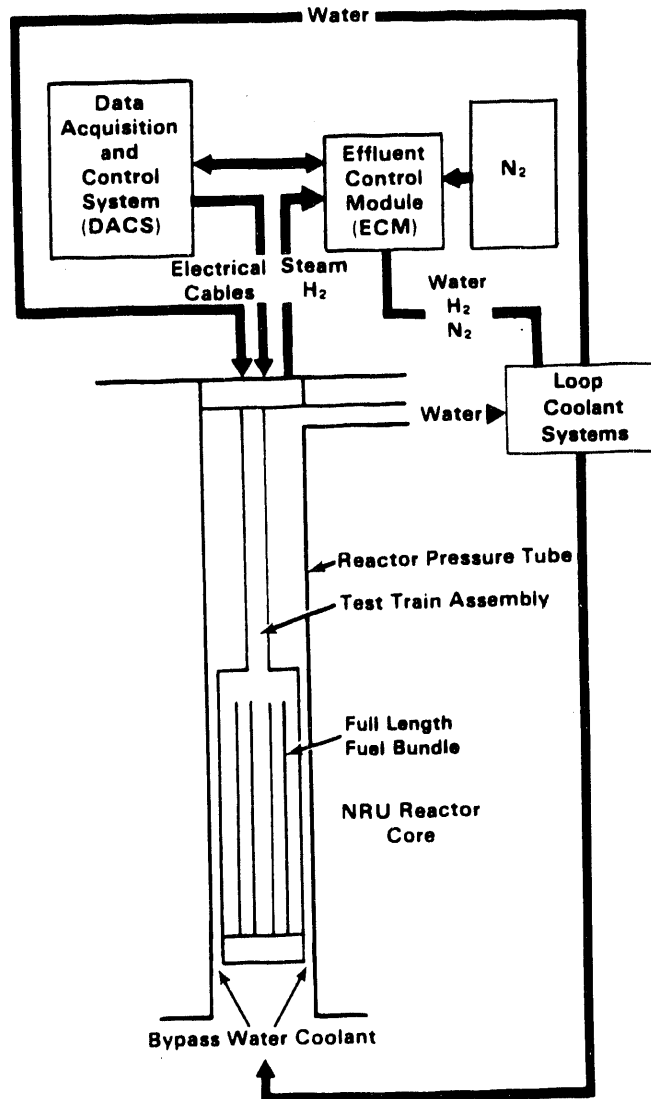


FIGURE 2.1. FLHT-5 Hardware Arrangement

The effluent line penetration through the FLHT-5 closure plug is thermally isolated from the plug to help prevent premature steam condensation. The steam flows through the inside tube of two concentric tubes. The region between the tubes is evacuated, thus forming a "thermos" bottle. A metal bellows is welded to the inner tube below the closure plug to accommodate axial differential thermal expansion between the two tubes. The outer tube is seal-welded to the closure plug.

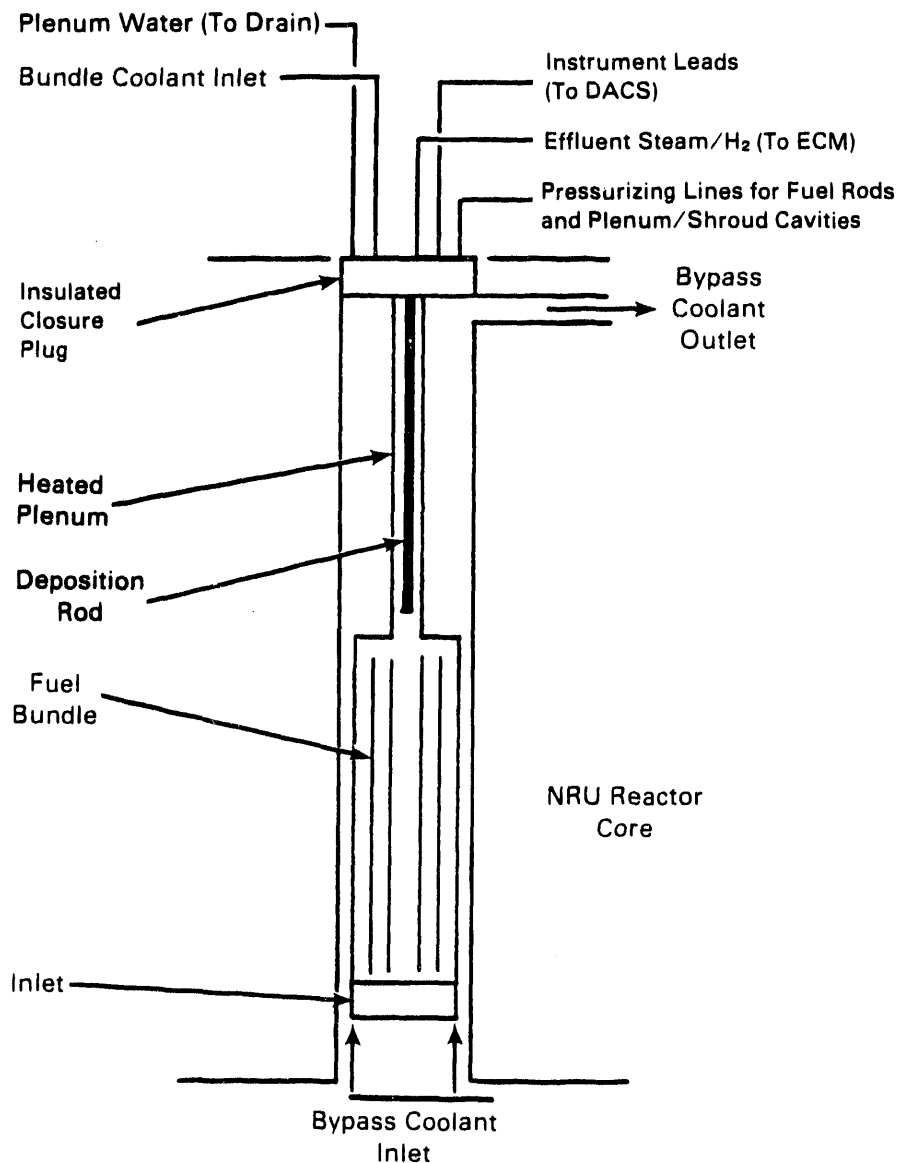


FIGURE 2.2. FLHT-5 Test Train Assembly

The test train instrument lines and pressurization tubes penetrate the closure plug through four feed-through plugs. As many as 55 leads can penetrate one instrument feed-through plug. The pressure boundary for the feed-through plug is provided by graphite packing gland seals. The pressure boundary for the flush line and the three bundle coolant lines is provided by standard autoclave fittings. The flush line will be used after the test to

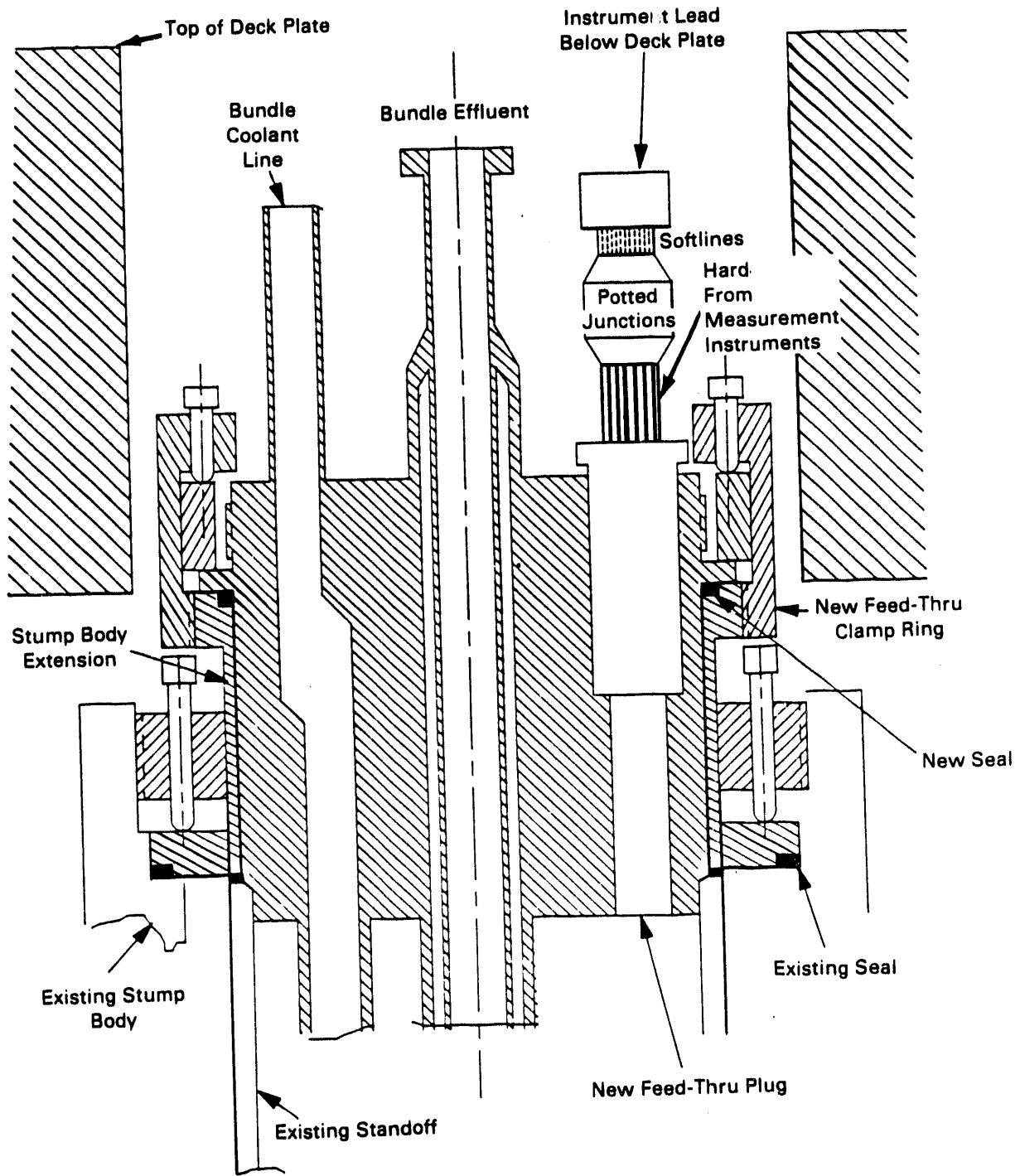


FIGURE 2.3. FLHT-5 Closure Schematic

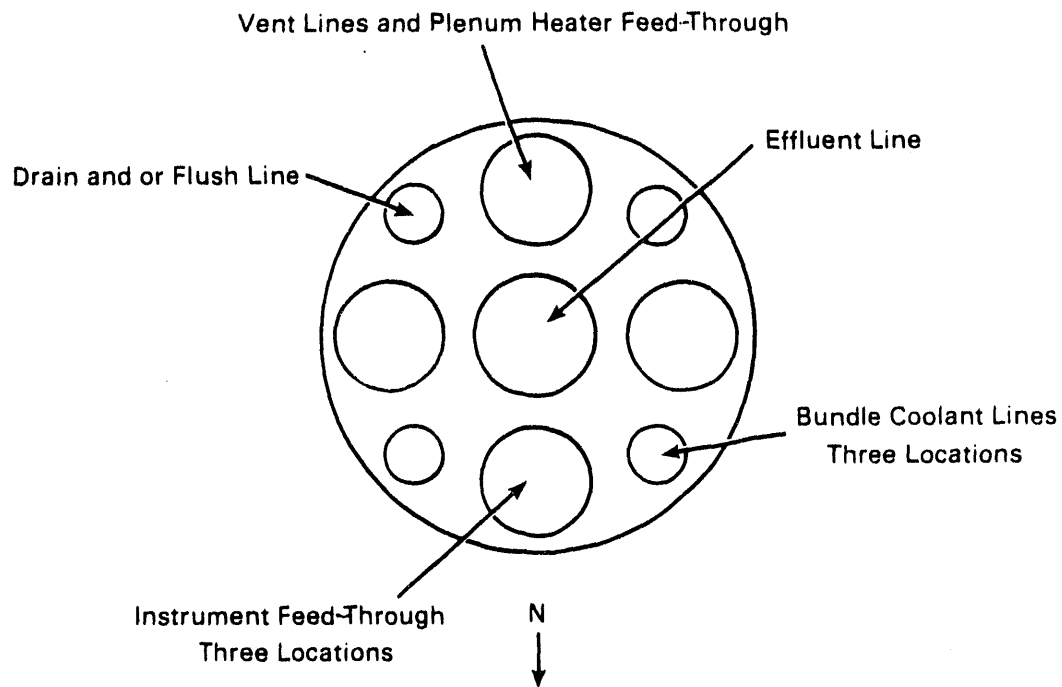


FIGURE 2.4. Closure Region Feed-Throughs for FLHT-5

reduce radiation levels near the closure region and thus provide easier personnel access during the test train assembly discharge operation.

All pressure boundary seals are tested during and after final test train assembly. The seal of the closure plug to the reactor pressure tube is tested after the test train is loaded into the reactor but before other experiment hardware is put into place.

2.1.2 Plenum Region

The approximately 4-m-(12-ft) long, 3-in.- (7.6-cm) diameter plenum section (Figure 2.5) connects the closure section to the core section, which contains the test fuel assembly. The plenum provides appropriate mechanical features to support and position the lower portions of the test train. It also provides the insulated and heated effluent pathway [1-in. (2.54 cm) diameter steam tube] from the core region to ECM. Within the effluent line is a 0.375-in. (0.95 cm) diameter "deposition rod" for collecting samples of fission products that deposit by aerosol deposition, chemisorption, and plateout along that 4-m length. The basic design of the plenum is two coaxial Zircaloy tubes, or

"rounds." The inner round is the effluent line and the outer one supports the insulation and heaters. Between the two tubes are annular sections of low-density ZrO_2 insulation, and nickel-chromium heater wires are wrapped around the steam tube between it and the insulation (see Figures 2.5 and 2.6).

There are a total of eight heaters along the 4-m length of the plenum, with one active and one inactive heater in each of four equal-length zones. The inactive heater will be used in case the active one malfunctions or more heat is needed to maintain the desired steam temperature along the plenum length. The heaters are equipped with indicator and control thermocouples (TCs). The heater controllers provide over-temperature and ground-fault protection. The heaters will control steam temperatures so that the exit temperature from the plenum will be between 288 and 343°C (550 to 650°F).

The deposition rod assembly is shown schematically in Figure 2.7. This 0.375-in.-dia, 4-m-long rod is suspended within the steam line from the deposition and access stub above the deck plate. It has eight TCs along its length to monitor local temperatures during the test. After the test, this rod will be pulled directly from the plenum into a shielded cask (in dry condition) and transport it to a hot cell for examination.

A set of Belleville springs near the bottom of the plenum compensates for thermally driven changes in the lengths of the inner and outer Zircaloy tubes.

The bottom end of the plenum contains the plenum drain and the bottom flange. The bottom flange connects to the top flange of the core region of the test train assembly.

2.1.3 Fuel Rod Region

The fuel rod region that hangs below the plenum contains two major components: a full-length 11-rod LWR fuel bundle and a multi-component shroud that surrounds and insulates the fuel bundle (see Figure 2.8).

The fuel bundle and shroud layout is shown in Figure 2.9. Shroud details are shown in Figure 2.10. The fuel bundle consists of 10 fresh (unirradiated) PWR fuel rods, one irradiated PWR rod (from the H. B. Robinson Reactor), and one stainless steel filler rod. The rods are held in a square array with a

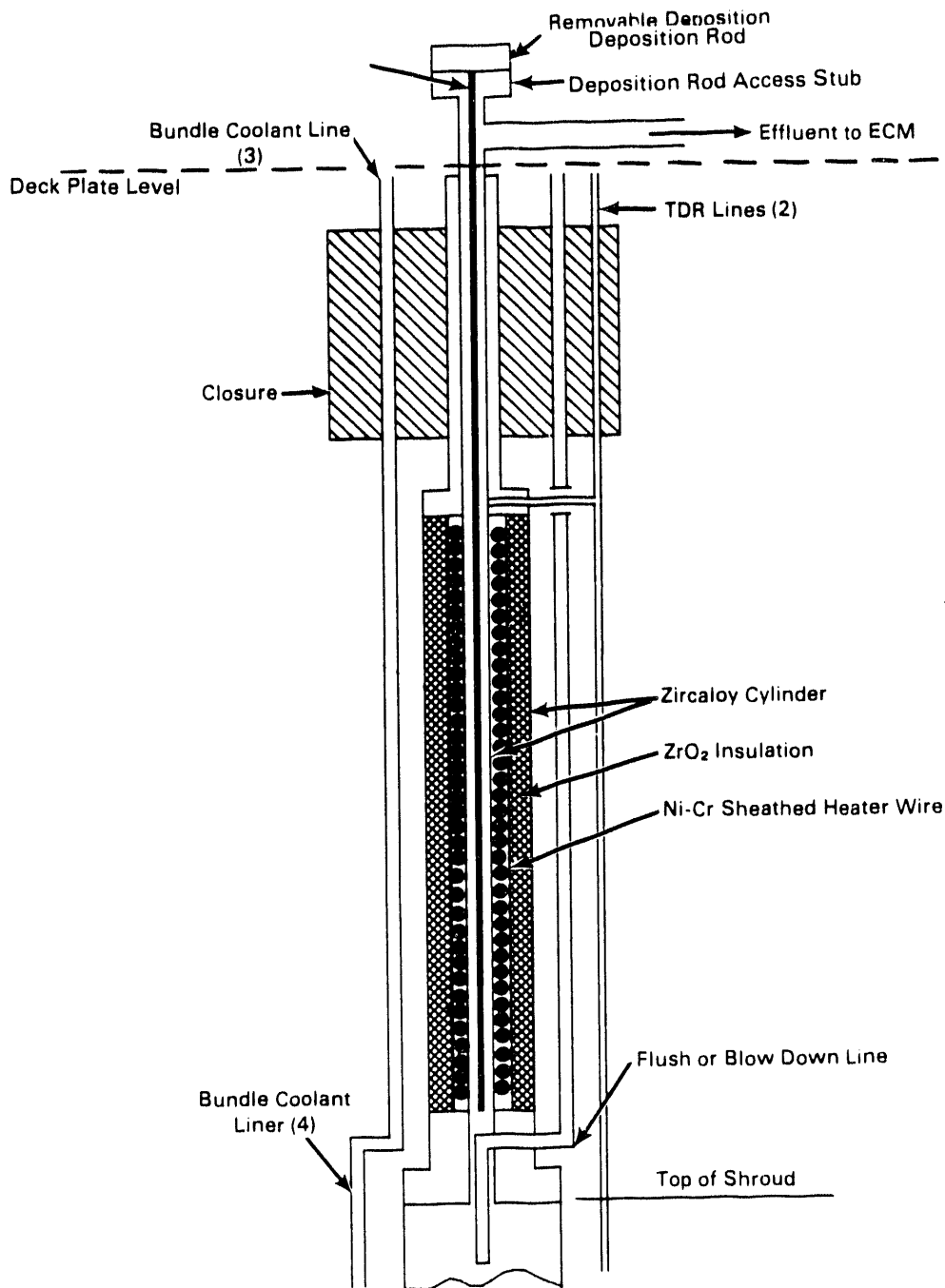


FIGURE 2.5. Axial Cross Section of the FLHT-5 Insulated Closure and Heated/Insulated Plenum

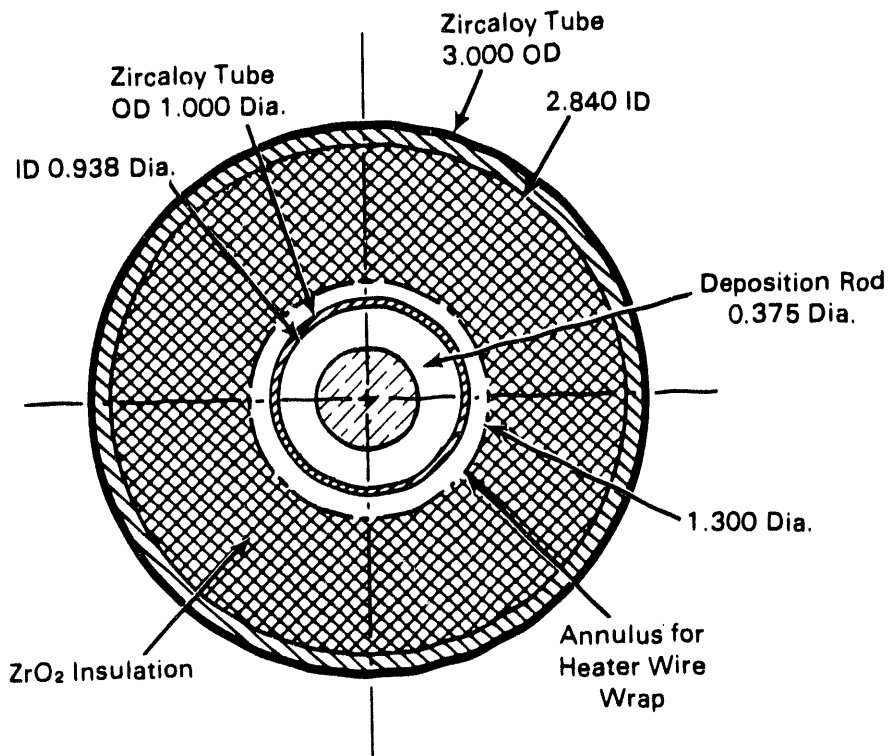


FIGURE 2.6. Transverse Cross Section of the Insulated Plenum for FLHT-5 Showing Nominal Dimensions (all dimensions are in inches)

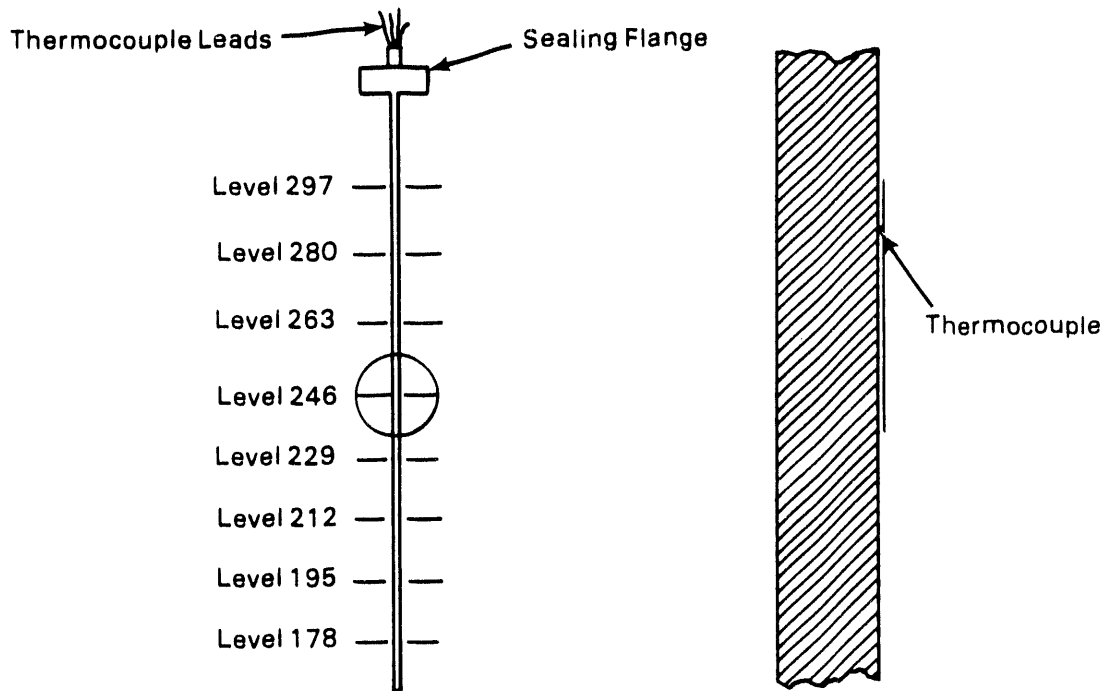


FIGURE 2.7. Deposition Rod for FLHT-5 ("Levels" are distances above the bottom of the fuel column in inches)

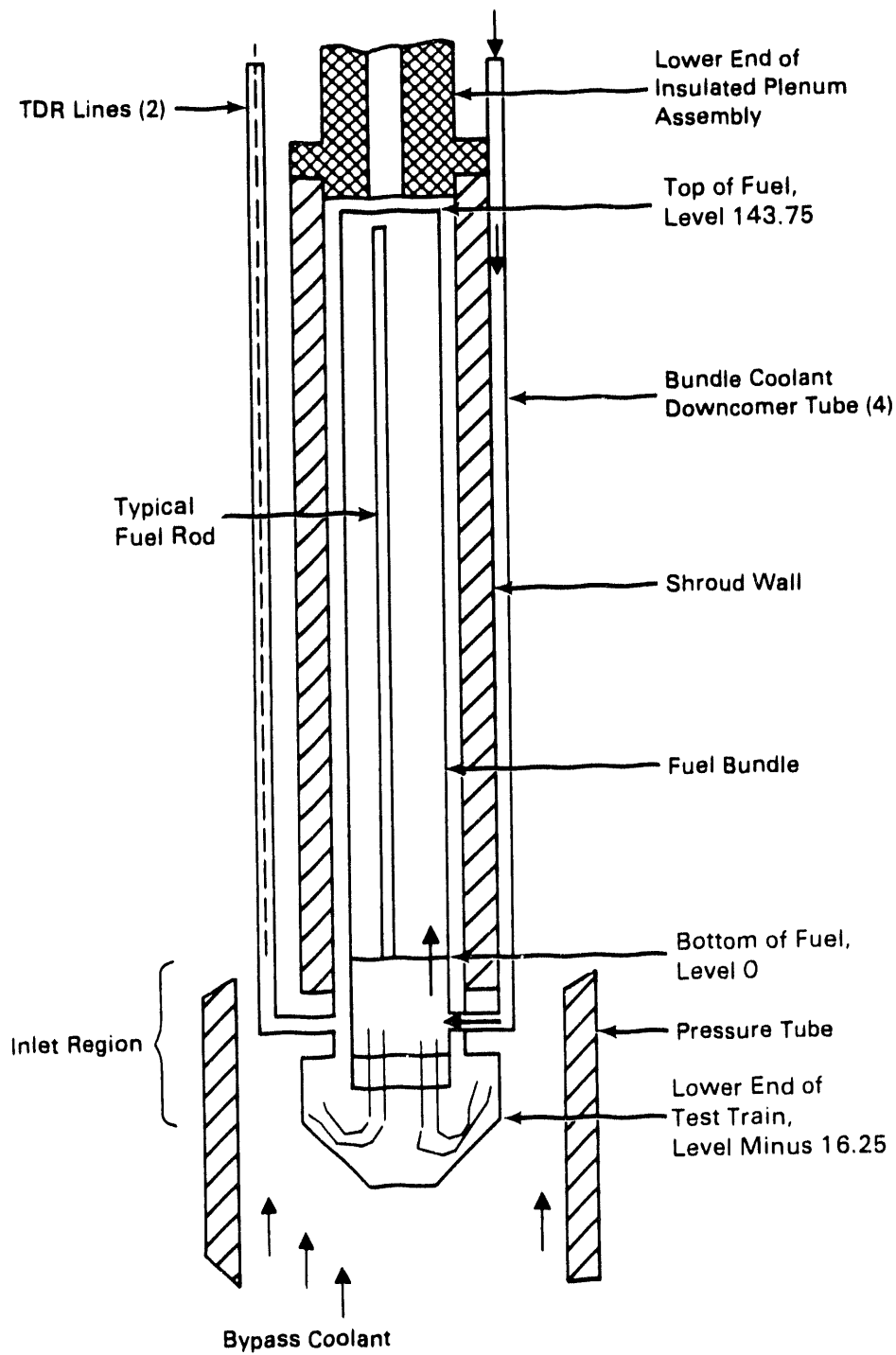


FIGURE 2.8. Axial Schematic of FLHT-5 Fuel Rod Region

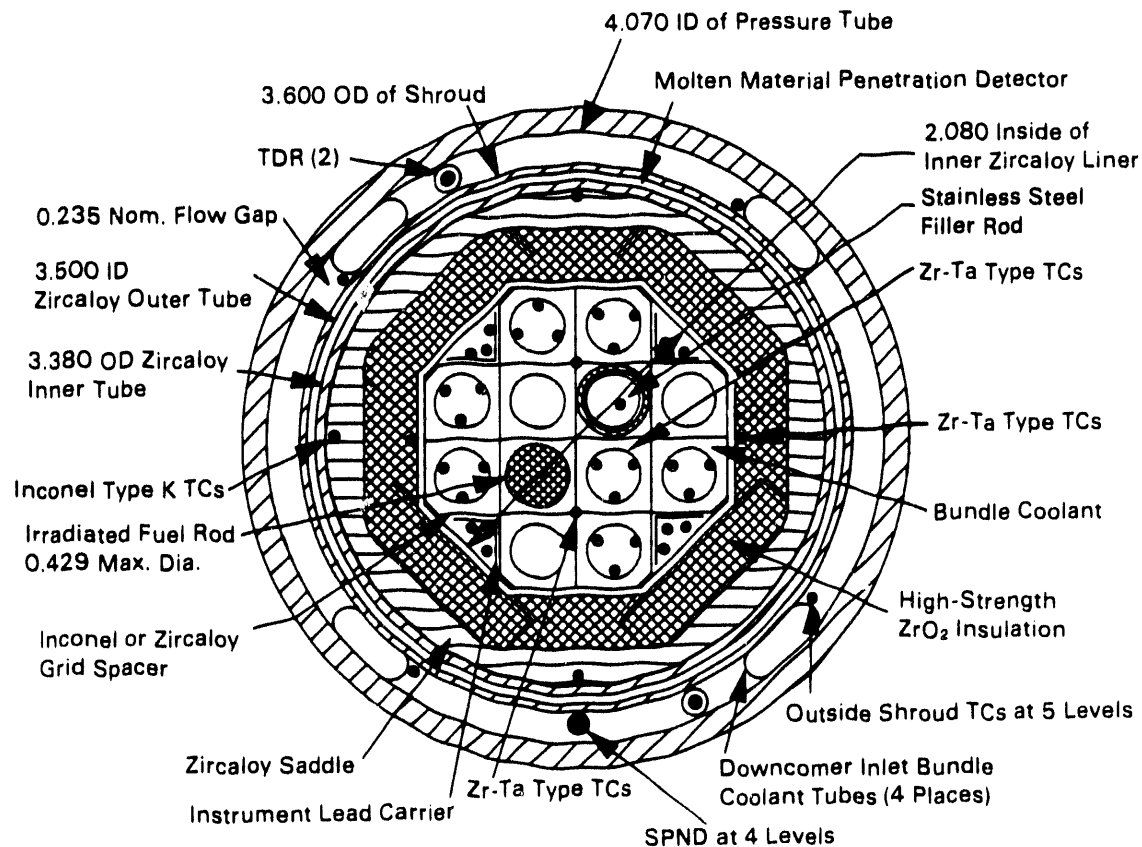


FIGURE 2.9. Cross Section of FLHT-5 Test Assembly Core Region (Dimensions in Inches)

1.3-cm pitch by eight grid spacers. The top spacer is made of Inconel, next four of Zircaloy, and the bottom three of Inconel; the spacers are located at equal spans along the length of the rods. Each unirradiated fuel rod contains a 3.63-m column of sintered UO_2 dished pellets, clad in a Zircaloy-4 tube with welded end caps at each end. The U-235 enrichment of the unirradiated rods is adjusted to the equivalent enrichment of the H. B. Robinson rod, i.e., 1.76%. The TCs are resistance-welded to the cladding interior surface at various elevations. The TC leads exit through the bottom of the rods. An Inconel spring is located in the plenum space at the top of the fuel rod to provide a compressive force on the column and thus prevent formation of axial gaps during handling and shipping.

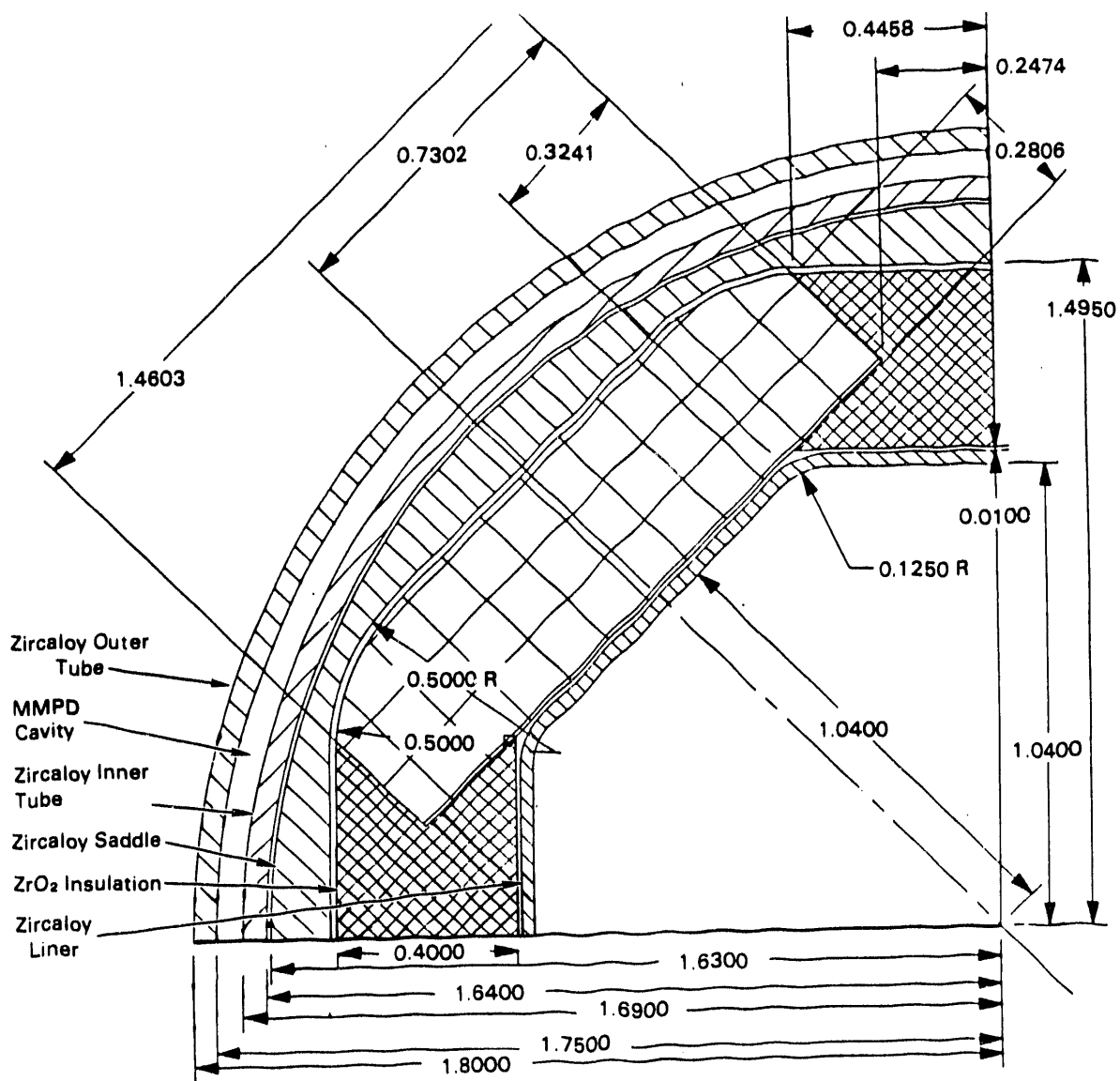


FIGURE 2.10. FLHT-5 Shroud (All dimensions in inches)

The lower end of each rod has a special duplex Zircaloy/stainless steel end cap that permits the end cap to be welded to the Zircaloy cladding and the TC leads to be brazed to the stainless steel section of the end cap. The bundle is supported from the bottom by a plate at the bottom of the test assembly; the rods are free to expand upward.

The shroud consists of two concentric Zircaloy tubes called "rounds"; Zircaloy saddles; zirconia thermal insulation tiles; and a Zircaloy liner (Figure 2.10). The two rounds form a double-walled capsule to isolate and protect the reactor pressure tube from the high-temperature fuel bundle components. Each round has a minimum yield strength (0.2% offset) of 400 MPa (58,000 psi), which equates to an internal yield pressure of 11.7 MPa (1700 psi) for the inner tube and 11.0 MPa (1600 psi) for the outer tube.

The two shroud rounds are maintained concentric by eight 1-mm-dia wires wrapped side-by-side around the outside of the inner tube. Each of the eight wires is about 180-m (560-ft) long. Four of the eight wires act as continuous TCs to indicate changing temperatures along the inner round. These four sensors are called molten metal penetration detectors (MMPDs) because their function is to indicate the presence of hot (molten) material near the inner tube.

Zircaloy saddles located inside the inner round provide compressive support and a smooth transition from the circular inner round to the octagonal-shaped blanket of insulation that surrounds the fuel bundle. The thermal insulation is a low-density (approximately 30% TD) rigid high-strength zirconia fiberboard in the shape of interlocking tiles. The low density helps provide high thermal resistance. The rigid high-strength fiberboard provides easy handling and machining plus resistance to compressive loadings that exist during the test. The interlocking design is used to keep the tiles from moving into the bundle region.^(a) The insulation is required so that high bundle temperatures can be reached; it is not required to protect the double-walled capsule or the reactor pressure tube. The double-walled capsule provides the mechanical support for the insulated fuel bundle.

The shroud includes a Zircaloy inner liner that protects the insulation during shipping and bundle insertion. During the early portions of the test, the liner prevents water from permeating the insulation. Such water ingress

(a) Post-test inspection of the FLHT-2 assembly showed tile cracking but no movement, even in regions exposed to the most severe conditions for several minutes

would reduce the thermal resistance of the insulation. During the high-temperature part of the test, the Zircaloy liner simulates a thin-wall BWR channel or additional fuel rods surrounding the existing fuel rods.

An annulus of flowing water exists between the shroud outer round and the pressure tube. This water annulus is called the bypass coolant and is the key safety component for the FLHT-5 test. It cools the outer round and indirectly cools the inner round. If these rounds remain cool, they will contain the hot bundle components and protect the reactor pressure tube. The reactor pressure tube forms a secondary containment for the test assembly.

2.1.4 Inlet Region

The inlet region contains the fixture that supports the bottom of the bundle, seals the bundle region to the bottom of the shroud, and provides sealed passageways for the bundle coolant, instrument, and pressurization lines and two time domain reflectometer (TDR) tubes used to measure bundle liquid level. The bundle leads that exit through the inlet housing are sealed to the housing using graphite gaskets like those used in the closure region.

2.2 EFFLUENT CONTROL MODULE

The ECM is located on top of the reactor and consists of two interconnected compartments that provide shielding and secondary confinement for the portion of the effluent line that extends across the top of the reactor. The compartments contain hardware that accomplishes many other functions detailed below (see Figure 2.11).

The first compartment is a small (1.2 m x 0.6 m x 0.8 m) lead-walled box (10-cm wall thickness) that covers the effluent line as it exits vertically from the top of the reactor and bends 90° to enter the primary ECM confinement cubicle. This box is designated the steamline closure cave (SCC). It contains an antideposition device (to sweep fission product clear of the effluent line wall over a short length) and six sample bombs to take grab samples of the effluent stream at designated times during the test. The SCC also shields the deposition rod access stub, through which the deposition rod will be removed after the test.

The SCC connects to the ECM proper, which is a 2.0 x 1.8 x 1.9 m cubicle of 3 mm (1/8-in.) steel plate, forming a secondary confinement about the exposed steam line. The air in this confinement is circulated from the reactor service space to the ECM and through a HEPA filter and a charcoal filter back to the service space. This circulation of confinement air is a defense against a possible leak of radioactive contamination from the steam line. (No such leak occurred during the FLHT-4 or FLHT-2 experiments.)

Inside the ECM confinement is another lead-lined steel box (10-cm wall thickness) with outside dimensions of 1.2 x 0.6 x 0.7 m, which contains the remaining ECM hardware and the main effluent line. The flow paths inside this box are shown in Figure 2.11. The main effluent flow path includes a condenser and separator, float valves, an iodine filter (sampler) and a pressure regulator valve. The valve responds to pressure transducer readouts through the DACS to maintain system pressure at 1.2 MPa (190 psig).

The condenser condenses the steam and separates the liquid and gaseous fractions. The gaseous effluent passes through the iodine filter and exits the ECM. That line is joined by the condensate (liquid) line, and a large dilution N₂ flow is added downstream of the ECM. The recombined effluent goes to a catch tank in the NRU basement. The noble gases in the effluent continue onto the reactor stack.

Two sample lines branch off the main effluent line. One of these, upstream of the condenser, conducts a sample through the mass spectrometer for measuring H₂/H₂O ratios and fission gas fractions. The second line, downstream of the condenser, conducts a gaseous effluent sample through a heater to the palladium hydrogen partial pressure meter and then through a chiller to a Beckman thermal conductivity meter that measures the hydrogen fraction in the sample mixture. Two bypass lines vent the main effluent line through safety relief valves in case it clogs at certain points. One bypass line goes around the iodine filter; and a second bypasses the entire ECM. The valve on the second bypass line will open at 2.4 MPa (350 psig).

Pressurized nitrogen is injected upstream and downstream of the condenser valve that responds to changes in system pressure. The ~60 (R.T.) liter minute N₂ flow sweeps the effluent through the condenser and importantly provides

2.15

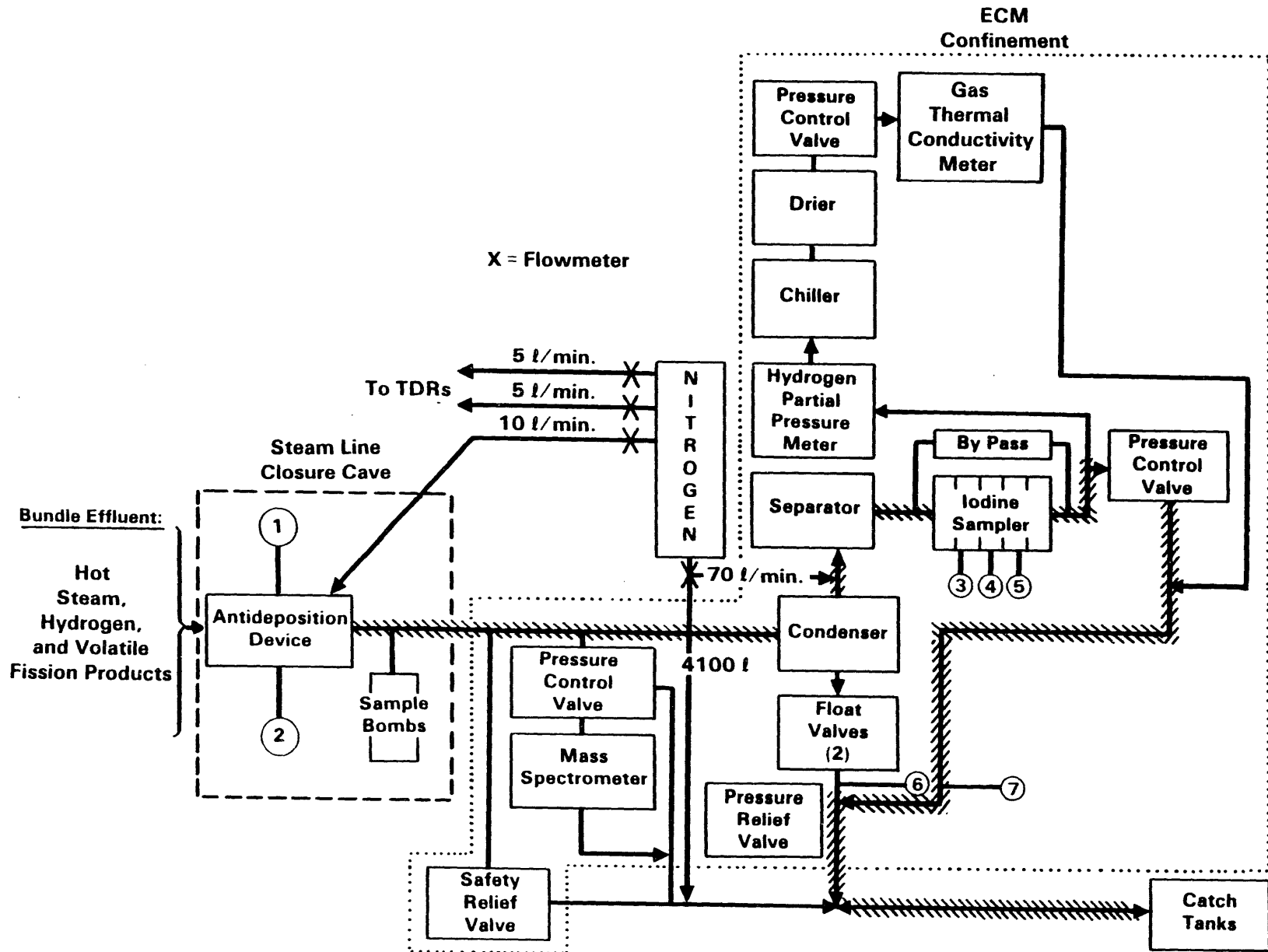


FIGURE 2.11. Flow Paths in the Effluent Control Module (cross hatching indicates main effluent flowpath). The circled numbers indicate locations of 7 gamma spectrometers.

a N₂ known flow standard, from which the Beckman data and the output of a turbine flow meter (on the gaseous effluent line) can be used to deduce absolute hydrogen flow.

The hardware of the ECM also includes two pressure relief valves, one preset to open at 1.6 MPa (240 psig) and the other at 2.4 MPa (350 psig). The two float valves on the liquid stream from the condenser serve different functions. The smaller valve handles condensate flows during the actual boildown transient, and the larger valve handles the much larger flows of solid water during pretransient operation.

The ECM hardware also includes numerous valves and fittings for services, such as chiller water and condenser cooling water; electrical leads for the heaters and heater types (plus control thermocouples for the heating devices); and the various nitrogen injections.

The ECM also provides access (beam ports) through the shielding for seven gamma spectrometers at the following locations:

- steam line at the SCC (2)
- the multistage iodine filter (3)
- the liquid and gaseous waste lines (1 each).

2.3 REACTOR/LOOPS

The NRU Reactor is operated by the Atomic Energy of Canada Limited (AECL). Full-length fuel bundles with commercial enrichment levels can operate in the reactor at nominal LWR power levels. The 130-MW-rated heavy-water-moderated-and-cooled reactor has two loops (U-1 and U-2) that can be connected to various pressure tubes for experiments. The Zircaloy-2 pressure tube used for the FLHT tests has an inside diameter of 10.4 cm (4.07 in.) and spans the length of the 9-m (30-ft) reactor vessel, including the active core length of 2.8 m (9 ft). It will be connected to the U-2 loop for the FLHT-5 experiment.

The U-2 loop can provide cooling water for steady-state and transient thermal-hydraulic conditions that simulate BWR and PWR coolant systems. The

loop can supply water at pressure up to 10.3 MPa (1500 psi) at inlet temperatures up to 315°C (600°F). The U-2 loop will supply the bypass and bundle coolant during the FLHT-5 test.

System pressure is maintained by a pressurized nitrogen source. Nitrogen is also injected downstream of the ECM in the gas waste line to provide hydrogen dilution.

The bypass coolant supplied by the U-2 loop enters the bottom of the reactor pressure tube and flows up the annulus between the pressure tube and the test train assembly. The water exits through the top of the pressure tube and flows back to the U-2 loop pumps.

Separate loop hardware supplies the bundle inlet coolant for the test from several pressurized tanks (accumulators). The water flows from the tanks to the top of the reactor through three bundle coolant lines at the top of the test train. Past the closure region, one of the three streams splits so that four coolant tubes pass alongside the shroud in the annulus between the shroud and the pressure tube. The flow streams enter the bundle region through four penetrations in the inlet fixture.

Once injected into the inlet region, the bundle coolant flows up along the fuel rods, is heated by fission power, and converted to steam, which in turn reacts with the high-temperature Zircaloy cladding and liner to form hydrogen and release heat. The bundle steam/hydrogen effluent then flows through the plenum, the closure, the steam line, and through the ECM to the catch tank.

Loop systems also provide a source of water (from another pressurized tank) for the ECM condenser and chiller. Loop hardware also supplies nitrogen gas for the ECM pressurization and hydrogen dilution.

2.4 INSTRUMENTATION

More than 250 instruments will be used in the FLHT-5 experiment to measure local pressure, temperature, flow, neutron flux, liquid level, and hydrogen generation. A listing of all the test instruments in the bundle and plenum regions is provided in this section. Test train instruments and their location are listed in Tables 2.1, 2.2, and 2.3. Major ECM instruments are shown in

TABLE 2.1. Fuel Bundle Instrumentation Summary

Instrument Type	Location	Distance Above Bottom of Fuel Column	
		m	in.
Type C Thermocouple	Inside Cladding Rods 1B-4C	1.02	40.0
Type C Thermocouple	Inside Cladding Rods 1C	1.22	48.0
Type C Thermocouple	Inside Cladding Rods 3C-3A	1.42	56.0
Type C Thermocouple	Inside Cladding Rods 2A-3D	1.63	64.0
Type C Thermocouple	Inside Cladding Rods 1B-4C	1.83	72.0
Type C Thermocouple	Inside Cladding Rods 1C	2.03	80.0
Type C Thermocouple	Inside Cladding Rods 3C-3A	2.24	88.0
Type C Thermocouple	Inside Cladding Rods 2A-3D	2.44	96.0
Type C Thermocouple	Inside Cladding Rods 1B-4C	2.64	104.0
Type C Thermocouple	Inside Cladding Rods 1C	2.84	112.0
Type C Thermocouple	Inside Cladding Rods 3C-3A	3.05	120.0
Type C Thermocouple	Inside Cladding Rods 2A	3.25	128.0
Type C Thermocouple	Inside Cladding Rods 3D	3.35	132.1
Type K Thermocouple	Carrier Mounted, Cells 1A	0.51	20.0
Type K Thermocouple	Carrier Mounted, Cells 1A	0.61	24.0
Type K Thermocouple	Carrier Mounted, Cells 1A	0.71	28.0
Type K Thermocouple	Carrier Mounted, Cells 1A	0.81	32.0
Type K Thermocouple	Carrier Mounted, Cells 1A	0.91	36.0
Type K Thermocouple	Carrier Mounted, Cells 1A-4D	1.02	40.0
Type K Thermocouple	Carrier Mounted, Cells 1A-4D	1.12	44.0
Type K Thermocouple	Carrier Mounted, Cells 4A	1.22	48.0
Type K Thermocouple	Carrier Mounted, Cells 4A	1.32	52.0
Type K Thermocouple	Carrier Mounted, Cells 4A	1.42	56.0
Type K Thermocouple	Carrier Mounted, Cells 4A	1.52	60.0
Type K Thermocouple	Carrier Mounted, Cells 4A	1.63	64.0
Type K Thermocouple	Carrier Mounted, Cells 4A	1.73	68.0
Type K Thermocouple	Carrier Mounted, Cells 4A	1.83	72.0
Type C Thermocouple	Spacer Mounted, Rods 1B-4C	1.61	63.5
Type C Thermocouple	Spacer Mounted, Rods 1B-4C	3.21	126.5
Type C Thermocouple	Spacer Mounted, Rods 1B-4C	3.75	147.5
Type K Thermocouples (3)	In flow stream, bundle inlet region		-10.0
Pressure Transducers (8 rods)		sensors at level	-5.00

TABLE 2.2. Shroud Instrumentation Summary

Instrument Type	Location	Distance Above Bottom of Fuel Column	
		m	in.
Type C Thermocouples	Outer Liner Surface, 0-180°	1.42	56.0
Type C Thermocouples	Outer Liner Surface, 90-270°	1.63	64.0
Type C Thermocouples	Outer Liner Surface, 0-180°	1.83	72.0
Type C Thermocouples	Outer Liner Surface, 90-270°	2.03	80.0
Type C Thermocouples	Outer Liner Surface, 0-180°	2.23	88.0
Type C Thermocouples	Outer Liner Surface, 90-270°	2.44	96.0
Type C Thermocouples	Outer Liner Surface, 0-180°	2.64	104.0
Type C Thermocouples	Outer Liner Surface, 90-270°	2.84	112.0
Type C Thermocouples	Outer Liner Surface, 0-180°	3.05	120.0
Type C Thermocouples	Outer Liner Surface, 90-270°	3.66	144.0
Type C Thermocouples	Outer Liner Surface, 0-180°	3.86	152.0
Type K Thermocouples	Outer Surface of Saddle, 0-180°	0.20	8.0
Type K Thermocouples	Outer Surface of Saddle, 90-270°	0.41	16.0
Type K Thermocouples	Outer Surface of Saddle, 0-180°	0.61	24.0
Type K Thermocouples	Outer Surface of Saddle, 90-270°	0.81	32.0
Type K Thermocouples	Outer Surface of Saddle, 0-180°	1.02	40.0
Type K Thermocouples	Outer Surface of Saddle, 90-270°	1.22	48.0
Type K Thermocouples	Outer Surface of Saddle, 0-180°	1.42	56.0
Type K Thermocouples	Outer Surface of Saddle, 90-270°	1.63	64.0
Type K Thermocouples	Outer Surface of Saddle, 0-180°	1.83	72.0
Type K Thermocouples	Outer Surface of Saddle, 90-270°	2.03	80.0
Type K Thermocouples	Outer Surface of Saddle, 0-180°	2.23	88.0
Type K Thermocouples	Outer Surface of Saddle, 90-270°	2.44	96.0
Type K Thermocouples	Outer Surface of Saddle, 0-180°	2.64	104.0
Type K Thermocouples	Outer Surface of Saddle, 90-270°	2.84	112.0
Type K Thermocouples	Outer Surface of Saddle, 0-180°	3.05	120.0
Type K Thermocouples	Outer Surface of Saddle, 90-270°	3.25	128.0
Type K Thermocouples	Outer Surface of Saddle, 0-180°	3.45	136.0
Type K Thermocouples	Outside Surface of Shroud, 0-90-180°	-0.2	-8.0
Type K Thermocouples	Outside Surface of Shroud, 0-180°	1.83	72.0
Type K Thermocouples	Outside Surface of Shroud, 0-180°	2.29	90.0
Type K Thermocouples	Outside Surface of Shroud, 0-180°	2.79	110.0
Type K Thermocouples	Outside Surface of Shroud, 0-90-180°	3.66	144.0
Self-Powered Neutron Detectors	Outside Surface of Shroud, 180°	0.60	23.75
	Outside Surface of Shroud, 180°	1.14	44.75
	Outside Surface of Shroud, 180°	1.67	65.75
	Outside Surface of Shroud, 180°	2.20	86.75
Flux Wires	Outside Surface of Shroud, 0°	Full-Length	
TDR (Liquid Level Detectors)	Outside Surface of Shroud, 70°	Full-Length	-10" to 166"
	Outside Surface of Shroud, 250°	Full-Length	
MMPD's (Molten Metal Penetration Detectors)	In cavity between inner and outer shroud rounds	4 independent detectors	

TABLE 2.3. Plenum/Steam Line Instrumentation Summary

Instrument Type	Location	Distance Above Bottom of Fuel Column	
		m	in.
Type K Thermocouples	Outside of Inner Liner, 0-180°	4.52	178
Type K Thermocouples	Outside of Inner Liner, 0-180°	4.95	195
Type K Thermocouples	Outside of Inner Liner, 0-180°	5.38	212
Type K Thermocouples	Outside of Inner Liner, 0-180°	5.82	229
Type K Thermocouples	Outside of Inner Liner, 0-180°	6.25	246
Type K Thermocouples	Outside of Inner Liner, 0-180°	6.68	263
Type K Thermocouples	Outside of Inner Liner, 0-180°	7.11	280
Type K Thermocouples	Outside of Inner Liner, 0-180°	7.54	297
Type K Thermocouple	On Deposition Rod, 0°	4.52	178
Type K Thermocouple	On Deposition Rod, 0°	4.95	195
Type K Thermocouple	On Deposition Rod, 0°	5.38	212
Type K Thermocouple	On Deposition Rod, 0°	5.82	229
Type K Thermocouple	On Deposition Rod, 0°	6.25	246
Type K Thermocouple	On Deposition Rod, 0°	6.68	263
Type K Thermocouple	On Deposition Rod, 0°	7.11	280
Type K Thermocouple	On Deposition Rod, 0°	7.54	297
Type C Thermocouples	Outside Inner Liner, 0-180°	4.11	162
Type K Thermocouples	Outside Outer Liner, 0-90-180-270°	4.22	166
Type K Thermocouples	Outside Outer Liner, 0-180°	5.74	226
Type K Thermocouples	Outside Outer Liner, 0-180°	7.16	282
Type K Thermocouples	Outside Steam Line, 0-90-180-270° (above closure)	8.43	332
Pressure Transducers	Lower Plenum	4.22	166
Pressure Transducers	Upper Plenum	7.77	306

Figure 2.11. During a test, all critical test instruments are monitored by the test engineers. If it appears that test conditions (indicated by one or more instruments) are either becoming unsafe or are such that the main test objectives cannot be attained, the test will be terminated. If corrections can be made in a reasonable time (one or two days), they will be made and the test will be restarted. These contingencies are addressed in general in the Safety Concerns section of this report. Specific termination and recovery procedures are contained in the Experimental Operations Plan.

Most instruments used in the test enhance operational safety because they can indicate potentially unsafe conditions. However, some instruments monitor key test conditions that automatically cause termination of the test if preset limits are exceeded. The test will be automatically terminated when specified flow, temperature, pressure, power, or coolant accumulator weight measurements exceed preset high or low limits. Other instruments activate alarms that may lead to manual termination of the test.

Nearly all of the FLHT-5 safety instruments are the same type of instrument used in previous tests. All the instruments used in the previous tests to monitor for unsafe conditions performed satisfactorily. Just prior to the FLHT-5 test, each safety instrument circuit will be checked to be sure the limits are correctly set and the electrical circuits are operational.

2.5 DATA ACQUISITION AND CONTROL SYSTEM

The DACS is composed of the following major components: a Data General (DG) MV/6000 super-minicomputer, a NEFF A/D (analog-to-digital) subsystem, two Tektronix 4027 color graphics terminals, and several DG character terminals. The MV/6000 uses the AOS/VS virtual memory operating system and is equipped with two megabytes of semiconductor memory, two 1600-bpi tape drives, two 190-megabyte disk drives, and a line printer. A small dot matrix printer is attached to one of the terminals; two other terminals are connected to a Tektronix hard copy unit and either of them can initiate a data copy.

The DACS hardware and software are designed to accomplish the following operations:

- real-time data collection and scanning
- tape and disk input and output (I/O)
- on-line graphics and terminal I/O
- experiment control (calibration, startup, and controlling the bundle coolant flow)
- automatic experiment termination (NRU reactor trip)

- alarms on off-limit conditions (could lead to manual trip)
- post-test data examination and output.

The DACS is arranged in the configuration shown in Figure 2.12. One character terminal is used as the console to control the DACS; one character terminal and one graphics terminal are used by the test director for data monitoring and evaluation; and one character terminal and one graphics terminal are provided in a separate room for the use of test observers not involved in actually running the experiment. These terminals are equipped with a variety of monitoring functions, but no control functions. The major components and the personnel stations for operating and observing the experiment are shown schematically in Figure 2.13.

The DACS software is designed to use the function keys of the terminals to initiate desired routines. Certain functions available to the console operator are disabled in the other terminals. These special functions are necessary to operate the computer system, but they do not have any data reporting capability.

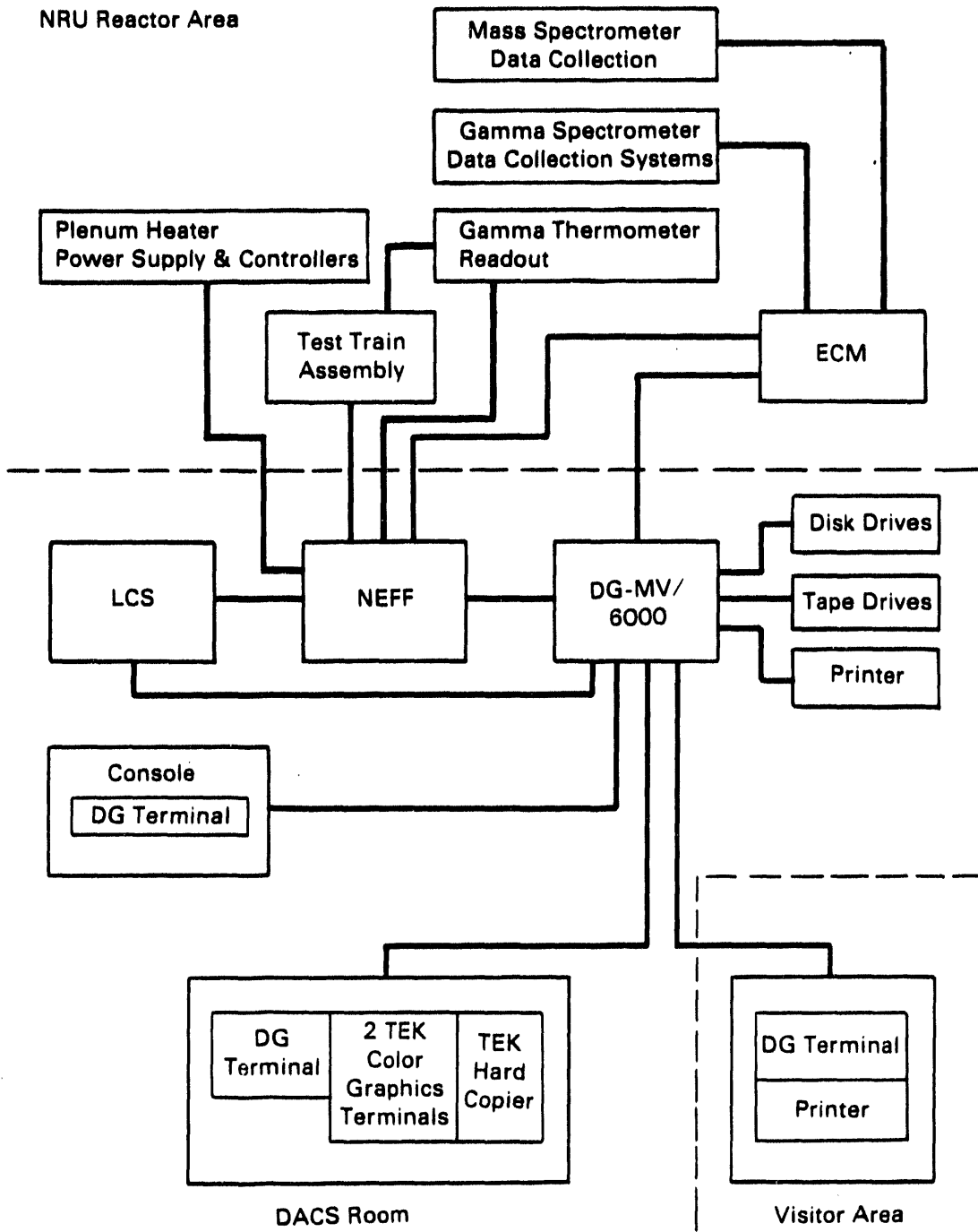
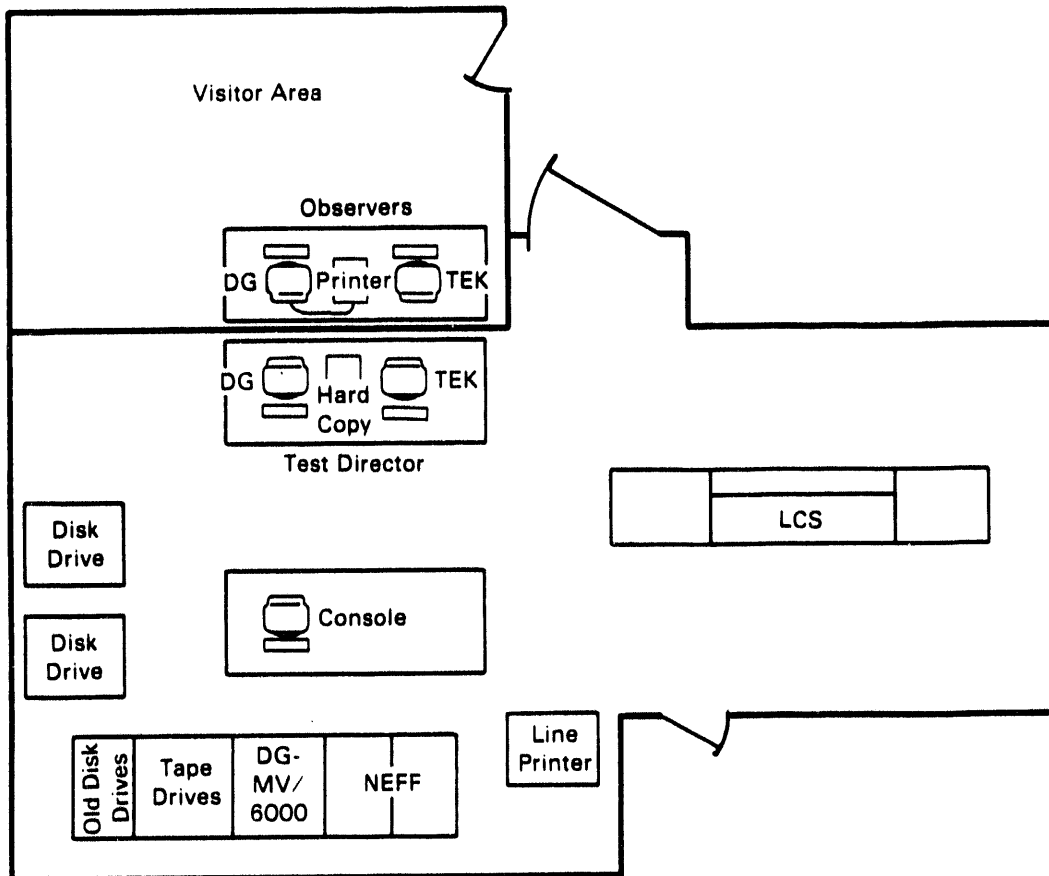


FIGURE 2.12. Electrical Connections for the DACS, LCS, ECM, Test Train, and Data Stations



LCS - Loop Control System
 TEK - Tektronix Color Graphics Terminal
 DG - Data General Terminals
 DG-MV/6000 - Computer
 NEFF - Analog-to-Digital Data Acquisition System

FIGURE 2.13. Sample Floor Plan of the Data Acquisition and Control System

3.0 EXPERIMENT PROCEDURES, CONDITIONS, AND CONTROLS

This section provides an overview of the planned conduct of the FLHT-5 experiment, including: pretest hardware preparation and installation; test sequence and conditions; post-test disassembly and removal activities; and the procedures and controls planned to maintain safety throughout the entire campaign. More detailed discussion of the predicted test events and conditions and the safety analysis is reserved for Section 4.0 (Safety Concerns).

3.1 TEST HARDWARE PREPARATION AND INSTALLATION

The goals of the pretest preparations are: to complete bundle and shroud assembly and connections; to install the test train in the NRU reactor loop; and to make all final closures, instrument connections, and instrument calibrations and checkouts for loop, ECM, and assembly operation. Assembly, plenum, and ECM leak checking are also an essential part of the installation procedures.

3.1.1 Bundle and Shroud Assembly and Connections

The FLHT-5 assembly will contain one irradiated H. B. Robinson fuel rod, as did FLHT-4. The irradiated rod will be installed in the assembly under water in the NRU rod bay. This will necessitate transporting the bundle and shroud to and from the NRU basin as well as shroud/assembly connection and instrument hardline/softline connection and potting at the basin. The test train assembly will proceed as described below.

The bundle (minus the irradiated rod) and the shroud will be preassembled at PNL before arriving at CRNL. After layout, inspection, and inventory at CRNL, the bundle will be inserted into the shroud from the bottom; the coolant lines and TDR's will be installed, followed by the bundle/shroud inlet fixtures. The latter will be leak-checked. The bundle and (external) heated plenum leads will be run through the feed-through plug.

All the above will be done horizontally on layout tables. Then the shrouded bundle and the plenum will be installed on a strong back with an offset between the bundle and plenum, which will not yet be connected. The

entire test train will be hoisted to the NRU basin where the train will be lowered into 30 ft of water, such that the irradiated rod (already in the basin) can be moved into position and inserted into the bundle under water. A guide tube will be used to facilitate this operation.

The shrouded bundle and plenum assembly will then be raised until the flange area clears the water. The plenum will be moved over and onto the shroud and bolted to it. Based on radiation fields experienced during similar operations during FLHT-4, the dose rate to personnel during this and subsequent basin operations should be acceptably low (<50 mR/h).

The attachment of instrument leads to the plenum exterior can then be completed and the test train removed from the strong back. The final pull of leads through the feed-through plug can be accomplished and the seals pressed. The instrument-potted junctions can then be made with the test train still in the basin.

3.1.2 Test Train Installation

The test train will be hoisted carefully into a shielded cask on the reactor top face, lowered into the L-24 loop position, and leak-checked. The closure plug will then be installed and final connections to the ECM and the DACS will be made. A leak check of the entire effluent line (assembly through ECM) completes the preparation procedures.

The entire flow path, including the heated plenum and the ECM will be "commissioned" by injecting superheated steam into the system near the top of the assembly and observing the performance of various measurement and control systems such as the plenum heaters, the pressurizers, the flow meters, the control valves, and the hydrogen monitors. Further checks for leak tightness and flow control will be made at this time.

3.2 PRECONDITIONING OPERATION

The assembly will be calibrated for power production at low neutron power to ensure that the power levels during the subsequent higher power "preconditioning" operation are well known. The purposes of the preconditioning operation are to prototypically crack the fresh fuel pellets (thus, providing

prototypic fission product release pathways from the fuel), to promote fuel/cladding contact to enhance chemical interaction, and to build up an inventory of medium-lived isotopes, notably iodine isotopes, that can be detected by the gamma spectrometers during the test and during post-test examination of the deposition rod. Occurrence of a peak linear heat rating greater than 25 kW/m is required for the first objective. Several slow ramps to the 700 to 800 kW level are planned in the course of several hours operation at approximately 700 kW. The delay-to-test will be 12 to 24 h, depending on the total effective full-power hours of preconditioning operation. The actual delay imposed will in any case keep the calculated radionuclide inventory at the time of the boilaway less than or equal to the projected levels used in this FSAR.

There is a remote possibility that a fuel rod (in particular the pressurized irradiated rod) could fail during the preconditioning period, resulting in a release of very radioactive fission products into the coolant loop water. Because the bundle coolant inlet and outlet lines extend across the reactor top face during the preconditioning operation, the exposed portions of these lines will be shielded with 4 in. of lead to mitigate radiation hazard in the remote possibility of a fuel rod failure.

The peak operating conditions during the preconditioning are summarized in Table 3.1. Note that the peak linear heat rating (31 kW/m) is sufficient to produce pellet cracking, but is not sufficient to cause abnormally high cladding temperatures or fuel temperatures. Also note that the margin to dryout is quite sufficient under the specified coolant conditions (MDNBR = 2.82).

During the preconditioning, the ECM will be isolated from the test train (there will be no water or steam flow through it).

3.3 TEST PHASE SEQUENCE AND CONDITIONS

The ECM will be reconnected to the flow path following preconditioning and cooldown. After the appropriate delay period, neutron power (30 kW) and bundle and bypass flow (each 1 kg/s) will be re-established. The bundle flow will be reduced to about 11.3 g/s (90 lb/h) and held for a period of time, during which the plenum heaters will be turned on and adjusted. A steady-state pretransient condition is expected to be established at this flow rate in which the plenum

TABLE 3.1. FLHT-5 Preconditioning Operating Conditions

<u>Coolant in Bundle</u>	
Inlet temperature,	38°C (100°F)
Outlet temperature	165°C (330°F)
Flow rate	1.51 kg/s (12,000 lbm/h)
Outlet pressure	1.38 MPa (185 psig)
<u>Bundle Parameters</u>	
Maximum total power	800 kW
Peak linear heat rating	31.8 kW/m (9.7 kW/ft)
Average linear rating	19.9 kW/m (6.1 kW/ft)
Maximum cladding temperature	<217°C (420°F)
Maximum fuel center temperature	1240°C (2264°F)
Minimum DNB ratio	2.82
<u>Bypass Annulus Coolant</u>	
Inlet temperature	38°C (100°F)
Outlet temperature	42°C (108°F)
Flow rate	1.01 kg/s (8000 lbm/h)
Outlet pressure	1.38 MPa (185 psig)

and ECM piping are dried out (no condensation) and the liquid level and steaming rate in the bundle are stabilized. About 1/3 to 2/3 m (1 to 2 ft) of the top of the assembly will be uncovered (but steam cooled) at that point.

The bundle flow will then be reduced to 1.26 g/s (10 lb/h), which will initiate the coolant boilaway and cladding heatup phase of the transient. Based on FLHT-2 and FLHT-4 experience, the coolant two-phase level will rapidly fall toward an equilibrium level at roughly 0.75 m above the bottom of the fuel stack. During that time, the upper region cladding and fuel will be heating up (due to nuclear and oxidation heating) at a rate of about 2 to 3°C/s until a temperature of 1400 to 1500°C is reached. Then local accelerated oxidation and a rapid rise in temperature into the 2200 to 2600°C (4000 to 4700°F) range will occur. These conditions will progress downward along a moving front (due to steam starvation of levels above the front and continued heating of the levels below it). Based on FLHT-4 data, the downward front movement will probably be relatively rapid.

The steadily closer proximity of the front to steam cooled components will bring an end to the downward front movement. Based on FLHT-4 experience, the front will then move slowly upward until the top of the assembly is reached.

During the downward and upward "burning" and subsequent heating, cooling, and oxidation of fuel, a significant fraction of the gaseous and volatile fission products (up to 80%) are expected to be released from the assembly. Transport and deposition analyses and FLHT-4 experience demonstrate that some of this released inventory--composed mainly of Xe, Kr, Cs and I, but not Te--will be carried by the effluent to the condenser, where the Cs and I, will be deposited. The noble gases will pass on to the NRU stack, together with the generated hydrogen, which will be diluted to less than 4 vol% in the large flow of nitrogen injected just downstream of the ECM. The 4 vol% represents a safe flammability limit.

A summary of the expected test operating conditions appears in Table 3.2, and results of code calculations for oxidation and temperatures appear in Appendix A. Based on FLHT-4 experience, the anticipated heat losses are such that the bundle temperature would peak at far less than the melting temperature of UO_2 (i.e., 2800°C or 5000°F) even if the oxidation front movement does not truncate the temperature rise at considerably lower values (~2200°C, ~4000°F). In any case, the safety of the test depends on the coolability of the shroud outer rounds, and these are expected to remain acceptably cool, as indicated in Table 3.2 and explained in Section 4.0.

A hold period of up to 60 min, with 30 kW nuclear heating and 1.26 g/s (10 lbs/h) coolant flow, is planned after rapid oxidation first occurs and temperatures >2200°C are first attained. This hold period duration is subject to re-evaluation during the test. If a melting blockage and debris bed heatup situation develops, as indicated by TDR and saddle TC data, the test will be terminated sooner; on the other hand, if oxidation and hydrogen production progresses under known and controllable conditions up to the 60-min mark, the test may be extended until hydrogen production finally ceases.

3.4 POST-TEST DISCONNECTION AND DISASSEMBLY

The post-test activities include a bundle restart to very low power to check thermocouple performance; a cooldown period (up to 24 h); a flush of the ECM line to reduce radiation fields; removal and gamma-scanning of the deposition rod; crimping and cutting the ECM inlet/outlet effluent lines and

TABLE 3.2. FLHT-5 Test Phase Operating Conditions

Flow Rate	Value
Bundle coolant - operation	0.00126-0.00252 kg/s (10 to 20 lbm/h)
Bundle sweep gas (nitrogen) (post-test)	10 L/min (0.35 ft ³ /min) STP
Bypass coolant	1.0 kg/s (8000 lbm/h)
ECM condenser water	315 g/s (2500 lbm/h)
ECM chilled water	0.038 L/min (0.01 gpm)
ECM nitrogen (injections for pressure)	~90 L/min (3.18 ft ³ /min) NTP (Total of 4 injection points)
Gaseous waste stream nitrogen dilution	4100 L/min
Power	
NRU reactor	approximately 6 to 8% neutron full scale
Fuel rod - linear (peak) Bundle	1.16 to 1.36 kW/m (0.35 to 0.41 kW/ft) 30 to 35 kW
Temperature	
Peak fuel cladding	2200 to 2600°C (4000 to 4700°F)
Peak shroud saddle interior	<700°C (1300°F)
Peak inner round	<330°C (630°F)
Peak outer round	<150°C (300°F)
Bundle coolant inlet	38 to 93°C (100 to 200°F)
Bundle coolant saturation	194°C (382°F) at 185 psig
Bypass coolant inlet	38 to 93°C (100 to 200°F)
Bypass coolant outlet	50 to 105°C (122 to 222°F)
Bypass coolant saturation	194°C (382°F) at 185 psig
Peak plenum inner wall	<1090°C (2000°F)
Peak plenum outlet steam	<370°C (700°F)
Pressure	
Bundle coolant	1.38 MPa (200 psig)
Fuel rod cold fill gas pressure (a)	(a)
Bypass coolant	1.38 MPa (200 psig)
MMPD cavity (helium filled)	0.1 MPa (0 psig)
Shroud insulation cavity (inert gas filled)	0.3 to 0.7 MPa (50 to 100 psig)
Plenum insulation cavity (evacuated)	<0 MPa (0 psig)

(a) To be presented in the FLHT-5 Experiment Operations Plan (approximately 50 psig).

disconnecting instruments and services; crimping/cutting the assembly effluent, inlet, flush, and drain lines and instrument leads; and removal of the test (to the basin), the steam closure cave (to a hot cell), and finally the ECM (to storage and eventually disposal).

3.4.1 Deposition Rod Removal

The deposition rod will be removed utilizing design and procedures that confine contamination throughout the process of hoisting the rod into a canister inside a vertical shielded cask. The rod will be gamma-scanned as it is lifted slowly into the cask. The deposition rod access stub will be crimped, cut and sealed. The assembly/effluent line will then be flushed, while a gamma scan is made of the flush stream (i.e., the liquid waste line) to determine efficacy of the flushing.

3.4.2 Crimping and Cutting Effluent and Connector Lines

Crimping and cutting tools and procedures are designed to minimize personnel exposure and the spread of contamination during the disconnection of the ECM, steam closure cave, and test train. Typically, a line will be flattened tightly in three sequential locations, then sheared in the center of the middle flattened area. Duplicate sets of hydraulic-actuated long-handled mashing/shearing heads have been obtained to eliminate switching contaminated heads. Radiation and contamination surveys will be performed before, during, and after the disconnection operations. Surveillance of airborne contamination will also be maintained, and breathing masks will be worn during the cutting of contaminated piping. Appropriate protective clothing and personnel dosimetry will also be required.

3.5 CONTROLS AND PROCEDURES TO MAINTAIN SAFETY

This subsection focuses on controls and procedures designed to maintain safety during the transient test phase of the experiment. Safety-related features of the pretransient and post-test phases have been indicated in the previous section.

The major emphasis of the design and procedural controls is to protect the pressure tube in which the test train resides. Thus, all foreseen situations that

could lead to pressure tube damage are protected by multiple sensors that will trip (shut down) the NRU reactor on an N-out-of-M(M>N) logic. These automatic trip circuits are set to actuate if predetermined limits ("setpoints") are exceeded. The automatic trip parameters and setpoints are listed in Table 3.3.

Other parameters will be monitored because they could indicate approach to an undesirable condition. These parameters include the MMPD (wire wrap continuity and cavity pressure) at the inner Zircaloy round and the bundle steam flow/differential pressure/exit temperatures, which could indicate flow blockage or (in the latter case) accelerated Zircaloy oxidation in the plenum region. These indications could lead to a manual reactor trip, based on the test director's judgment, within the guidelines of the EOP.

TABLE 3.3. FLHT-5 Experiment Safety Trip Functions

<u>Automatic Trips</u>	<u>Set Points</u>	<u>Responsibility</u>
<u>Temperatures</u>		
Shroud saddle exterior - high	982°C (1800°F)	PNL
Bypass coolant outlet - high	175°C (347°F)	CRNL
Plenum steam outlet - high	370°C (700°F)	CRNL
Plenum outside (level 166) - high	200°C (391°F)	PNL
<u>Pressure</u>		
ECM system pressure - low	0.59 MPa (85 psig)	PNL
<u>Coolant Flow Rate</u>		
Bypass coolant - low	0.756 kg/s (6000 lb/h)	CRNL
Bypass coolant - high	1.26 kg/s (10000 lb/h)	CRNL
Bundle accumulator weight - low	11.3 kg (25 lb)	CRNL
U-2 Surge tank level - low		CRNL
<u>Power Change</u>		
Mean power log rate - high	15%/s	CRNL
<u>Manual Trips</u>		
<u>Sensor</u>		
Bundle coolant differential pressure - high		PNL
Bundle effluent temperature - high		PNL
MMPD cavity pressure - high		PNL
Bundle coolant - low accumulator weight		CRNL

4.0 SAFETY CONCERNS DURING NORMAL OPERATION

Topics involving safety concerns for the FLHT-5 experiment include release of radioactive fission products, radiation fields, reactivity changes, hydrogen generation, materials at high temperature, steam explosion, and steam pressure pulses. The radioactive fission products include those in the irradiated H. B. Robinson rod plus those produced in all the fuel rods during the preconditioning phase and transient phase. The radiation fields are created by the decaying radioactive fission products and the decaying neutron activation products. Once the test train assembly is loaded into the NRU Reactor, predicted reactivity changes have been calculated for the removal of the bundle water from the core region and a hypothesized axial movement of UO_2 in the test bundle. (No evidence has yet been found in FLHT-2 or FLHT-4 data for significant axial relocation of UO_2 .) Hydrogen is produced from the chemical reaction of Zircaloy with steam during the high-temperature portion of the transient test. A steam explosion could only occur if a molten mixture (U, Zr, O) reacted with water under certain specific conditions. A steam pressure pulse would occur in the bundle region if hot material, including Zircaloy, fell into the water pool at the bottom of the fuel bundle region. (No such pulse was observed during FLHT-2 or FLHT-4).

All of the above hazards were analyzed for the FLHT-2 and FLHT-4 tests. Two analyses that still basically apply are those for steam explosion and steam pressure pulses. The potential for these occurrences was reanalyzed, assuming the somewhat more severe predicted conditions for FLHT-5. The prior conclusion (that several criteria for these occurrences are not met) was reached again in the updated analysis. The updated analyses are shown in Appendix C.

Analysis of the other hazards is slightly altered from that presented in the PSAR by the inclusion of only one irradiated rod (three were assumed in the PSAR). This change reduces the predicted radiation fields, especially at long times post-test.

4.1 RADIOACTIVE FISSION PRODUCTS

The presence of radioactive fission products (contamination) is an inherent hazard associated with nuclear energy. Proper hardware design and handling procedures provide for safe working conditions. The fission product inventory in the FLHT-5 test will be greater than that generated in the FLHT-4 test because of the longer pretest conditioning period at 700 to 800 kW bundle power and because of the increased nuclear power during the transient phase. The release fractions are also expected to be higher because of long transient operation at higher fuel temperatures and consequent greater oxidation and liquification of the fuel. In this section, conservative estimates for inventory, release, and deposition of the fission products are presented along with estimated post-test radiation fields.

The primary containment system (bundle steam/hydrogen flow path) was designed for and will be tested for leak tightness at pressures of 2.4 MPa (350 psig); the operating pressure during the test phase will be <1.38 MPa (200 psig). Should a leak develop during the test, the only hazardous location for such a leak will be downstream from the test train closure plug. The steam/hydrogen flow path from the top of the closure has a secondary confinement (maintained at a slightly negative pressure) to prevent the release of gases into the reactor hall. During the transient phase of the test (in which the fission product release will occur), personnel access to the vicinity of the ECM will not be permitted and the radiation fields and airborne contamination will be monitored remotely. Access to the ECM and vicinity after the test will be permitted only after a thorough radiation survey of the area by CRNL Health Physicists.

The air from the ECM confinement space is routed through HEPA and charcoal filters prior to release to the reactor service space and ultimately the NRU/NRX stack. A liquid detector on the ECM confinement floor will detect any gross liquid leaks from the condenser or liquid effluent piping.

Components in the ECM have different pressure and temperature design limits, all of which are comfortably above the operating conditions. Lower limit components are the floats inside the float valves. The floats inside the

float valve will collapse above 3.1 MPa (450 psig) at 260°C (500°F). The condensate from the condenser that flows into the float valves has a maximum (saturation) temperature of 194°C (382°F), and the maximum operating pressure will not exceed 200 psig.

4.1.1 Radiation Fields Resulting From Fission Product Release

Radiation fields associated with FLHT-5 are due to the presence of both fission and activation products; however, activation products are not expected to contribute significantly to the post-test working background radiation levels. Actual radiation levels during the FLHT-5 test are expected to be up to twice as high than those for FLHT-4 due to higher release fractions and higher test-phase nuclear power, and longer preconditioning.

Krypton gas will be used in the insulation cavity in FLHT-5, as it was in FLHT-4. The relative activity of this krypton was negligible during FLHT-4. The insulation cavity will be evacuated during preconditioning and pressurized with krypton before the transient phase. This will minimize the neutron activation of the krypton.

The irradiated H. B. Robinson rod contains about 400 Ci of long-lived radioactive isotopes (strontium-90, cesium-137, yttrium-90). In addition, the planned preconditioning period will contribute on the order of 10,000 Ci of medium-lived iodine isotopes (iodine-131, -133, -134, and -135) at the time of the transient test. The FLHT-4 inventory of such isotopes was on the order of 5000 curies. A listing of expected fission product inventories and release fractions of 13 selected elements is given for the FLHT-5 experiment in Table 4.1. These inventories and release fractions are compared with those from the PBF SFD 1-4 test, which was also a high-temperature severe fuel damage test involving irradiated fuel. The predicted release fractions for FLHT-5 were calculated by integrating the CORSOR release rates (Appendix B) using a fuel temperature history predicted by the in-house code, "TRUMP", as described in Appendix A.

PNL retained a consultant, Dr. A. Cronenberg of Engineering Science and Analysis, Idaho Falls, Idaho, to calculate the fission product release and deposition for the FLHT-5 experiment. Cronenberg found that,

TABLE 4.1. Predicted FLHT-5 Curie Inventories and Release Fractions
(Compared to SFD 1-4 Test)

Element	FLHT-5 Calculations		SFD 1-4 Experience	
	Inventory, Curies (a)	Release Fraction, %	Inventory, Curies	Release Fraction, %
Kr	6,200	81	~10,000	30-50
Xe	13,000	81		
I	16,000	81	~3,500	24
Rb	9,000	81	--	--
Cs (137)	160	75	1,200	~40
Cs (Total)	8,400	75	--	--
Te	8,800	7.9	--	--
Ag	70	68	--	--
Sb	3,100	35	--	--
Ba	9,700	9.1	--	--
Mo	7,800	3.8	--	--
Sr	12,000	3.7	--	--
Zr	12,000	0.007	--	--
Ru	460	0.33	--	--

(a) At zero delay post-test (assuming 10-h preconditioning at 800 kW, 24-h delay, 4 h at 30 kW).

(b) Inventories are FISPROD code results for 11 fresh rods (Walker 1975).

due to high predicted flow velocities in the plenum and ECM piping, the vast majority of released cesium, iodine, and tellurium will not condense or deposit until they reach the steam condenser inside the ECM. There, however 80% of the released species (CsI, Cs₂, H₂Te and SnTe) will be trapped. Assuming the inventories and release fractions listed in Table 8, and the geometry of the condenser (inside the 10-cm lead shielding inside the ECM), radiation fields around the ECM were calculated with the QAD code (Cain 1977).

The resulting dose rates were influenced by distance to the ECM. For the ECM confinement, for example, the west side is the closest to the condenser and

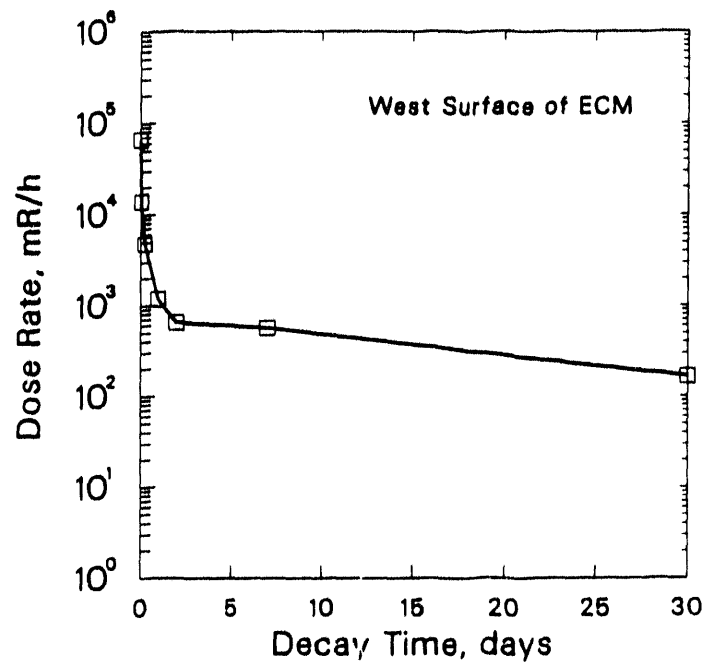


FIGURE 4.1. Maximum Predicted Post-Test Dose Rates on West Exterior Surface of the ECM

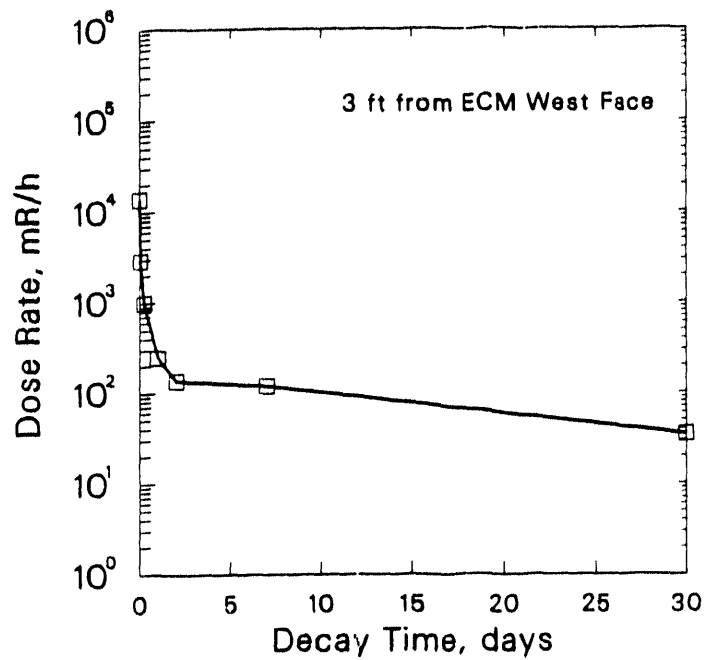


FIGURE 4.2. Maximum Predicted Post-Test Dose Rates Three Feet from the West Side of the ECM

thus has the highest dose rates. On this west surface, the maximum dose rates occur at the elevation of the condenser, and at a position in line with it. These maximum west-side surface dose rates are plotted vs. decay time post-test in Figure 4.1. A more realistic working field would be that 3 feet (arm's length) from the surface, and these rates are plotted in Figure 4.2.

For the lead-walled cave inside the ECM, the north face is closest to the condenser. The maximum north-face dose rates are plotted vs. time in Figure 4.3. This figure is included mainly to provide perspective to long-term dose rates that could be encountered in eventual disassembly of the ECM. During post-test operations, the ECM confinement will prohibit personnel access to the cave or the condenser itself.

It should be emphasized that these calculated dose rates are highly conservative. They are based on a very pessimistic temperature history and on release fractions appropriate to irradiated fuel. The predominance of unirradiated fuel in the FLHT-5 test, combined with a more realistic temperature history, would reduce the actual release by a factor of five or more, with

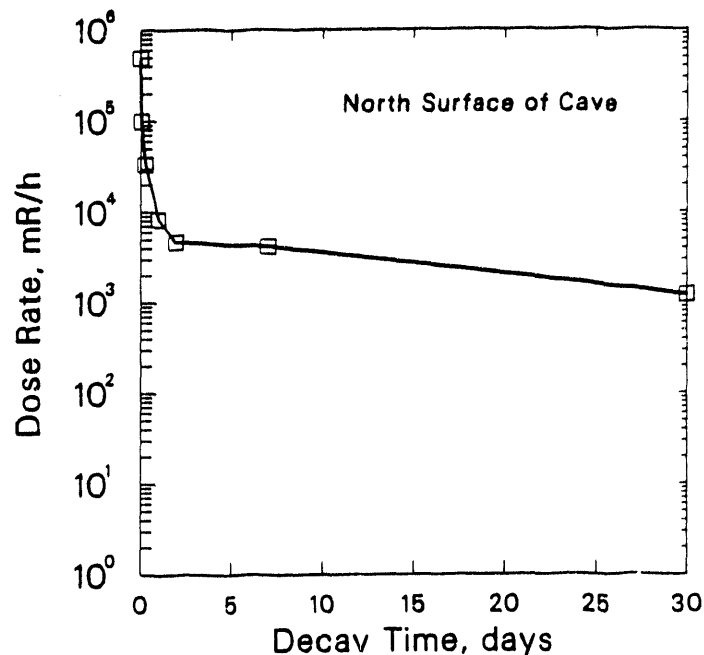


FIGURE 4.3. Maximum Predicted Post-Test Dose Rates on the North Side Cave Exterior

proportional reduction in the dose rates. Actual maximum ECM surface dose rates measured immediately after the FLHT-4 test were 5 R/h, and were <1 R/h 6 h later.

It also should be emphasized that these dose rates are calculated for the period prior to any water flush that would reduce the fission product inventory in the ECM. Based on PBF/SFD 1-4 and FLHT-4 experience, a reduction of Cs/I deposits and consequent dose rates by a factor of 20 to 200 may be expected from water flushing. Nevertheless, semi-remote operation of the ECM during the transient and for 24 h thereafter and numerous safety techniques (long handled pipe crimping/cutting tools, pre-designed quick disconnects, etc.) are planned to minimize personnel exposure during the disconnection/removal of the ECM and removal of the test assembly. Special design features and administrative procedures identified to date in this regard were presented in the preceding section.

4.1.2 Stack Releases of Radioactive Fission Products

Only stack release of the noble gases (Xe and Kr) and iodine are considered credible. The other released volatile elements (notably Te and Cs) will form species such as SnTe, CsI, and CsOH that will condense or chemisorb on the ECM components and/or dissolve in the liquid effluent, such that they will be contained in the test train, ECM, or the catch tank. It is probable that >99% of the iodine will similarly condense or absorb before reaching the stack filters. (Negligible iodine activity was found at the stack charcoal filters following the FLHT-4 test.) Nevertheless, 5% of the released iodine and 100% of the release Xe + Kr are assumed to reach the stack filters. The noble gases are assumed to pass through the stacks. The removal efficiency of the filters (HEPA + activated charcoal) for iodine is assumed to be 99.5%. Thus, the following stack releases are envisioned:

<u>Fission Product</u>	<u>Pre-Filter Quantity Available for Stack Releases</u>	<u>Stack Release</u>	<u>Derived Cumulative Weekly Limit for Stack Release</u>	<u>Stack Release of a Percentage of the Weekly Limit</u>
Noble Gases (units of Ci-MeV)	4,920	4,920	280,000	<2
Iodine (units of Curies of I-131 equivalent)	26.1	0.13	5.8	<3

In the above, the noble gases are limited on the basis of Ci-MeV (product of activity and gamma energy, summed over all the contributing isotopes). But the quantity "available for release" is judged as that at a 5-min delay from the release point to the site boundary dose point, recognizing that the transit time to and through the stacks is at least that long. The iodine is limited on the basis of I-131 curie equivalent, which is a weighted sum of the activities of the various iodine isotope activities. Based on the above, the estimated iodine release from the stack (by conservative estimates) is less than 3% of the weekly operating release limits and the estimated release of noble gases is less than 2% of the weekly limit.

4.2 REACTIVITY EFFECTS

The reactivity effects of voiding the (poison) light water from the bundle and bypass coolant regions and also the reactivity effects of a hypothesized axial relocation of fuel were calculated for the FLHT-1 experiment. These calculations were reviewed for FLHT-5 and found to be appropriate, conservative, and acceptable.

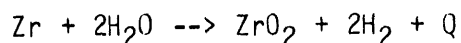
The CRNL staff calculate that complete voiding water from the bundle region increases the reactivity 0.71 mk and also increases the bundle power from 30 to 35 kW. Partial voiding of the bundle coolant is a planned part of the FLHT-5. Voiding of the bypass water increases the reactivity to 0.92 mk. The reactivity effect of the combination voiding of both bundle and bypass water is +1.66 mk. Measurements made during FLHT-2 indicate that this figure is actually less than 1.0 mk (with rod worth uncertainties accounted for).

The calculated reactivity effect of relocated fuel (described later) is +0.94 mk, and the total bundle power would increase slightly with relocation. These calculated reactivity changes are within the acceptable limit of +6.0 mk for the NRU Reactor; however, as mentioned earlier, the loss of bypass coolant is not an acceptable condition for continued operation because of the resulting damage due to the thermal loading on the shroud and reactor pressure tube.

4.3 HYDROGEN GENERATION

Hydrogen is one of the products of the FLHT-5 experiment. The measured generation rates during the course of the experiment are important data. The presence of hydrogen requires careful handling/processing because hydrogen/air mixtures can burn or explode. To prevent any hydrogen reactions (mainly with air), the hydrogen is diluted with nitrogen so that the hydrogen concentration is generally less than 4% (i.e., below the flammable limit). The attainable flow of nitrogen (4100 L/min) is capable of diluting hydrogen flows of 0.24 g/s (170 L/m) to less than 4%. The maximum predicted hydrogen rate during the course of the planned experiment is briefly 0.22 g/s (164 L/min), as shown in Appendix A, but quickly falls below 150 L/min.

Hydrogen is produced by the reaction of hot Zircaloy with steam. Zirconium, the main constituent in Zircaloy^(a), reacts with steam as follows:



where Q = the exothermic heat of reaction
= 143 kcal (598 kJ) per mole Zr
= 1555 cal (6506 kJ) per gram Zr
= 3972 cal (16.6 kJ) per gram H₂O
= 35.7 kcal (149 kJ) per gram H₂
= 3192 cal (13.4 kJ) per liter H₂.^(b)

(a) Zircaloy-4 contains 98.2% Zr, 1.5% Sn, 0.2% Fe, and 0.1% Cr.

(b) At 1 atm and room temperature.

The rate of hydrogen production depends on the surface area, temperature, and amounts of prior oxidation of the Zircaloy and available steam. The heat generation associated with the Zircaloy oxidation and hydrogen generation is addressed in Section 4.4. Plots of the predicted hydrogen production and the heat generation resulting from oxidation are shown in Appendix A.

The anticipated hydrogen flows for the FLHT-5 test are manageable from a safety standpoint. The corresponding released heat will drive the bundle temperatures above the cladding melt temperature (1970°C), but the bundle temperatures will remain below the UO₂ melting temperature (2790°C), as discussed in Section 4.4.

4.4 MATERIALS AT HIGH TEMPERATURE

The peak fuel bundle temperature estimated for the FLHT-5 experiment is 2600°C (4700°F), which is about 300°C (540°F) higher than the peak temperature attained in FLHT-4. Bundle region materials at high temperatures in contact with reactor components may cause damage. In this section, conditions are analyzed for the containment of bundle materials with temperatures as high as 2600°C. First, an analysis is presented that shows that the allowable heat flux through the Zircaloy inner and outer round (given bypass cooling) is much greater than the heat fluxes expected in FLHT-5. Next, effects of chemical power from the Zircaloy oxidation are presented to help quantify the experimental heat fluxes. Finally, the analysis in Appendix A is discussed to show that peak bundle temperatures are not expected to exceed 2600°C.

4.4.1 Heat Flux Through Inner and Outer Rounds

The primary pressure and molten material boundaries for these tests are the two shroud rounds; as long as they remain cool and intact, no hot materials containment problems will occur regardless of what happens inside the test train. The following analyses demonstrate that the inner and outer rounds will indeed be maintained cooled and intact. It is concluded that breach of the outer round is not possible. The shroud insulation, which may suffer minor cracking based on FLHT-2 examination, is not intended or needed as a safety feature. Rather, it is necessary to achieve the high temperatures desired for the fuel rods.

The inner and outer Zircaloy rounds are cooled by water flowing through the bypass annulus between the shroud and the reactor pressure tube. A flow of at least 1 kg/s (8000 lb/h) of water with an inlet temperature of less than 93°C (200°F) is planned. The mass flux, linear velocity, and heat transfer coefficients corresponding to this flow condition are 615 kg/s-m² (0.452 x 10⁶ lb/h-ft²), 0.7 m/s (2.3 ft/s) and (conservatively) 0.5 W/cm²-°C (875 Btu/h-ft²-°F).

The energy source to cause heating of the shroud rounds and the bypass coolant is the radial heat flow out through the shroud, driven by the temperature difference between the test assembly interior and bypass coolant. The peak magnitude of this heat flow rate was measured as 30 kW in FLHT-2. The measured heat flow rate into the bypass heat sink for FLHT-1 peaked at about 28 kW.

A maximum total-bundle radial heat flow of 50 kW was used to assess the cooling of the Zircaloy saddles and rounds for FLHT-4 (Lanning and Lombardo 1986). This represents a near steady-state condition at high oxidation rates, which is not anticipated to be achievable. The measured maximum heat flow for FLHT-4 was 40 kW. For the purpose of this analysis, a 57-kW total radial heat flow is taken from the in-house computer code output (Figure A.15). The 57-kW radial heat flow into the 1.0-kg/s bypass coolant will increase the coolant temperature by about 10°C (18°F) at the elevation of peak radial heat flow and by about 14°C (25°F) at the outlet. Assuming an inlet temperature of 93°C (200°F), the coolant outlet temperature and the peak outside shroud surface temperature are calculated to be about 107°C (224°F) and 145°C (293°F), respectively. Structural integrity of the Zircaloy tubes is expected at these low temperatures.

To provide an estimate of the safety margin, conditions required for bulk boiling at the bypass outlet were determined as shown in Table 4.2.

The conditions for bulk coolant outlet boiling should not be construed as safety limits. They are used to provide a convenient method of illustrating the safety margins in the radial heat sink. It can be seen that the margins are large.

TABLE 4.2. Bypass Coolant Margins (assuming 200°F inlet temperature) for Bulk Outlet Boiling

<u>Parameter</u>	<u>Required Change in Parameter to Cause Bulk Outlet Boiling</u>
Coolant flow	(divide by) 7.2
Radial heat flow	(multiply by) 7.2
Inlet temperature	(add) 87°C (156°F)

The peak temperatures of the inner and outer rounds of the shroud are of interest because excessive temperatures (>1000°C) would result in loss of strength. First, we note that pairs of TCs have been placed in the shroud saddles on 20 cm (8-in.) axial centers, beginning at the 345 cm (136-in.) elevation and extending down to the 20 cm (8-in.) elevation. These TCs are fed into the reactor trip circuit such that if three out of four adjacent TCs register above 982°C (1800°F) the reactor will trip and the test will terminate. Assuming that a steady-state heat flux causes this trip condition, it is possible to solve for that heat flow and then use the heat flow value to calculate inner- and outer-round temperatures corresponding to the saddle-trip condition.

The gross thermal resistance from saddle-to-coolant in the FLHT shroud has been established as 13.3°C/kW/m in previous tests. Since the coolant temperature at position of peak heat flux would be approximately 93 + 10 = 103°C, the heat flow required for saddle trip would be: $(982 - 103)/13.3 = 66 \text{ kW/m}$.

For that heat flow, the shroud inner and outer round temperatures calculate to be 367 (693°F) and 148°C (298°F), respectively. The rounds will maintain most of their room-temperature strength at these low temperatures.

For a more realistic estimate of maximum radial heat flow, we must turn to in-house code calculations (and compare to FLHT-4 data to see if such calculations are reliable). Calculated values for FLHT-4 peak saddle temperatures compared well with measured values of less than 650°C (1200°F). Assuming these

are near steady-state temperature values^(a), we can back-calculate the peak local heat flow: $(650 - 103)/13.3 = 41$ kW/m. This value compares favorably with the code-calculated value of 38 kW/m. Therefore, the code-calculated peak FLHT-5 radial heat flow (48 kW/m) is accepted as best-estimate (see Figure A.14).

Based on the maximum value of radial heat flow of 48 kW, margins for local boiling and dryout can be calculated. The results are given in Table 4.3. It can be seen that the margins are large.

4.4.2 Consequence of Loss of Shroud Insulation (and UO₂ Melt Temperatures)

The radial heat flow through the shroud as a function of insulation thickness was also examined. The following assumptions were used:

- High-temperature oxidation is at steady state with respect to the insulation (a very conservative assumption, based on FLHT-2/FLHT-4 experience).
- The inner surface temperature of the insulation is 2760°C (5000°F).
- Bypass coolant temperature is 103°C (218°F).
- The thermal resistance (R_{SC}) from the saddle to the coolant is derived from FLHT-1 data (13.3°C/kW/m) and confirmed by the FLHT-4 data.

TABLE 4.3. Margins for Local Boiling and for Dryout in the Bypass at 48 kW Radial Heat Flow

Parameter	Required change in Parameter to Cause:	
	Local Boiling	Dryout
Coolant flow	(divide by) 3.4	--
Radial heat flow	(multiply by) 2.6	7.0
Inlet Temperature	(add) 59°C (106°F)	--

(a) The lumped-parameter time constant for materials outboard from the saddles is less than 50 s. The duration of the saddle temperature transients (~250 s) implies that steady state is achieved in the outer shroud. (But it is not achieved within the insulation, which has an effective time constant of ~300 s.)

The temperatures and heat flows can be related by the equations

$$T_s - T_o = R_{sc} Q$$

and

$$\int_{T_s}^{T_I} k_{ZrO_2} dT = \frac{Q \ln(b/a)}{2\pi}$$

where a,b = shroud insulation inner/outer radii (1.04/1.44 in. or 2.64/3.66 cm)

$$\begin{aligned} k_{ZrO_2} &= \text{shroud insulation conductivity (in kW/m}\cdot\text{K)} \\ &= 0.204 \times 10^{-3} + 1.49 \times 10^{-7} T(\text{K}), \text{ (Based on laboratory measurements to 1900 K)} \\ &= 0.502 \times 10^{-3} * \left[\frac{T(\text{K})}{2000} \right]^3, T > 2000 \text{ K} \end{aligned}$$

and Q = radial heat flow (kW/m)

R_{sc} = thermal resistance from saddle-to-coolant (13.3°C/kW/m)

T_s = the saddle temperature (K)

T_I = inner insulation surface temperature (5000°F, 3033 K)

T_o = local coolant temperature (103°C, 376 K)

k_{ZrO_2} = shroud insulation thermal conductivity.

The heat flow was then calculated assuming that through any means whatsoever^(a) the inner surface of the insulation was maintained at 2760°C (5000°F) (UO₂ melting). The calculation was repeated for various insulation thicknesses. The results show a heat flow of approximately 30 kW/m (9 kW/ft) with the full thickness of insulation and an increasing heat flow as the insulation

(a) The "means" to attain UO₂ melting temperature across the entire bundle cross section involve peak-flux nuclear heating (26 kW/m) plus significant oxidation heating of a coherent debris bed. With full insulation thickness, 30-26=4 kW/m of oxidation power is required, which is credible. With no insulation, 200-26=174 kW/m is required, which is totally incredible.

is removed. A maximum of 200 kW/m (61 kW/ft) is calculated for the bounding case of no insulation remaining. The heat flux at the outer shroud surface, even for the case of no insulation, is not large--only 697 kW/m² (0.221 x 10⁶ Btu/h-ft²). This heat flux will cause local boiling, but is far from that required for dryout.

There is significant conservatism in the calculation leading to these results. The calculations assume that the inner insulation surface remains at 2760°C (5000°F) and does so long enough to reach steady state; in any real case, it would not. For significant insulation losses, the large heat loss would cause the temperatures of the material producing the 2760°C to decrease.

The saddle and inner Zircaloy round temperatures were also calculated for the heat fluxes arising from loss of insulation. At the point of trip for saddle temperature (55% insulation loss), the inner round temperature would reach only 368°C, a temperature at which the inner round would retain most of its room temperature strength. The outer round would be at a temperature of 147°C, which is also quite low.

These discussions indicate that, even based on the calculated inner tube temperatures, there are large safety margins for shroud temperatures. The outside Zircaloy tube will be even cooler and will provide another stronger barrier.

It must be emphasized that safety of the test requires that the rounds of the shroud MMPD, particularly the outer one, be maintained cooled. The cooling is controlled by the flow rate and inlet temperature of the bypass coolant and by the radial heat flow. It is insensitive to conditions inside the test assembly (nominal operation, debris bed, loss of bundle coolant, loss of insulation, or anything else) except as these phenomena affect the stress and the radial heat flow. Adequate cooling can be easily maintained by providing sufficiently subcooled inlet temperatures and sufficiently high flow rates for the bypass. The ability to provide these conditions is easily within the capabilities of the NRU reactor loop coolant systems.

Bypass coolant is required to prevent damage to the two shroud rounds and the reactor pressure tube that may be caused by high-temperature materials.

Loss of bypass coolant flow could create a hazardous condition. An analysis of the loss of bypass coolant and other safety concerns is presented in Section 5.0 (Safety Concerns During Accidents).

The course of the peak cladding temperature is illustrated in Figure A.11. The peak temperature goes through a series of oscillations with successive peaks at different axial nodes. The maximum peak cladding temperatures presented in Figure A.11 are felt to be slightly overpredicted because they are commensurate with complete oxidation of the cladding, whereas in reality some liquified Zircaloy may run downward from a given axial region prior to complete oxidation. Peak cladding temperatures calculated for FLHT-5 by the SCDAP-18 code, which includes the above effect, do not exceed 2610°C (4700°F).

Corrective actions will be taken if it is determined (by the test director) that bundle temperatures have exceeded 2600°C. Based on FLHT-4 experience, we anticipate that liner TCs will survive and will signal any change from predictions that could lead to temperatures in excess of 2600°C.

4.5 ANALYSIS OF STEAM EXPLOSION AND STEAM PRESSURE PULSES

The following paragraphs summarize work performed for PNL by Dr. Cronenberg of Engineering Science and Analysis. Three possible sources of overpressurization resulting from the interaction of hot material with water were analyzed:

- Energetic and extremely rapid thermal interactions between molten fuel rod debris and water, leading to shock pressurization above the reactor pressure tube dynamic pressure limit (called a steam explosion).
- Milder debris/water thermal interactions where slow overpressurization may result as a consequence of an overly constricted off-gassing system, with pressurization beyond the pressure tube static pressure limit (called a steam spike).
- Energetic oxidation of molten Zircaloy by water, which can lead to a shockwave or pressure spiking conditions depending on the configuration of the Zr-melt/water reaction mixture (called an energetic chemical reaction).

Pressure increases from any of these three sources, if of sufficient magnitude, would result in potential failure of the shroud rounds and the reactor pressure tube. The results of these analyses show that no such damaging pressures are expected.

For each class of interaction, the "necessary" conditions for inducement of debris/coolant interactions are evaluated in the context of the FLHT-5 test conditions, and conclusions are drawn. The updated analyses for FLHT-5 are presented in Appendix C.

4.6 UNCERTAINTIES ASSOCIATED WITH NORMAL EXPERIMENT OPERATION

The actual fission product inventory as a function of time depends on the specific FLHT-5 bundle power history. The calculational uncertainty is much less than $\pm 10\%$. Even if the actual inventory were greater, the hazards associated with radioactive fission products would not increase significantly.

The predicted radiation fields near the ECM are marginally higher for FLHT-5 than they were for FLHT-4. Actual fields during and after the test will in any case be monitored remotely and then mapped before personnel access is permitted around the ECM.

An example of the calculated radiation field as a result of fission product deposition in the ECM as a function of time after the test was shown in Figures 4.1, 4.2, and 4.3. The estimated uncertainty of these calculations is \pm a factor of five.

The accuracy of reactivity calculations for tests in the NRU Reactor for a fixed reactor loading is probably within $\pm 10\%$. Some uncertainty in the calculations occurs because the loading is not known until very near the test date. Greater uncertainty is associated with the configuration of the fuel bundle once fuel movement is possible.

The potential for fuel movement is greatest once bundle temperatures are high enough to melt the cladding. If the molten cladding should flow away from the pellets (which subsequently oxidizes), the pellet columns could "collapse" into a pile of rubble. If the molten Zircaloy flows down the pellet surfaces,

UO₂ is dissolved, thus relocating into coherent debris. The amount of dissolution, the rate of downward flow, and the location, size, and shape of the solidified debris are also uncertain, thus introducing uncertainties into the reactivity calculations. For this safety analysis, conservative values were assumed to maximize the possible reactivity effects. The results are quite acceptable from a reactor safety viewpoint.

The predictions of the hydrogen generation rate, the hydrogen flow rate, and the total hydrogen production are based on the following assumptions:

- the Zircaloy temperatures are known
- the Zircaloy oxidation rates as a function of time and temperature are known
- the local hydrogen concentration is a function only of the hydrogen generation rate (no hydrogen concentration occurs in the effluent system).

To ensure that combustible mixtures of hydrogen do not occur during and right after the test, the nitrogen dilution rate was set based on the predicted peak hydrogen generation rate.

Well before the initiation of the buildown transient, a limited flow of dilution gas will be sweeping air out of the gas flow path. Near the end of the test (last 30 min), the gas mixture will essentially consist of nitrogen and hydrogen. Even during the test period when the peak hydrogen generation occurs, the gas mixture downstream the ECM will be diluted to 4% hydrogen. This mixture is not flammable regardless of the amount of air in the system. No such air leakage is expected.

Many factors contribute to the uncertainty associated with predicting FLHT-5 temperatures. In determining the temperature distribution within the bundle and shroud regions, the greatest uncertainty lies in predicting the local peak cladding temperatures of the test fuel rods, due primarily to the uncertainty in predicting the chemical power and the combined convective and radiative heat transfer from the oxidizing cladding. However, the experience gained in the FLHT-4 test has reduced the uncertainty in the initial high-temperature phase of the FLHT-5 test. Much less uncertainty is associated with

predicting temperatures in the exterior of the shroud, specifically those of the inner and outer Zircaloy tubes, because of the low temperatures, the absence of the metal-water reaction, and the conduction-only heat transfer. Estimates of the uncertainty in the predicted maximum inner and outer round temperatures are $+0^{\circ}\text{C}$, -100°C for FLHT-5. The uncertainty in the temperatures is due primarily to the uncertainty in the shroud resistance and the actual peak heat flow. The safety of the test depends on maintaining the rounds at low temperature, and these temperatures can be accurately predicted ($\pm 20^{\circ}\text{C}$). Thus, the uncertainty associated with the bundle temperature predictions is not a safety issue, provided adequate margins exist for radial heat removal.

Thermal analysis based on the in-house code has uncertainties due to code limitations like node size, material properties, extent of material movement, and modeling of local steam starvation.

Quantification of the effects of these uncertainties is not possible. In fact, the test is being performed in part to supply this information. The arguments presented in this section point out that the effects are not large. In any case, the discussion concerning bypass cooling shows that the shroud rounds more than adequately protect against these concerns.

A trip based on saddle temperatures gives a huge conservatism relative to probable failure of the shroud to contain the high temperature and radioactive products of the test. The heat flow required to trip the reactor on high saddle temperature is 66 kW/m. This is far less than the 340 kW/m required for dryout of the outer round, and less than the 200 kW/m required to keep molten UO_2 at the saddle inner surface.

It is also concluded that an increase in the radial heat flow will cause the saddle TCs to reach their trip temperatures but that the outer round temperature would be no more than 148°C (300°F) and the inner round temperature would be no more than 370°C (700°F). These temperatures are the results of increased radial heat flow rates and are independent of the cause of the increase.

5.0 SAFETY CONCERNS DURING ACCIDENTS

Several specific, unexpected, potentially unsafe conditions could occur during the FLHT-5 experiment. These unplanned events raise safety concerns mainly about test hardware integrity and performance should any of these events occur. The following areas are addressed in this section:

- loss of bypass coolant flow
- loss of bundle pressure
- ECM pipe rupture
- loss of all power.

5.1 LOSS OF BYPASS COOLANT FLOW

The integrity of the two Zircaloy tubes of the shroud must be maintained to retain the hazardous products of the test. This requirement is easily achieved if the tubes remain cool. A continuous flow of bypass coolant is therefore essential for the safe operation of the FLHT-5 test. High and low bypass coolant flow reactor trips are provided to protect against a loss of coolant flow. The information given earlier confirms a large flow-safety margin. A reactor trip will be set at a flow of about 75% of normal. The results of calculations show that a flow reduction to 30% of normal would be necessary to cause bulk boiling of the bypass coolant, which in itself is a conservative definition of a hazardous condition. There is ample margin and ample time in the loop operation to manually trip the reactor if a low-flow condition should occur. That action will terminate the steaming in the test section and thus almost instantly terminate the oxidation reaction.

Even though the reactor trips automatically on a high/low bypass flow signal, it is important that at least stagnant water be maintained in the bypass annulus tube. Calculations indicate that vaporization of only about 7 kg (15 lb) of stagnant bypass coolant would remove the stored energy in the fuel rods, the insulation, and the shroud components if the loss of bypass flow occurred when the peak temperature was 2600°C (4800°F).

A question has been raised concerning the need to remove heat above that of the stored energy if debris should fall into the water pool at the time of

the trip. Calculations were therefore made starting with a debris defined by Cronenberg. A mass of coherent (molten) debris of 2844 g (6.3 lb) with a temperature of 2130°C (3861°F) and a heat capacity of 394 J/kg-K (0.094 Btu/lb-°F) could fall into the pool.

The assumption was made that all the energy of the debris vaporized water from the pool. Further conservative assumptions were made that all of the steam reacted with Zircaloy and all of the energy released passed into the bypass. The calculations show that 0.9 kg (1.98 lb) of water would vaporize from the pool and 14.6 MJ (13,890 Btu) would be generated when the vapor reacted with Zircaloy. Putting this much heat into the bypass annulus would vaporize an additional 6 kg (13 lb) of coolant to give a total of 13 kg (29 lb). Because there is about 20 kg (44 lb) of water in the bypass annulus above the test assembly, about 50% more water is available than is necessary to remove even this conservatively calculated amount of heat. Therefore, this scenario, unlikely as it is, would not result in overheating of the shroud outer and inner rounds.

5.2 LOSS OF BUNDLE PRESSURE

The consequences of a loss of fuel bundle pressure would depend on the scenario by which the pressure loss occurred. If such a loss occurred, the reactor would automatically trip on low system pressure sensed in the ECM (Table 7). Should the loss of pressure be due to a failure of the bundle inlet tubing, the small amount of coolant water in the bundle would be discharged into the upper service space or ECM secondary containment system and be replaced by nitrogen from the ECM. The test fuel would then be slowly cooled to the bypass coolant system temperature. Any escaping fission products would be drawn into the ECM. The charcoal absorber in the ECM ventilation system would retain at least 99% of the radioiodines, resulting in only a small release to the reactor stack.

If a sudden loss of pressure occurred, reduction of the system pressure from 1.38 to 0.1 MPa (200 to 14.7 psia) would result in approximately 18% of the water below the liquid-steam interface flashing to steam. The time taken

to flash would depend on the nature of the failure and the time taken to reach atmospheric pressure. The increased steam production could conceivably increase the Zircaloy-steam reaction temporarily. Calculations were performed to provide information concerning the possible magnitude of the increased chemical reaction.

First, if the loss of pressure were sudden, the steam in the test assembly would undergo a nearly isentropic expansion. The temperature would drop by about 350°C (660°F), which would inhibit the degree of the Zircaloy/steam reaction. Moreover, a sudden drop in the test assembly pressure implies removal of most of the gaseous contents. In other words, in this case the steam flashed from the pool would almost instantaneously be swept from the test assembly and would not react.

However, if the conservative assumption is made that all the steam reacts (e.g., during a pressure loss at the end of the test when cladding temperatures are highest), less than 0.32 kg (0.7 lb) of steam would react. Its reaction would release 5.35 MJ (5080 Btu). Instantaneously placing this much heat into the assembly above the water level would raise the average assembly temperature by less than 260°C (460°F).

5.3 ECM PIPING RUPTURE

Fission products that are released from ruptured FLHT-5 fuel rods will flow through the effluent piping to the ECM from the test train head closure. A postulated rupture of that pipe could release fission products to the reactor building.

Rupture of the effluent pipe is extremely unlikely. The stainless steel tubing that connects the ECM to the test train head closure and other ECM components is designed for a pressure rating of 2.41 MPa (350 psia), which is 75% greater than the planned operating pressure of 1.28 MPa (185 psig). In addition, the ECM is anchored to the NRU deck with seismic anchors designed to withstand a 0.25-g horizontal load, precluding rupture of outlet piping due to unplanned ECM movement. The piping is also protected by 10-cm (4-in.)-thick lead shielding and a 3.2-mm (0.125-in.)-thick sheet steel cubicle, which

provide protection from a seismic event and falling objects. Further, the piping will be leak tested during commissioning. No credible failure mechanism is foreseen.

The same 3.2-mm (0.125-in.) thick sheet steel cubicle prevents any secondary leakage and directs liquid, gas, or vapor to the NRU radioactive waste disposal systems. A double-ended rupture of the effluent pipe was analyzed to estimate the maximum discharge flow rate. About 86 g/s (0.19 lbm/s) of steam/H₂ could be released from the ECM, and about 149 g/s (0.33 lbm/s) could be released from the test train outlet. Both flow rates decrease as the system depressurizes through the rupture pipe and the NRU reactor would be tripped by the effluent low-pressure sensor. The reactor building ventilation and exhaust system is designed to process any accidentally released vapor or gas from the ECM and upper service space through the activated charcoal filter system and dispose of it through the plant stack. There is a liquid sensor on the floor of the ECM. Any leaking liquids would be piped directly to the loop catch tanks after the test.

5.4 LOSS OF ALL POWER

During the course of the FLHT-5 experiment, it is possible that all off-site power to the NRU facility could be lost. The worst possible time for that to occur would be at the completion of the transient when fuel cladding temperatures are still very high. The NRU Reactor would be tripped by the loss of power, but the energy stored in the fuel bundle and test train would have to be dissipated without endangering NRU operating limits.

The analysis of this accident assumed that a 95°C (200°F) overshoot resulted after the NRU Reactor was tripped and that a temperature distribution with a peak at 1980°C (3600°F) was used to initiate the calculations. The enthalpy was calculated for each of 11 axial segments using the saturation temperature--194°C (382°F)--of the bypass coolant as the base. The total stored energy included contributions from the fuel bundle and shroud. Dividing the total stored energy by the latent heat of vaporization gives an estimate of the water mass that must be boiled away to remove the stored

energy. Less than 5 kg (11.3 lbm) of water is required, which is about 25% of that in the bypass region above the fueled core region. The stored energy of a core debris bed was also estimated to be about 10% greater than that of a structured fuel bundle. However, much more water is available around and above the test train than is needed to dissipate the stored energy.

Whether the fuel rod bundle is structured or a debris bed, the maximum stored energy in the FLHT-5 test assembly will be easily converted into a small fraction of the bypass coolant vaporization. The temperature of the shroud exterior and the pressure tube will also remain below the bypass coolant saturation temperature. Loss of all power is not a significant safety hazard.

The foregoing examples serve to illustrate that, even if unlikely off-normal events do occur, the design features of the reactor, loop system, test train, and ECM mitigate possible consequences to the facility, its personnel, and the public.

6.0 REFERENCES

Cain, V. R. 1977. A User's Manual for QAD-CG, the Combinatorial Geometry Version of the QAD-PSA Point Kernel Shielding Code. NE-007, Bechtel Power Corporation, Gaithersburg, Maryland.

Lanning, D. D., and N. J. Lombardo. 1986. Final Safety Analysis for FLHT-4 Experiment. PNL-5869 published in September 1993, Pacific Northwest Laboratory, Richland, Washington.

Walker, W. H. 1975. FISPROD-2 an Improved Fission Product Accumulation Program. AECL-5105, Atomic Energy of Canada Limited, Chalk River, Ontario.

APPENDIX A

IN-HOUSE CODE AND SCDAP CODE POST-TEST CALCULATIONS FOR
FLHT-4 AND PRETEST CALCULATIONS FOR FLHT-5

APPENDIX A

IN-HOUSE CODE AND SCDAP POST-TEST CALCULATIONS FOR FLHT-4 AND PRETEST CALCULATIONS FOR FLHT-5

Both the in-house code and the SCDAP code have been used to make predictions of cladding/shroud temperatures bundle oxidation/hydrogen generation rates and shroud heat flows for FLHT-5. Before making the FLHT-5 predictions, post-test FLHT-4 simulations were made with both codes and compared with measured values of temperature and hydrogen flow. Alterations in SCDAP input techniques that were made as a consequence of this exercise improved the code/data comparison. The results of the FLHT-4 code/data comparison are presented first, followed by the FLHT-5 predictions. Based on the code/data comparisons, the in-house code predictions for FLHT-5 are considered the more appropriate for safety analysis purposes, because the code (in the 7-node configuration) appears to yield best-estimate to slightly conservative code results with respect to parameters of major interest for safety analysis.

COMPARISONS SCDAP AND IN-HOUSE CODE CALCULATIONS TO FLHT-4 DATA

The in-house predictions presented here come from a simulation that presumes a heatup to a steady state at 75 lb/h inlet flow and 26 kW bundle nuclear power before flow reduction to a constant 10 lb/h at time = 0. The nuclear power increases to 30 kW as the water boils down. The SCDAP run assumes steady state at ~480 K and 23 kW constant bundle nuclear power before flow reduction, and the subsequent flow is taken as the fluctuating flow rate measured during the test. These differences explain some of the differences in the predicted results.

Bundle Oxidation Heat Generation Rate and Hydrogen Production Rate

The bundle exit hydrogen flow rate was assessed with three different measurement instruments: a noncondensable gas flowmeter, a palladium partial pressure meter, and a Beckman thermal conductivity meter. The noncondensable flowmeter data is currently considered the most reliable, especially with respect to flow rate, and hence, production rate. The bundle oxidation heat generation

(in kW) is taken to be proportional to the hydrogen production rate (in R.T. L/min) with the proportionality being 0.208 kW per R.T. L/min. Figure A.1 shows measured hydrogen flow rate and calculated hydrogen production rates for FLHT-4. Note that the in-house and SCDAP curves both agree fairly well with the data initially; the in-house curve does not follow the fluctuations in hydrogen production as does SCDAP simply because in-house code input does not follow the coolant inlet flow fluctuations, whereas SCDAP input does. SCDAP, however, predicts progressively less vigorous oxidation as the oxidation front moves up the assembly; whereas the in-house code (and the data) indicate full vigor to the end of the test. This dynamic effect is probably related to the rate and extent of the liner Zircaloy oxidation, as discussed below.

The corresponding bundle oxidation power is shown in Figure A.2. Clearly, local Zircaloy metal temperature, oxide thickness, oxidation rate, and heat generation and heat flow are all synergistically interrelated; and it is difficult to determine whether SCDAP is drifting away from the data because of 1) modeling deficiencies in first principal matters such as oxidation rate, heat flow, etc.; 2) input deficiencies such as axial node size; or 3) test data/measurement difficulties that relate to inlet flow, pressure control, etc., and do not relate to the code except in the choice of input.

Peak Cladding Temperature

In any case, although the in-house code, SCDAP, and the data diverge on the timing and vigor of the oxidation, there appears to be good agreement on the peak cladding temperature and the general progression of accelerated oxidation and high cladding temperatures within the assembly. Consider first the data for cladding and saddle temperatures (Figures A.3 and A.4, respectively). The cladding temperatures appear to reach peak temperatures near 2300°C (4200°F, 2573 K), based on a study of the liner temperatures. The saddle TCs that survived the test indicate a rapid downward burn from Levels 104 through 64, followed by a much slower upward burn throughout the rest of the test (see Figure A.4). Both SCDAP (Figure A.5) and the in-house code (Figure A.6) predict this same pattern. A specific comparison of the two codes against cladding temperature data at bundle midplane is given in Figure A.7.

Again, neither code matches the timing for the temperature rise at this elevation, but both predict the peak temperature within 100 K.

Total Bundle Oxidation/Hydrogen Production

It is in the matter of liner oxidation that the two codes diverge the most, with hydrogen data from FLHT-4 data favoring the in-house predictions. This is made clear from Table A.1. The discrepancy in liner oxidation leads to a discrepancy in total predicted hydrogen produced, as noted above.

TABLE A.1. Code/Data-Comparisons of Bundle Oxidation for FLHT-4

Comparison Item	FLHT-4 Data (Deduced from Total Hydrogen Production)	Code Predictions	
		In-House Code	SCDAP
Fraction of total bundle Zircaloy oxidized, %	45 to 61	63	44
Fraction of exposed bundle Zircaloy oxidized, % (75% of length above water)	>81(a) } 81 avg	84 } 84 avg	75 } 56 avg
Fraction of exposed liner + carriers oxidized (ignoring steel and Inconel)	<81(a) }	~84 }	38 }
Total hydrogen produced, R. T. liters	2100 to 3200 (best est. = 2600-2900)	3000	2100

(a) Assuming the highest value (61%) for oxidation of total bundle Zircaloy.

FLHT-5 PRETEST PREDICTIONS

The same basic differences regarding input were carried on to FLHT-5 predictions with the two codes; i.e., the in-house run assumes a steady state at 75 lb/h before flow reduction to a constant 10 lb/h, and SCDAP assumes a steady state at 480 K before flow reduction and fluctuating flow (8 to 12 lb/h) as encountered in FLHT-4. However, the boildown and steaming rates from the

in-house code were input to SCDAP for the first 1000 s, leading to similarity in the results from the two code throughout the first 1500 s. The in-house projection for boildown was considered more reliable than that of SCDAP, based on prior experience. In the in-house code, 30 kW bundle nuclear power was the initial value, which increased to 34 kW as the bundle voided. In SCDAP, a constant 30 kW was input for one run and 38 kW for a second run.

Bundle Oxidation Heat Generation and Hydrogen Production Rates

The projected bundle hydrogen production rates are shown in Figure A.8. As a consequence of the coordinated steaming rate inputs, the code projections follow each other closely out to ~1500 s; then they diverge, with SCDAP having the lower values, as with the FLHT-4 predictions. The divergence is related to the extent of liner oxidation and results in a divergence in the estimate of total hydrogen produced. The corresponding bundle oxidation heat generation curves are shown in Figure A.9.

Peak Cladding Temperature

As with FLHT-4 predictions, the divergence in predicted oxidation vigor and extent does not prevent semi-quantitative code-to-code agreement with respect to the timing and axial location of accelerated oxidation and high cladding temperatures within the assembly. As before, both codes predict a downward burn followed by a slow upward burn (Figures A.10 and A.11). A direct comparison between the two codes (for bundle midplane cladding temperatures) is shown in Figure A.12. Note that the in-house code displays a cooldown pattern that is more consistent with the data; the SCDAP cooldown is more extended.

Peak Saddle Temperatures and Radial Heat Flow

The in-house code was reasonably successful in predicting bypass power and shroud peaks saddle temperatures for FLHT-4, indicating that its radial heat flow predictions are reasonable. The predicted saddle temperatures, local (nodal) radial heat flow to the bypass, and total bundle heat flow to the bypass for FLHT-5 are shown in Figures A.13, 14, and 15 respectively.

Total Oxidation and Hydrogen Production

As with FLHT-4 predictions, the two codes yield divergent results on the extent of liner oxidation, which relates to a divergence in total hydrogen production, as shown in Table A.2.

TABLE A.2. Predicted Bundle Oxidation and Hydrogen Production for FLHT-5

<u>Comparison Item</u>	<u>Units</u>	<u>FLHT-5 Predictions</u>		
		<u>SCDAP^(a)</u>	<u>In-House Code</u>	<u>SCDAP^(b)</u>
Peak cladding temperature	°C	2610	2600	2620
Peak bundle oxidation power	kW	28	34	36
Peak hydrogen production rate	R.T. L/min	135	164	174
Total hydrogen produced	R.T. liters	2300	3600	2200
Fraction of total bundle Zircaloy oxidized	%	49	75	47
Fraction of exposed bundle Zircaloy oxidized (80% above the water)	%	89	94	35
Fraction of exposed liner oxidized	%	27	94	23

(a) Run 11/23/86: 10 axial nodes; steaming rate input from in-house run; 5 dummy rods; 30 kW bundle power.

(b) Run 1/1/87: 10 axial nodes; steaming rate input from in-house run; 5 dummy rods; 38 kW bundle power.

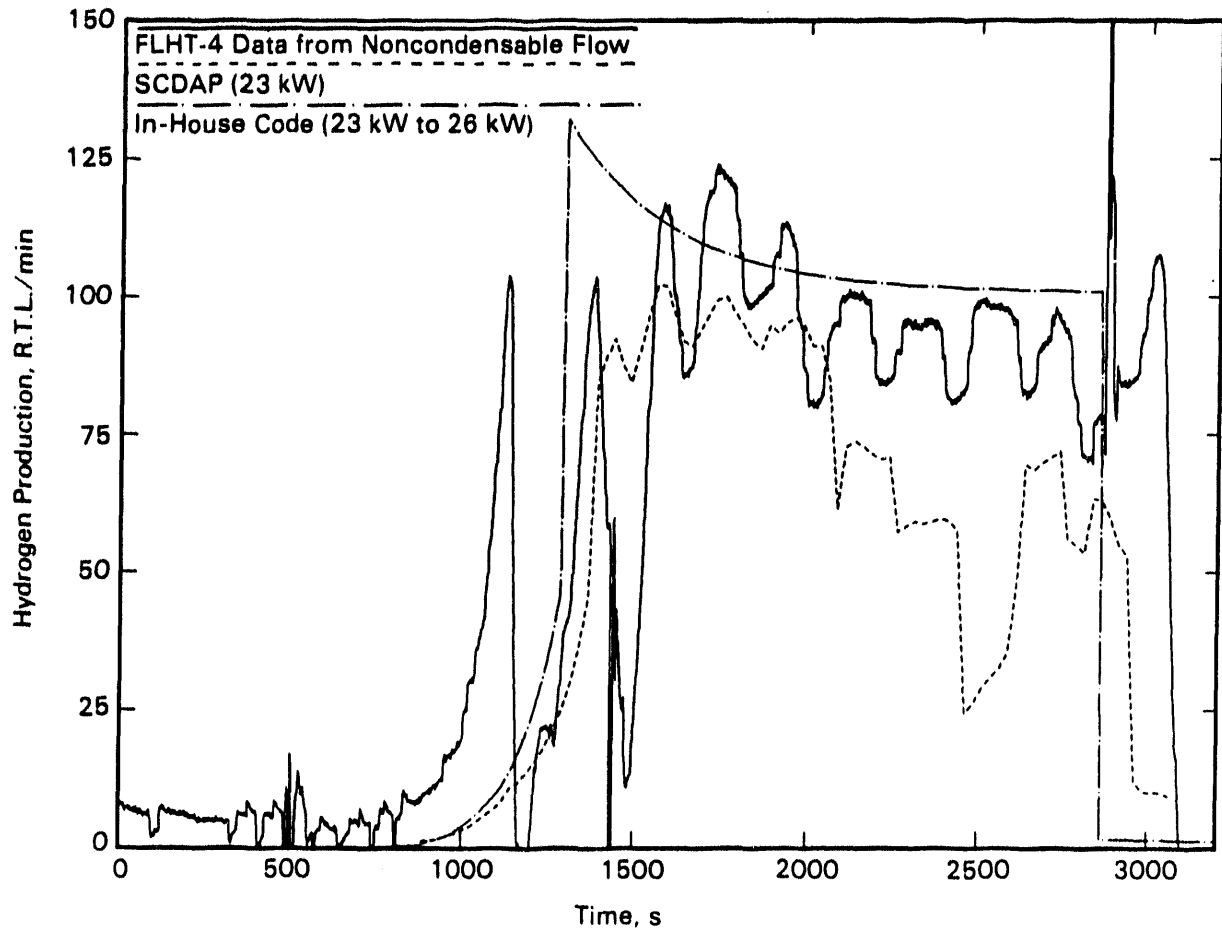


FIGURE A.1. FLHT-4 Hydrogen Generation Rate Data Compared with SCDAP and In-House Calculations (note flow reduction occurs at approximately 500 s)

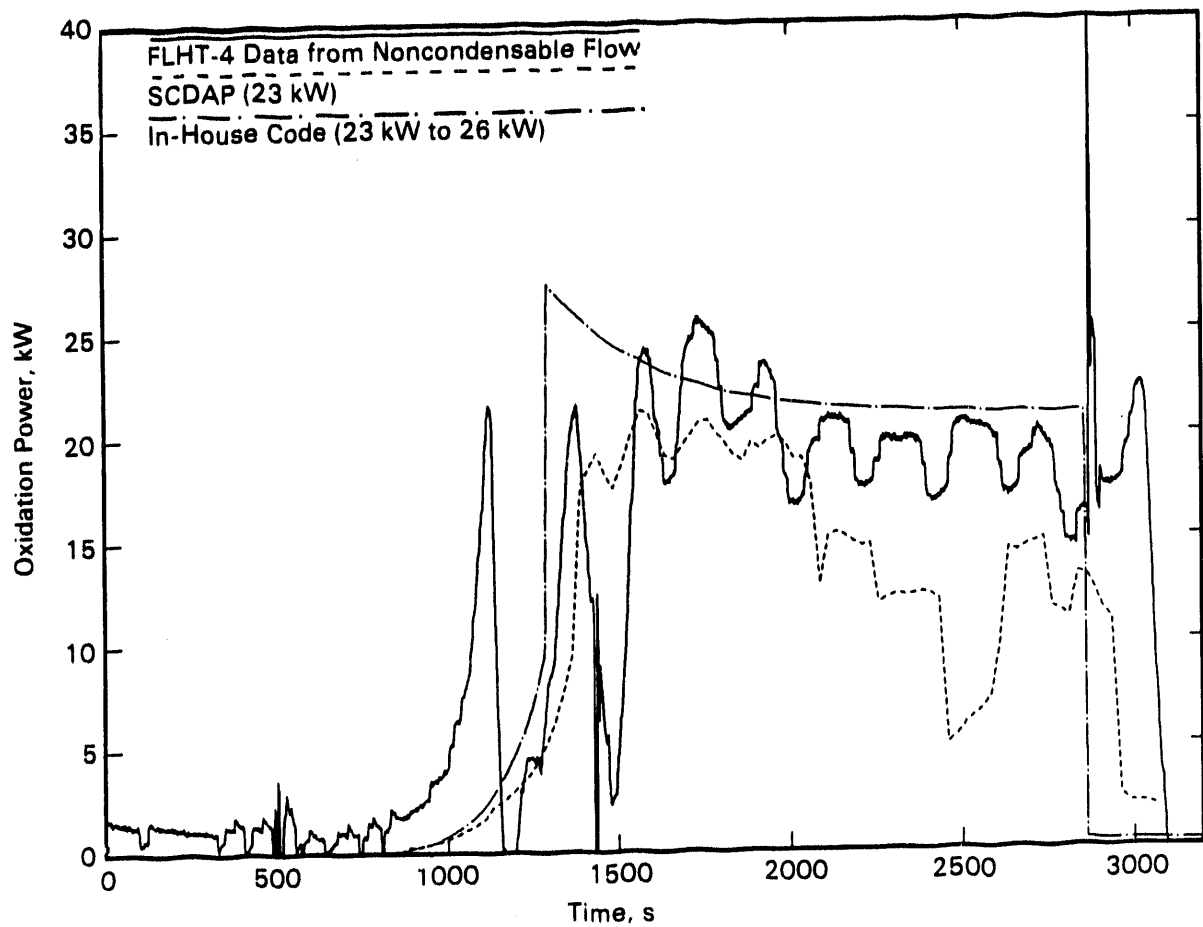


FIGURE A.2. Calculated Bundle Oxidation Heat Generation Rate for FLHT-4, Compared to Values Derived from Hydrogen Flow Measurements

A.8

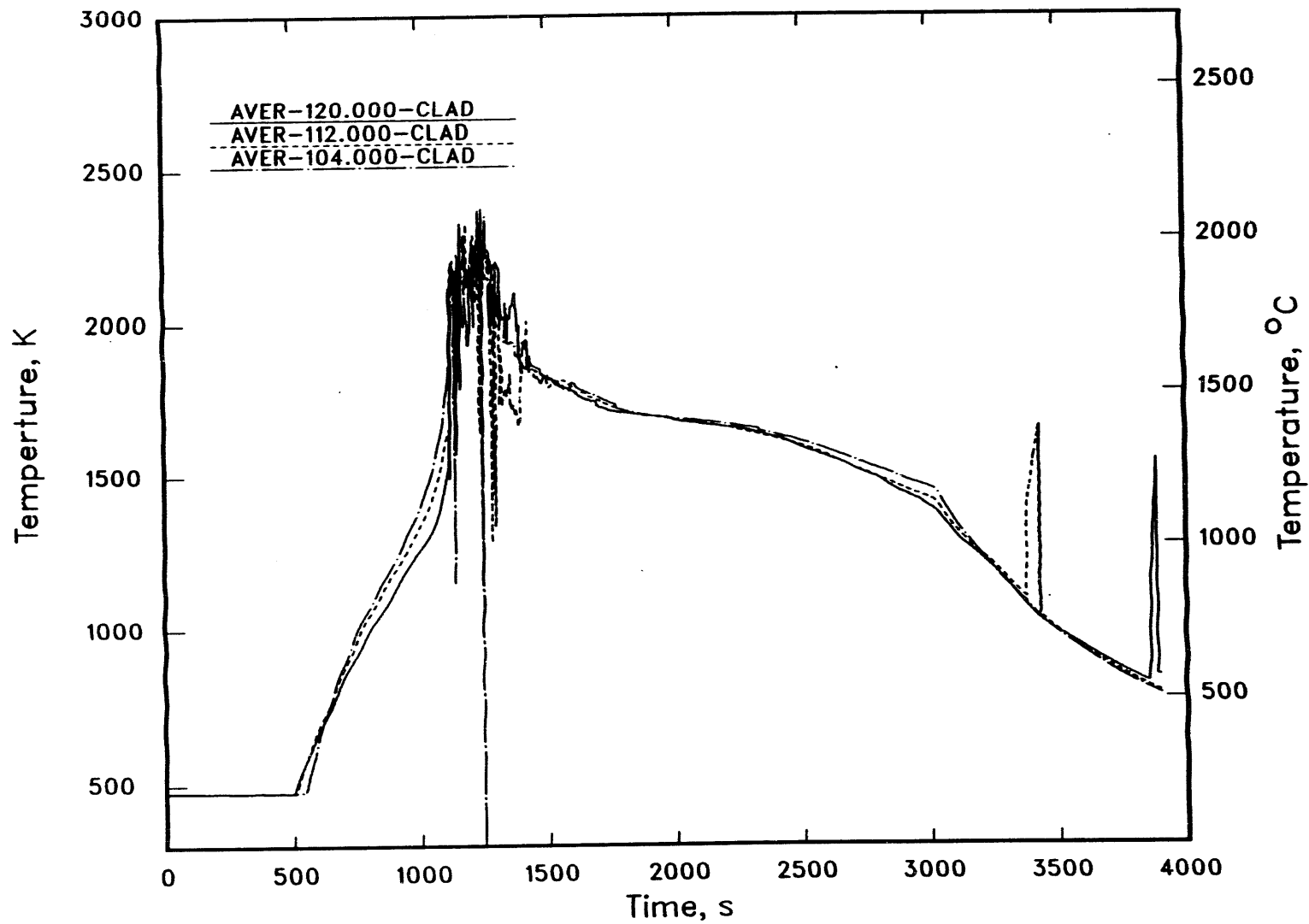


FIGURE A.3. Typical Cladding Thermocouple Readings from FLHT-4

A.9

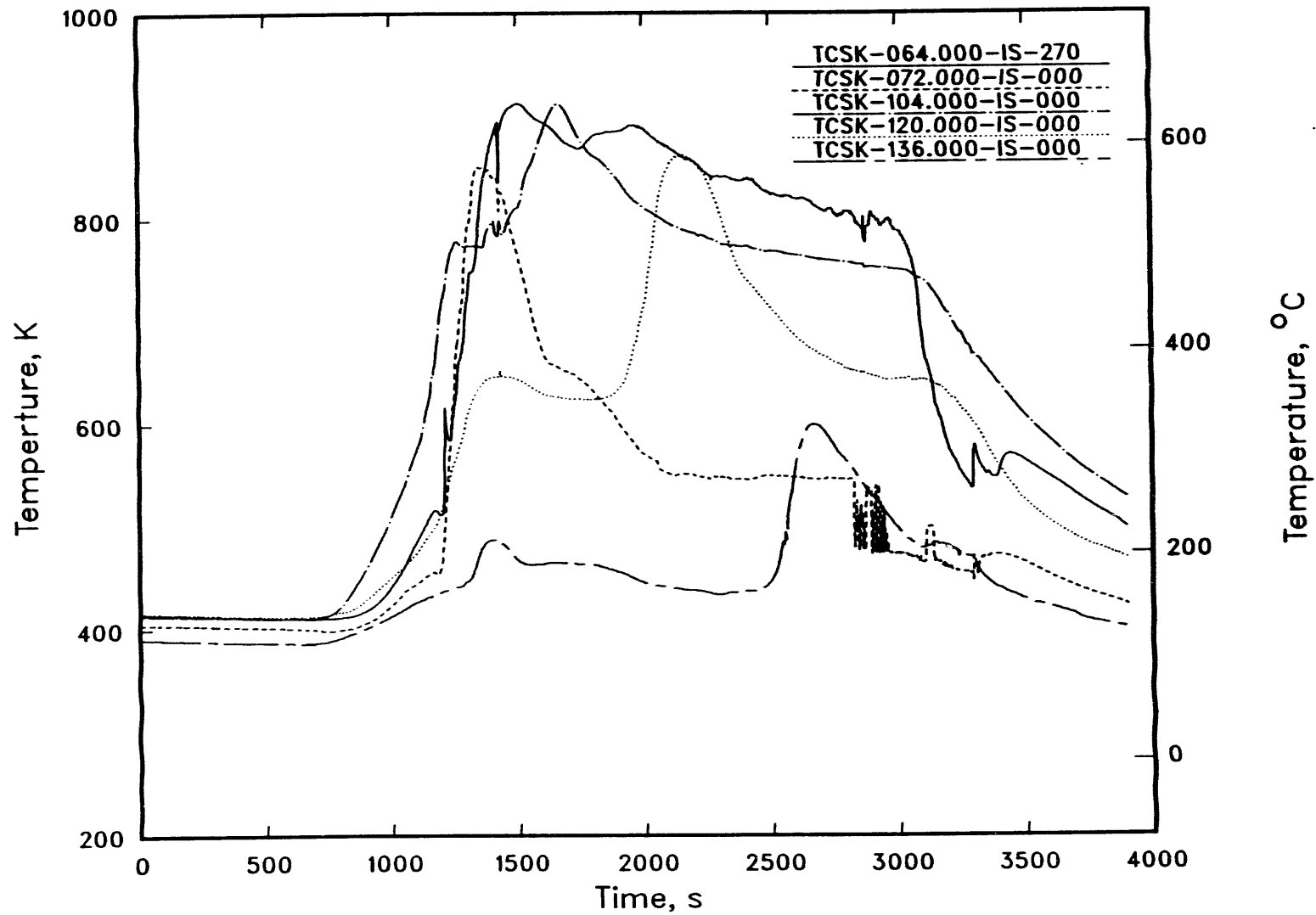


FIGURE A.4. Saddle Thermocouple Readings During FLHT-4. Curve labels indicate elevation (above bottom of fuel column) in inches.

A.10

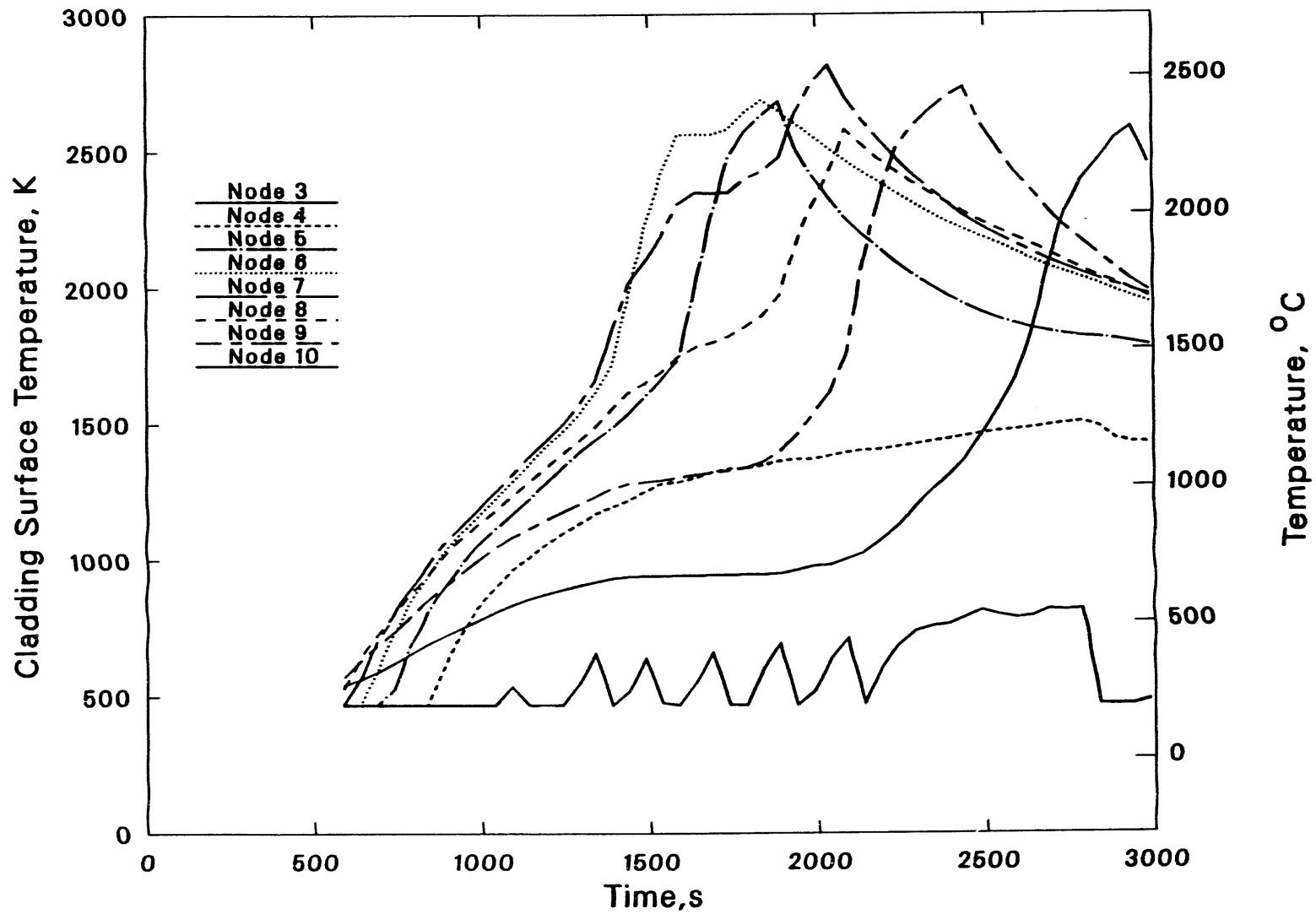


FIGURE A.5. SCDAP Nodal Cladding Temperatures Calculated for FLHT-4. The 10 axial nodes are equally spaced from bottom (Node 1) to top (Node 10) of the fuel column.

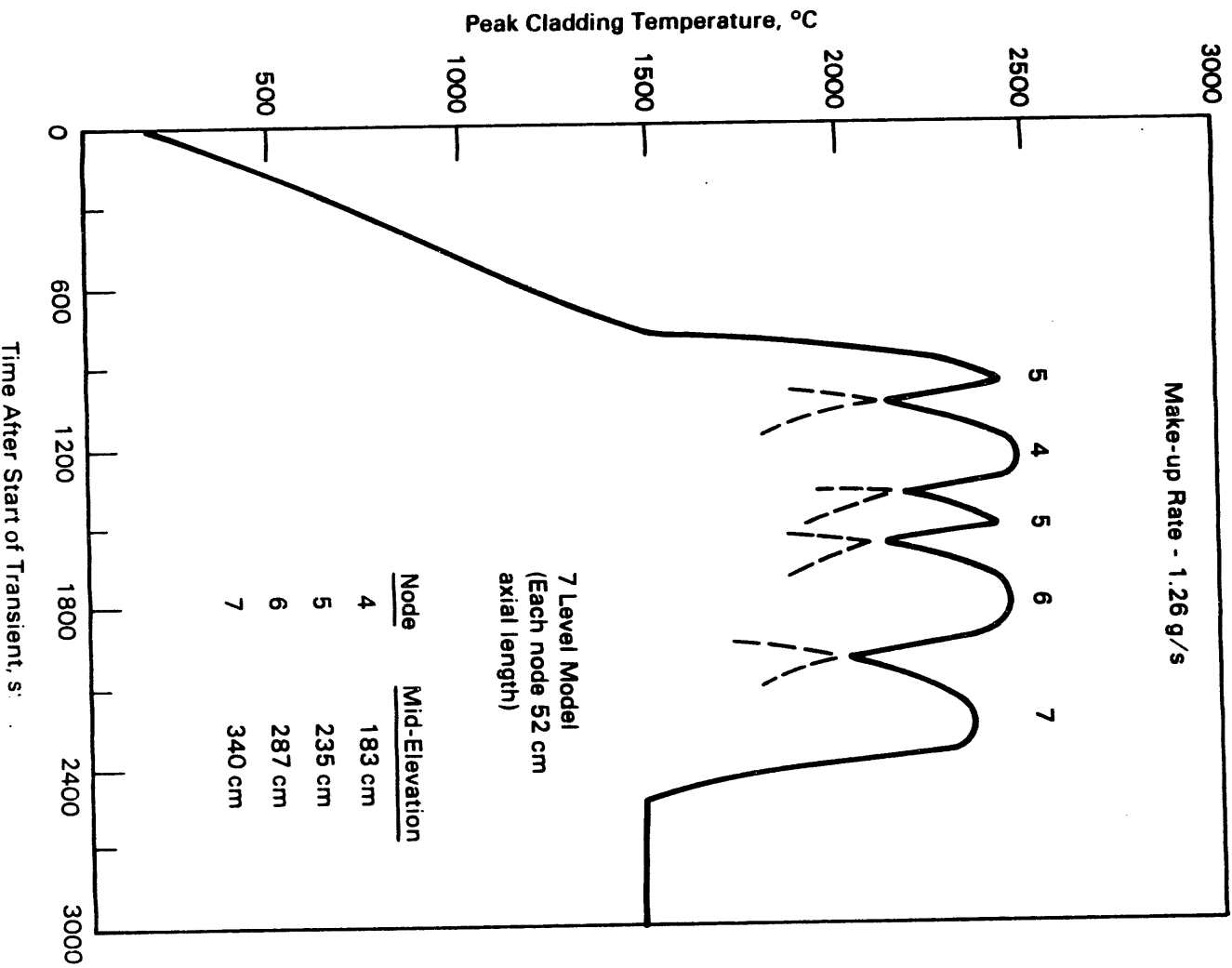


FIGURE A.6. In-House Code Nodal Temperatures Calculated for FLHT-4 (7 Nodes Total). The peaks occur due to individual successive axial nodes reacting autocatalytically with the steam. The mode numbers are noted for each peak.

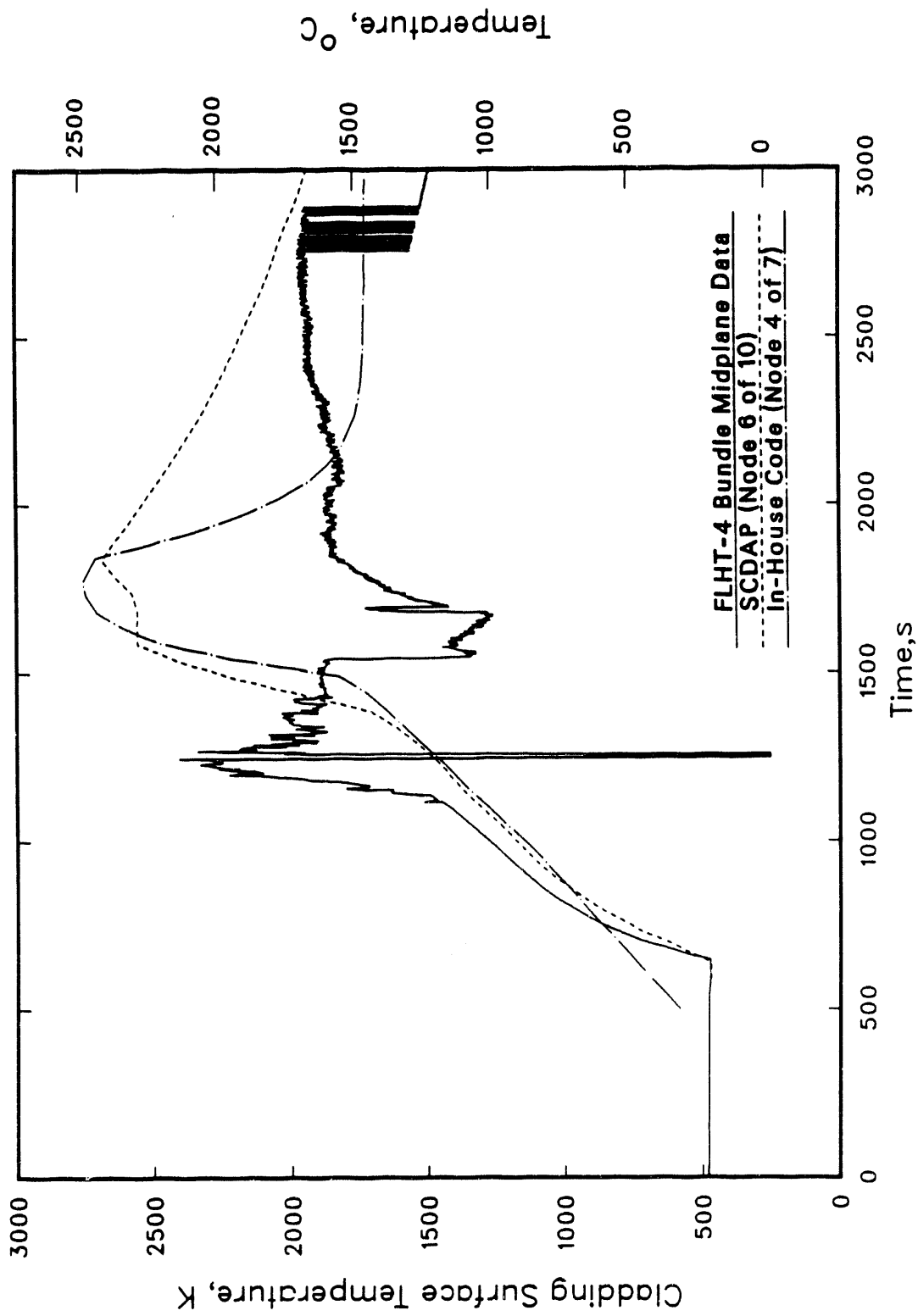


FIGURE A.7. SCDAP and In-House Code Mid-Plane Peak Cladding Temperatures Versus Data for FLHT-4

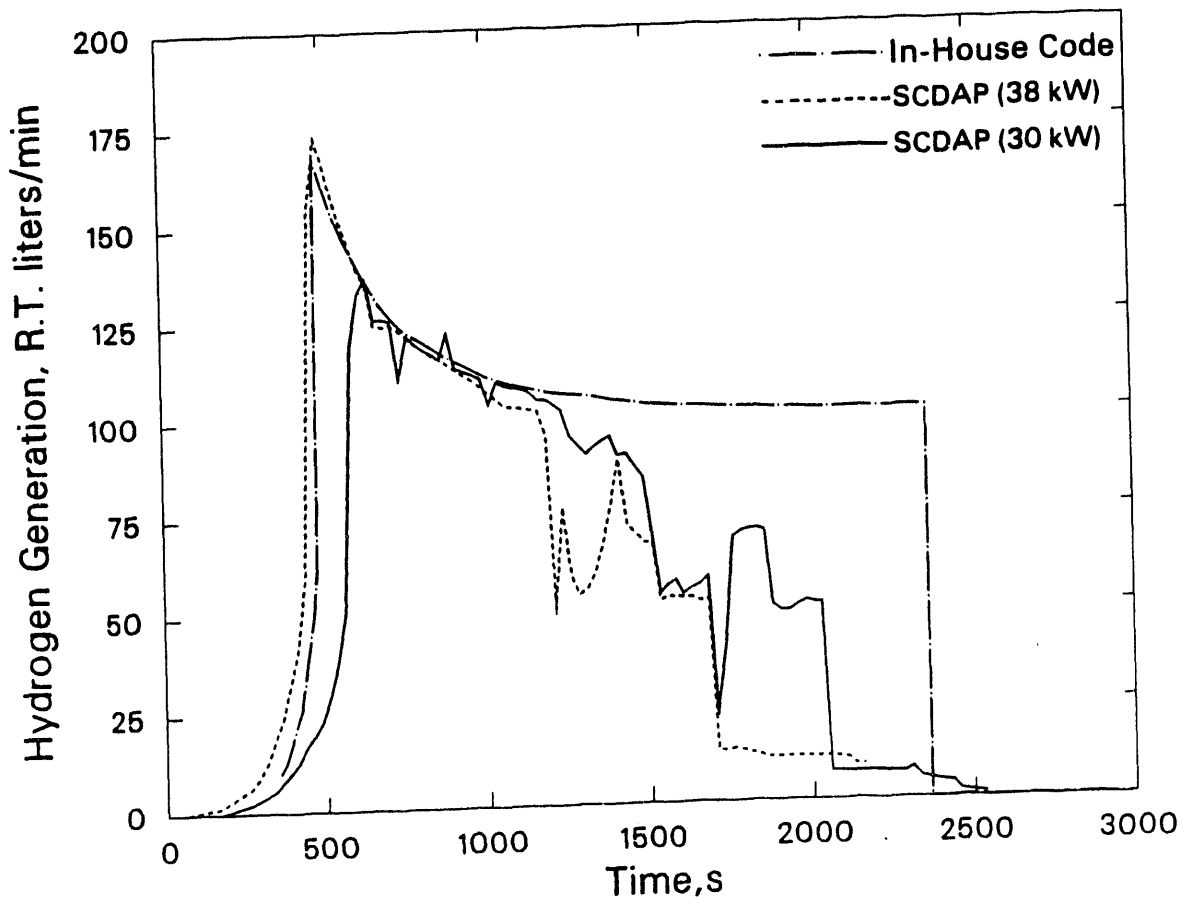


FIGURE A.8. Hydrogen Production Rates Predicted for FLHT-5
(flow reduction is at 0 s)

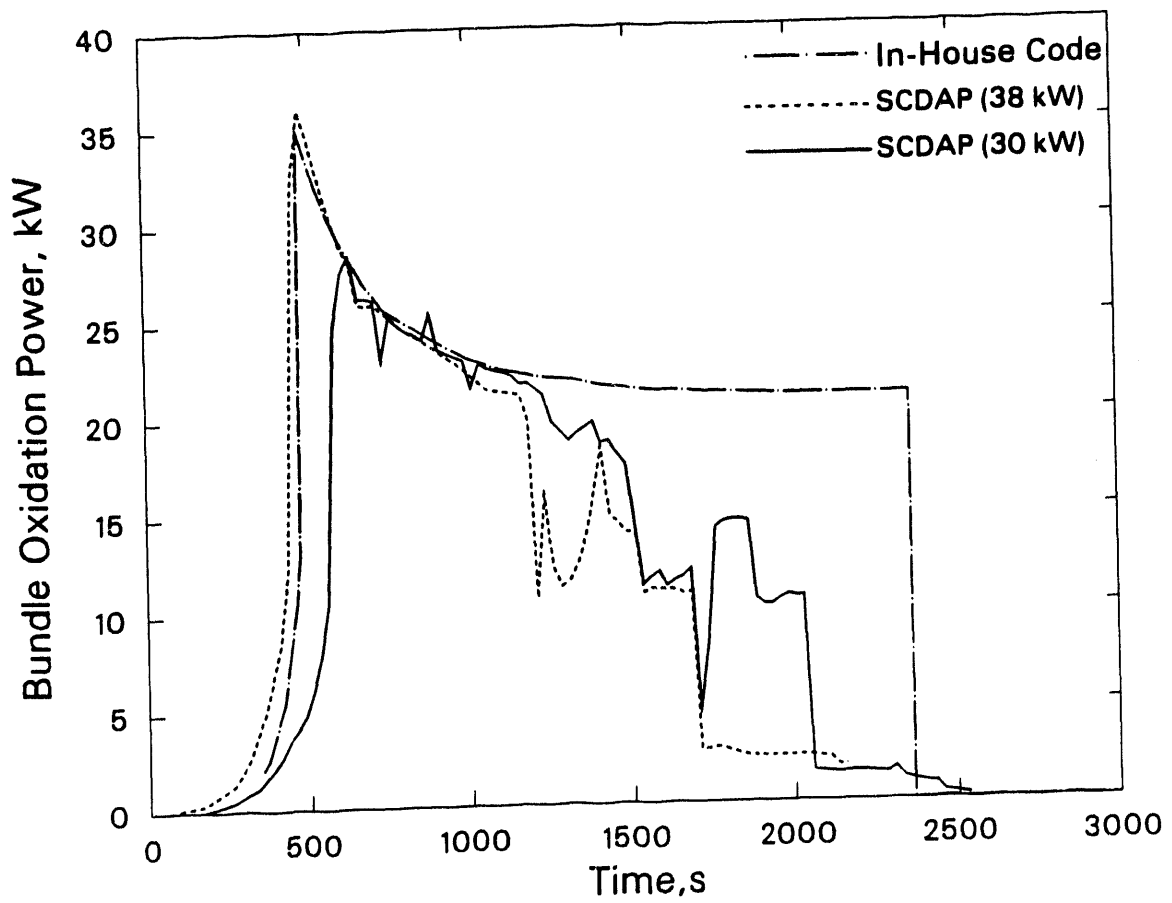


FIGURE A.9. Bundle Oxidation Heat Generation Rates Predicted for FLHT-5

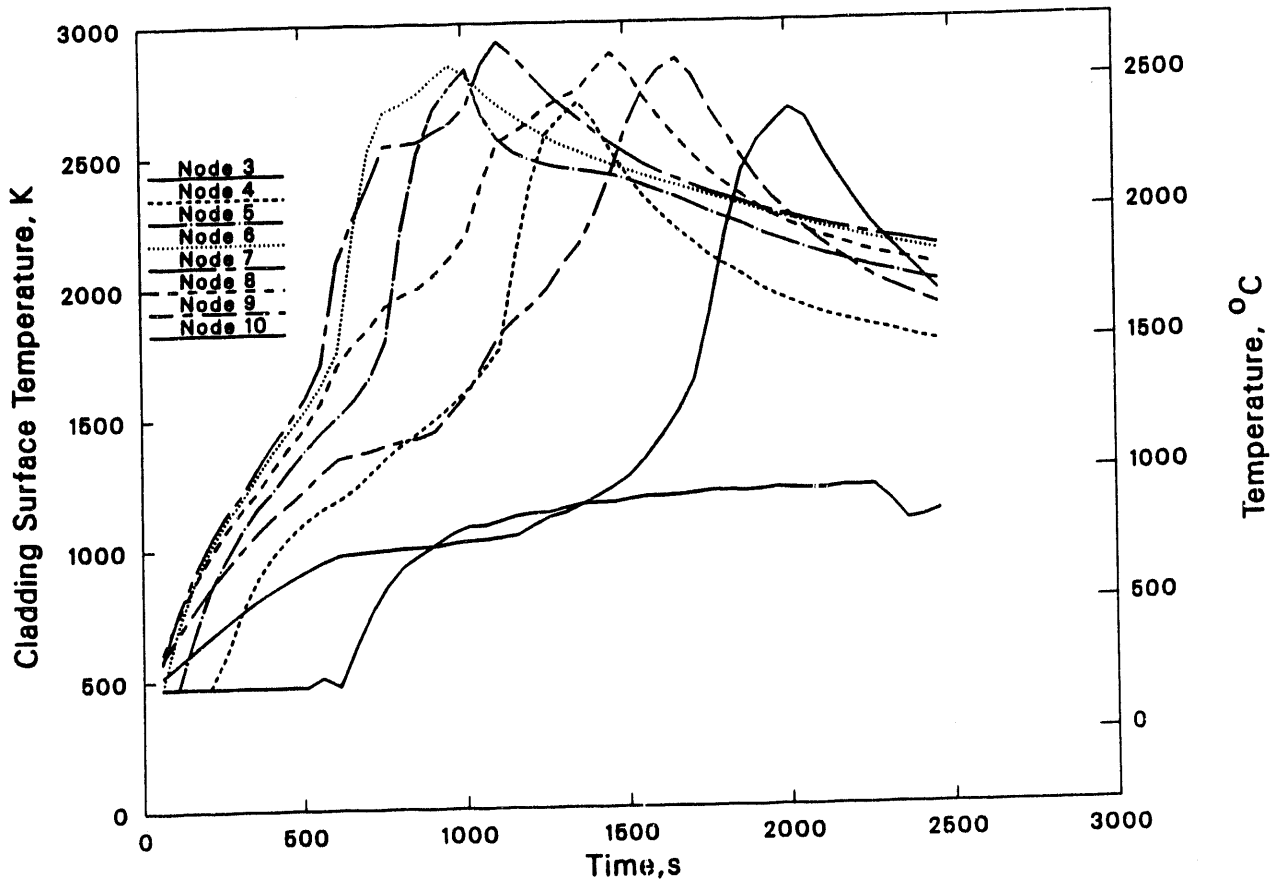


FIGURE A.10. SCDAP Nodal Temperatures Calculated for FLHT-5 (10-node calculations)

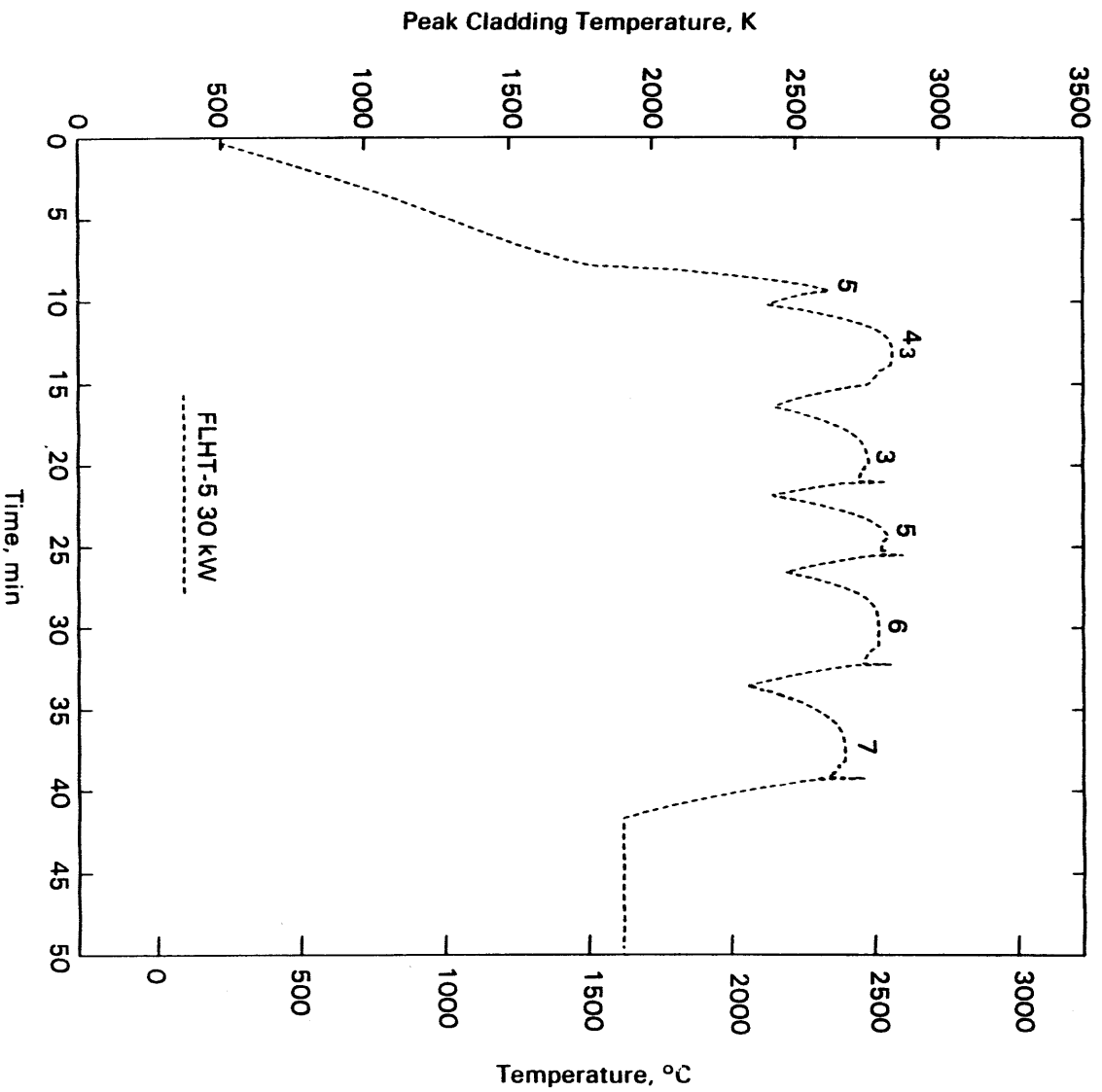


FIGURE A.11. In-House Code Nodal Temperatures Calculated for FLHT-5 (7-node calculation). The peaks occur due to individual successive axial nodes reacting autocatalytically with the steam. The mode numbers are noted for each peak.

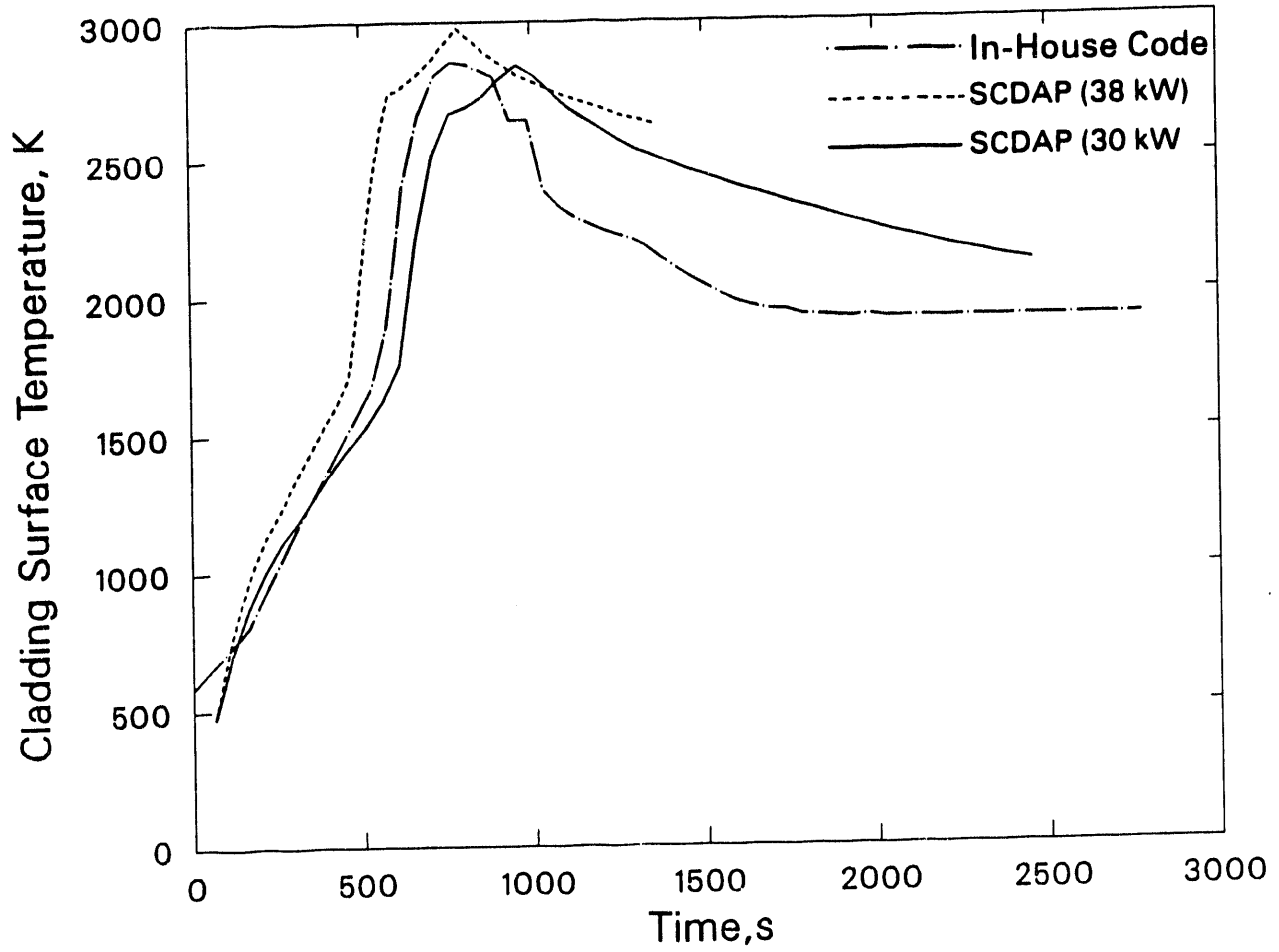


FIGURE A.12. SCDAP and In-House Calculated Mid-Plane Peak Cladding Temperatures for FLHT-5

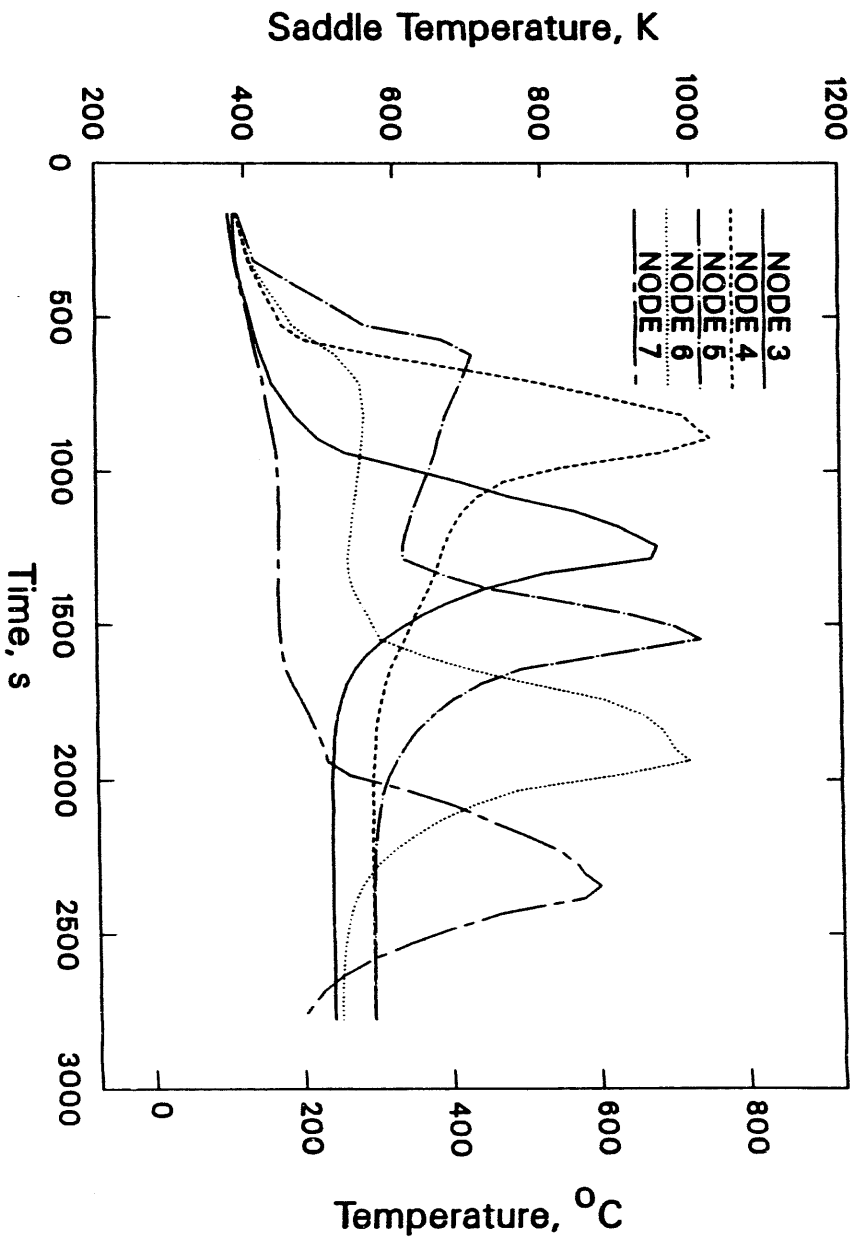


FIGURE A.13. In-House Code Nodal Saddle Temperature Calculated for FLHT-5

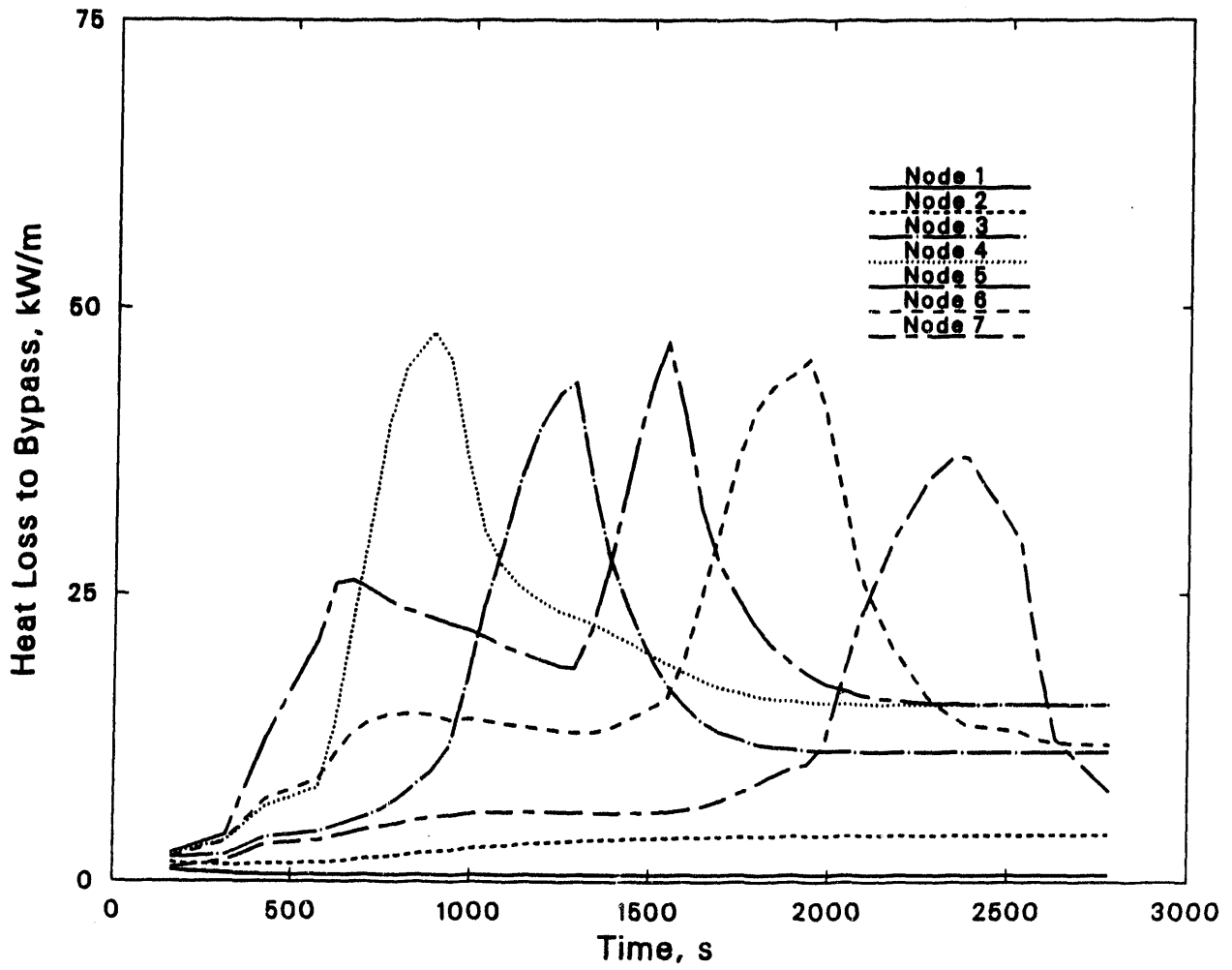


FIGURE A.14. In-House Code Nodal Radial Heat Loss Calculated for FLHT-5

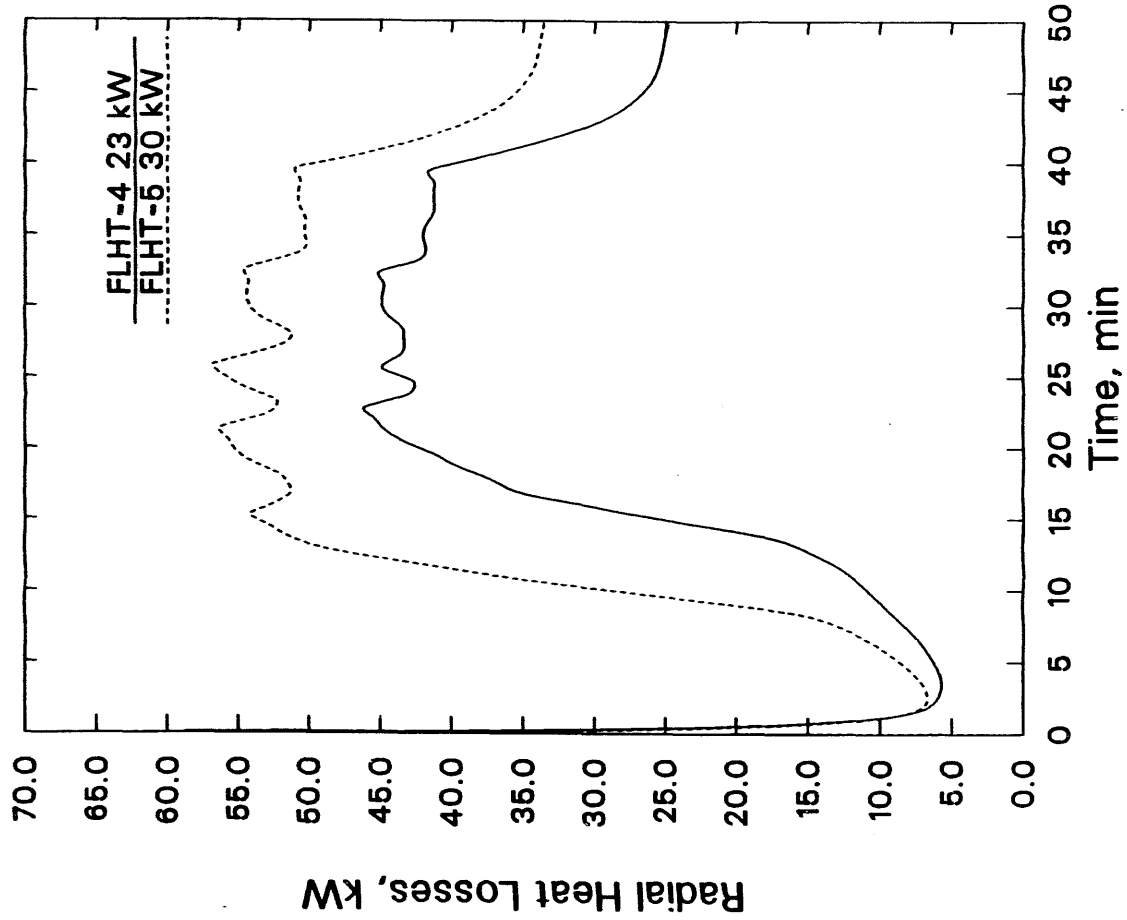


FIGURE A.15. Total Bundle Radial Heat Loss to Bypass as Predicted by the In-House Code for FLHT-5

APPENDIX B

CORSOR FISSION PRODUCT RELEASE CALCULATIONS

APPENDIX B

CORSOR FISSION PRODUCT RELEASE CALCULATIONS

In the document BMI-2122, a method is outlined for estimating fission product release rate, R (fraction per minute) according to the relation

$$R = A \exp (BT)$$

where T is average temperature in the fuel (°C). Values for "A" and "B" are given for 15 different elements. This method was applied to the FLHT-5 predicted fuel temperature history in the following way:

- 1) The hottest node in a given axial region at a given time step was taken to represent all the fuel in the region (the variation among nodes was usually less than 200°F).
- 2) The time history was divided into 51 steps.
- 3) The current relative inventory in each axial node was taken to be proportional to the axial form factor at the start of the transient. This inventory was corrected at the end of each time step by the release during that step (product of release rate times the step duration).
- 4) The cumulative release for the node for the step is the ratio of the initial inventory minus the current inventory, divided by the initial inventory.
- 5) The total cumulative release for the bundle is calculated as the average of the cumulative releases for the seven axial nodes, weighted by the form factor.

The results for the 15 subject elements are shown in Table B.1. Such results for release have been shown to be grossly conservative (i.e., high by an order of magnitude) in short-term heat-up of fresh fuel, both in PBF/SFD tests and in the FLHT-2 test. However, FLHT-5 will include one irradiated

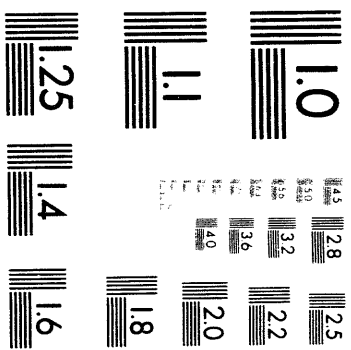
TABLE B.1. CORSOR Calculated Release Fractions for FLHT-5

<u>Element</u>	<u>Release Fraction, %</u>
Kr	81
Xe	81
I	81
Rb	81
Cs	75
Te	7.9
Ag	68
Sb	35
Ba	9.1
Mo	3.8
Sr	3.7
Zr	0.007
Ru	0.33

rod, and will include a relatively long time at high temperature, coupled with partial fuel liquification, fuel oxidation, and rapid partial cooldown. Given these facts, it is not clear what margin of conservatism the figures in Table B.1 contain. Similar predictions on FLHT-4 were within a factor of two of the stack release of Xe + Kr as-measured by a calibrated sample line and Geiger counter at the NRU stack.

APPENDIX C

UPDATED STEAM EXPLOSION AND
PRESSURE SPIKE ANALYSIS FOR FLHT-5



2 of 2

APPENDIX C

UPDATED STEAM EXPLOSION AND
PRESSURE SPIKE ANALYSIS FOR FLHT-5

A letter report from A. W. Cronenberg is presented here as an assessment of the potential for steam explosions or steam spikes during FLHT-5. Note: Cronenberg refers to the PNL in-house code as the "TRUMP" code.

AUGUST CRONENBERG - CONSULTING ENGINEER
836 Claire View - Idaho Falls, Id. 83402 - (208) 523-8480

January 14, 1987

Mr. D. Lanning
Battelle Pacific Northwest Lab.
Box 999
Richland, WA 99352

**Subject: ASSESSMENT OF ENERGETIC THERMAL AND CHEMICAL INTERACTION POTENTIAL
FOR THE FLHT-5 TEST**

Dear Don:

This letter is in reply to your request to assess the safety implications relative to energetic interaction potential of molten fuel rod debris with water, for the FLHT-5 experiment. Of particular concern are the somewhat higher temperatures and inventory of melt debris expected in the FLHT-5 test, as compared to FLHT-2 and FLHT-4.

To address this concern I make reference to the two previous reports on this subject (Refs. a and b), where an assessment of the potential for initiating energetic thermal/chemical interactions were assessed for the FLHT-2 and -4 experiments. In those two documents three classes of energetic interactions were investigated, namely:

a. A. W. Cronenberg, "FLHT-2; Experiment Safety Analysis Report," Engineering Science and Analysis, (January 18, 1985).

b. A. W. Cronenberg, "FLHT-4 and 5 Experiment Safety Analysis Report: Volume 1 Assessment of Energetic Thermal and Chemical Interaction Potential," ESA Report (December 1985).

1. Steam explosions: which can be characterized as thermal interactions between molten fuel rod debris and water, leading to rapid steam formation and the inducement of shockwave pressurization on a time-scale less than that for acoustic pressure relief.
2. Steam spikes: which can also be characterized as thermal interactions between melt debris and coolant, but where pressurization occurs on a time-scale longer than that for acoustic relief.
3. Energetic chemical reactions: where large-scale molten metallic zircaloy oxidation in water can lead to rapid energetic chemical interactions.

Although the FLHT-5 test is to be conducted under similar boildown conditions as the FLHT-2 and -4 experiments, somewhat higher temperatures and molten debris inventory are expected in FLHT-5, which poses the question of whether there exists an increased potential for an energetic interaction. To address this concern I first present an overview of the test conduct and expected differences with respect to peak temperatures and inventory of melt debris for the FLHT-4 and 5 experiments. Noting differences in test conditions, I then discuss potential differences with respect to the three classes of energetic interactions. Bottom-line conclusions are then summarized.

Description of Test Conduct:

Each FLHT test consists of ~12 ft long zircaloy-clad UO_2 -fuel rods, arranged in an octagonal array of 12 rod positions. Twelve fresh fuel rods were used in the FLHT-2 test, whereas one high-burnup rod and one gamma thermometer were incorporated into the FLHT-4 test assembly. In the FLHT-5 test bundle one previously irradiated rod will again be used. The fuel-destruction phase of each test is initiated by reducing coolant inlet flow to the bundle and increasing the reactor power, resulting in coolant boiloff, fuel rod overheating, cladding oxidation and fuel rod failure. Once

cladding temperatures in excess of about ≈ 1500 K are achieved, bundle heatup is driven by the exothermic reaction of the zircaloy with steam, which results in accelerated oxidation, Zircaloy melting, UO_2 dissolution and relocation, and release of hydrogen. Table 1 presents an overview of test conditions and expected results with respect to peak fuel rod temperatures and oxidation behavior. As indicated, the test conditions for FLHT-5 more closely approximate those of FLHT-4 than FLHT-2, so that a comparison of FLHT-5 with FLHT-4 is most relevant to the present discussion. Of particular interest are differences in peak temperatures and amount of melt debris for the FLHT-5 test compared to FLHT-4, which could influence molten debris/coolant interaction potential. Such differences are highlighted below:

Comparison of FLHT-4 and FLHT-5 Test Conditions

Figure 1 compares the TRUMP predicted boildown sequence for the FLHT-4 and -5 tests, where the makeup flow for these two tests is nominally 1.26 g/s. It should be noted that the liquid-level is somewhat lower for FLHT-5, with a corresponding higher oxidation power. The TRUMP calculated hydrogen production history for both tests are compared in Figure 2, using Prater oxidation kinetics. As indicated, the boildown transient (Fig. 1) results in a lower steady-state liquid level for FLHT-5 than for FLHT-4, due to the higher nuclear heat generation. The higher nuclear power causes a more rapid heatup after dryout in FLHT-5, which causes the oxidation excursion to happen earlier when higher steaming rates prevail, resulting in a higher peak hydrogen production rate (230 mg/sec for FLHT-5 versus 184 for FLHT-4). The differences in fuel temperatures and predicted oxide growth kinetics (SCDAP predictions) also affect the predicted total amount of H_2 generated for FLHT-4 versus FLHT-5, as noted in Table 1.

The cladding temperature histories are compared in Figure 3, where seven equal-spaced axial nodes were used in the TRUMP calculations, with the mid-node evaluation (above bottom of fuel) and assumed relative nuclear power as follows:

TABLE 1. Comparison of Test Conditions and Expected Results for the FLHT-2, FLHT-4, and FLHT-5 Experiments

Parameter	Units	FLHT-2		FLHT-4		FLHT-5
		TRUMP	Measured	TRUMP	Measured	TRUMP
Nominal makeup flow rate	g/s	1.26	1.4 ±20%	1.26	1.25 ±10%	1.26
Expected boildown level	m	0.9	0.9	0.9	0.9	0.75
Peak cladding temperature	K	2700	2500	2900	2600	2900
Maximum nominal nuclear power	kW	27	-- (a)	27	-- (a)	35
Peak bundle oxidation power	kW	27	16-31	27	16-26	34
Peak hydrogen production rate	g/s	0.18	0.11-0.21	0.184	0.11-0.17	0.23
Total hydrogen produced	g	42	39-40	243	175-240	300
Percent oxidation of total Zircaloy inventory	percent	11	10	61	45-61	75
Percent oxidation of cladding inventory above minimum liquid level	percent	15	>15 ^(b)	84	>81 ^(c)	94
Percent oxidation of carrier plus liner inventory above minimum liquid level ^(d)	percent	15	<15 ^(b)	84	<81 ^(c)	94

- (a) Calibration of fully flooded bundle was 23 kW ±5%; CRNL neutronics calculations indicate an overall increase of 15% for the voided bundle.
- (b) Partition of oxidation between liner and cladding is uncertain, but based on FLHT-4 experience plus post-test observation, we expect somewhat less fractional oxidation of the liner.
- (c) Assuming the higher (and more reliable) measurements of H₂ production are correct.
- (d) Note that the carriers plus liner account for 46% of the total bundle Zircaloy; the cladding accounts for 54%.

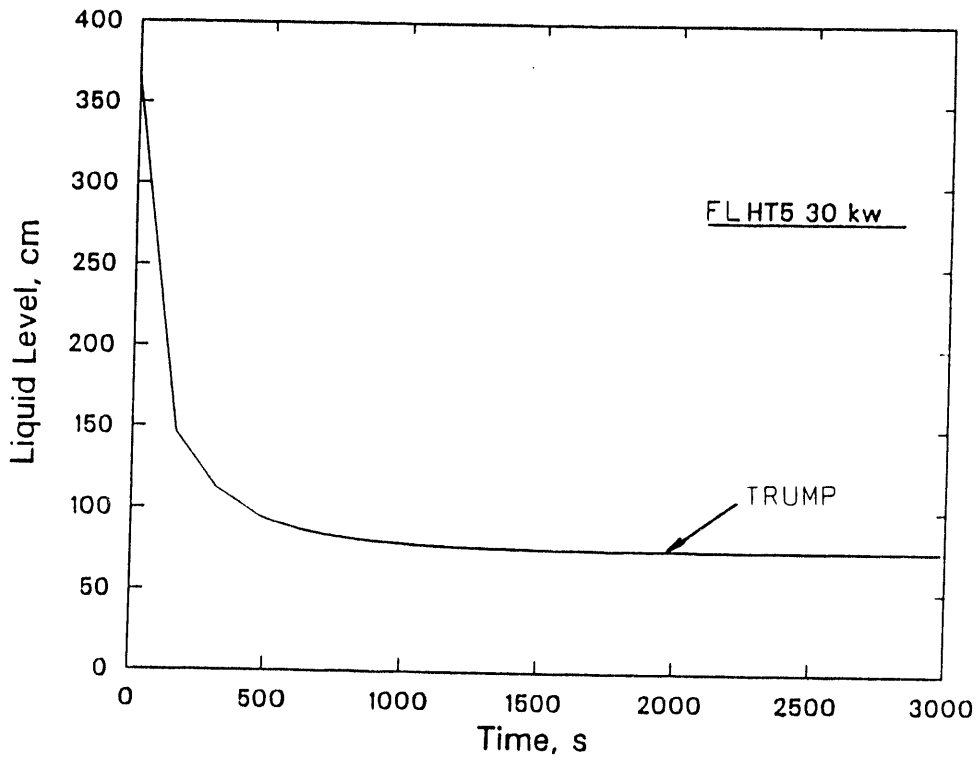
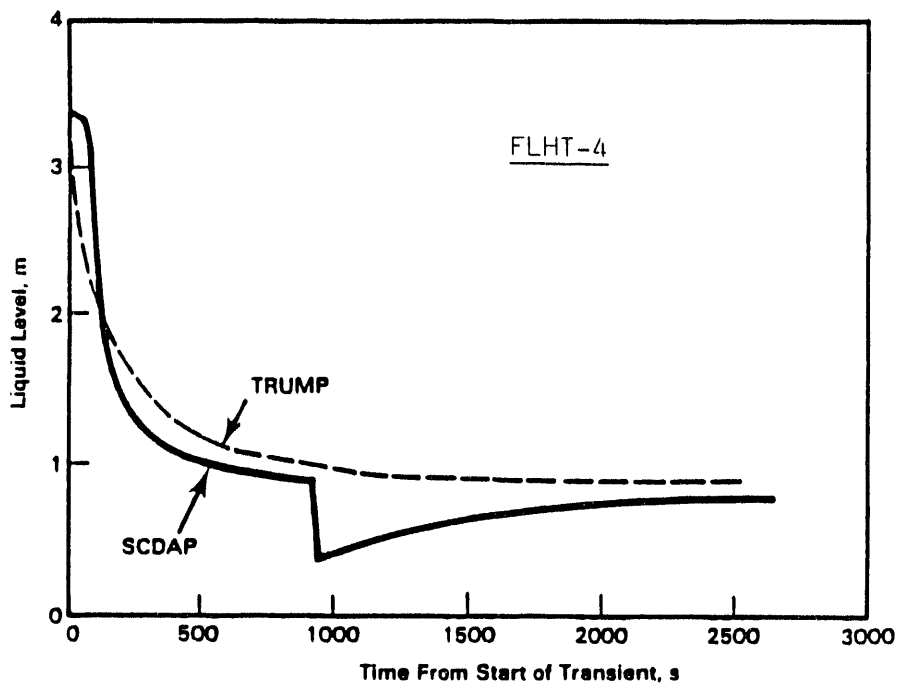


Figure 1. Comparison of SCDAP/TRUMP predicted boildown level for FLHT-4 (1.26 g/s) and FLHT-5 (1.26 g/s).

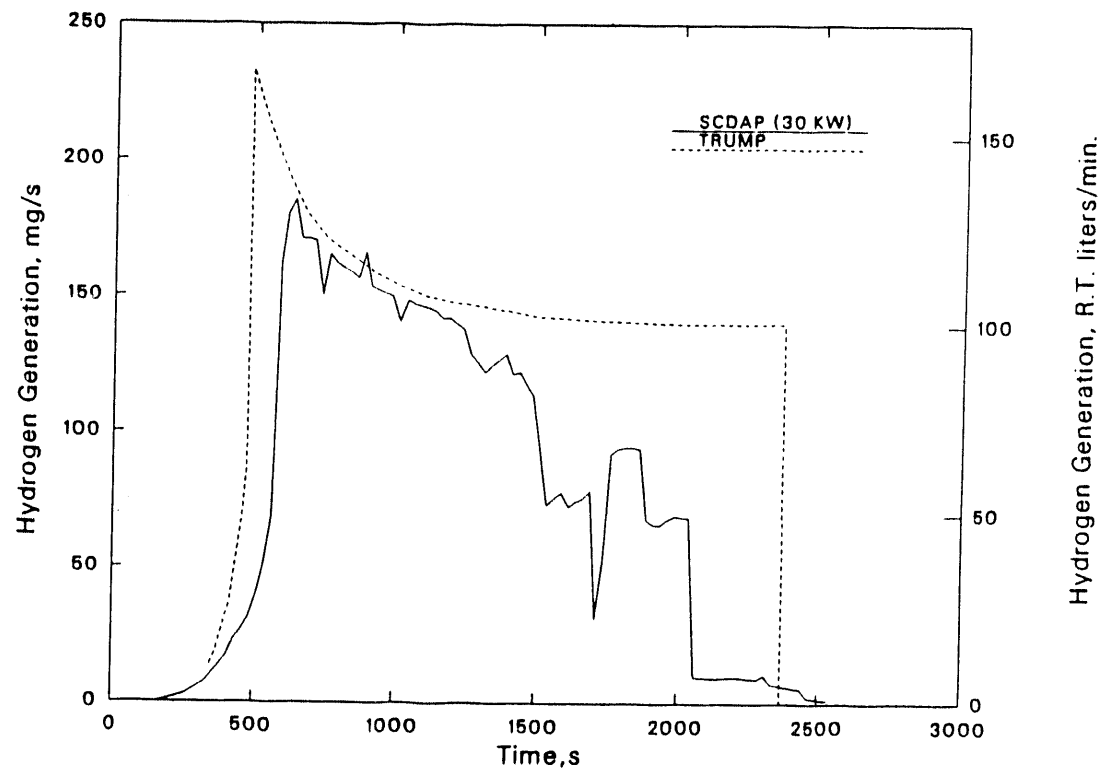
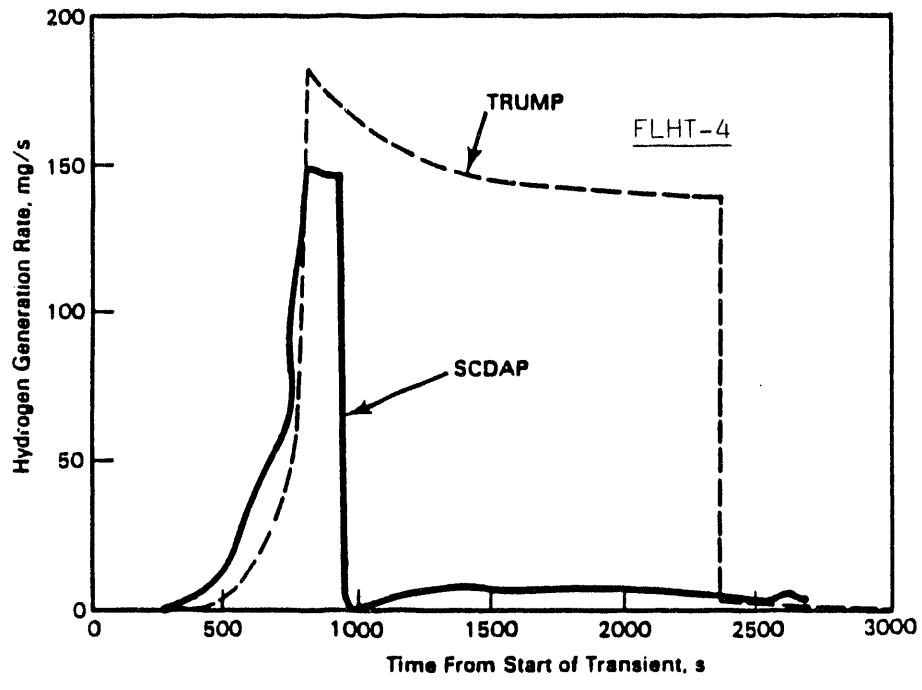


Figure 2. Comparison of SCDAP/TRUMP predicted hydrogen generation rate for FLHT-4 (1.26 g/s) and FLHT-5 (1.26 g/s).

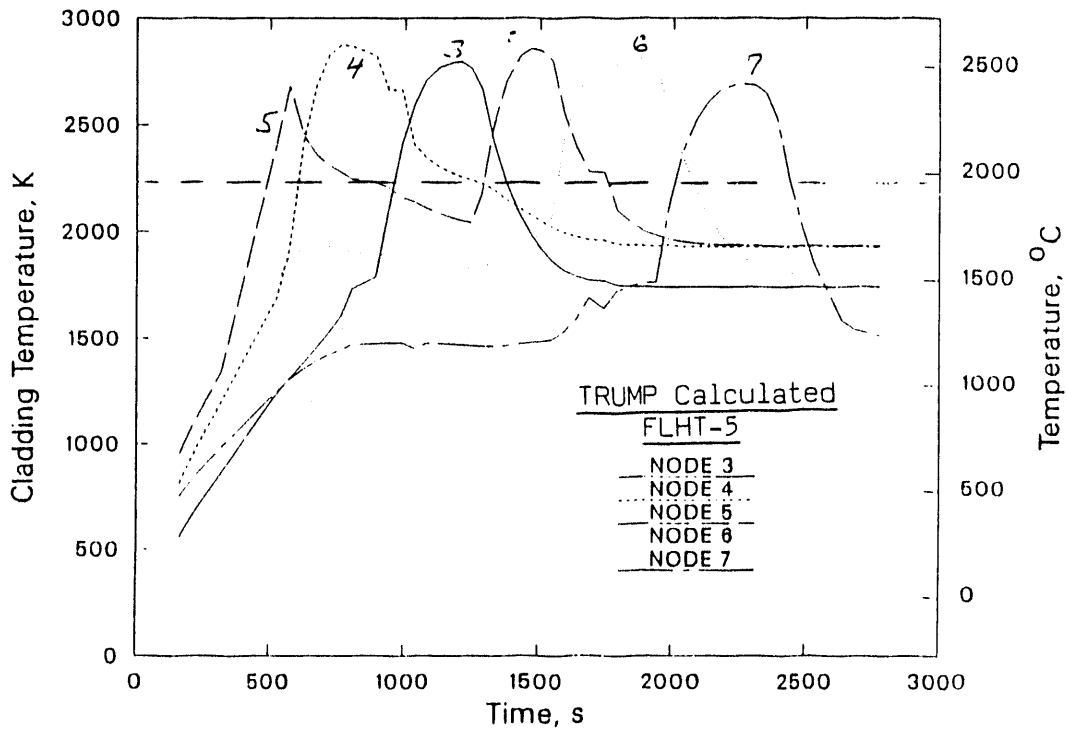
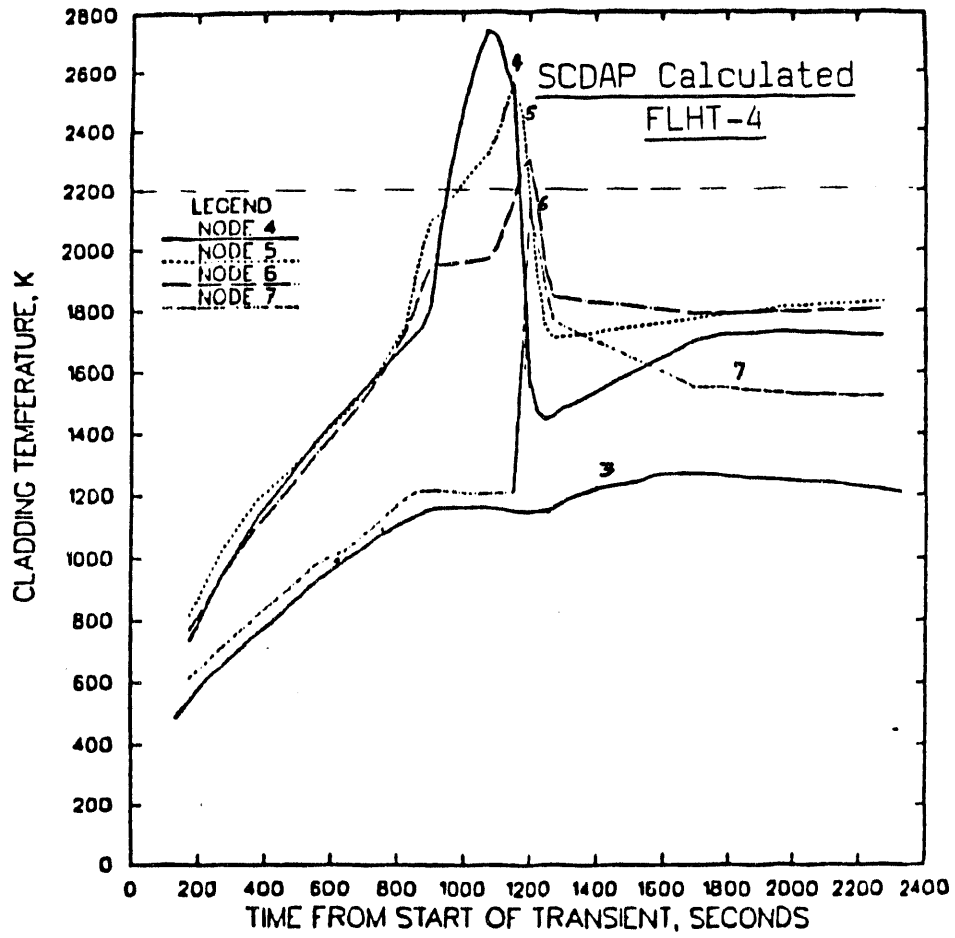


Figure 3. Comparison of SCDAP-FLHT-4 and TRUMP-FLHT-5 predicted cladding temperature histories at a makeup flow of 1.26 g/s for both tests.

FLHT-4 AND -5 AXIAL NODALIZATION FOR TRUMP

<u>Node</u>	<u>Mid-Node Elevation, m</u>	<u>Relative Power</u>
1	0.26	0.37
2	0.78	0.97
3	1.30	1.34
4	1.82	1.55
5	2.33	1.34
6	2.85	0.97
7	3.37	0.34

It should be noted that Figure 3 compares the SCDAP-FLHT-4 and TRUMP-FLHT-5 predicted cladding temperature histories, where somewhat different model assumptions exist with respect to cladding/fuel dissolution and melt relocation behavior. However, the salient feature to note is that both code predictions indicate similar heatup, where nodes 4 and 5 first experience peak temperatures on the order of 2600-2700 K, followed by Nodes 3, 6, and 7. It is also noted that because of the somewhat longer testing time and lower boildown level for FLHT-5, Nodes 3, 6 and 7 are predicted to attain somewhat higher temperatures than for FLHT-4. Thus, a somewhat greater (total) inventory of melt debris can be expected in the FLHT-5 experiment.

At the α -Zr(O) melt temperature (≈ 2270 K), cladding failure is expected and the initiation of loss-of-rod geometry due to molten alpha-Zr(O) dissolution of UO_2 fuel. Based on the results presented in Figure 3, it can be assumed that Nodes 4 and 5 experienced melt failure for FLHT-4, while Nodes 3 through 7 may experience melt failure for the FLHT-5 test. Falldown of this potentially coherent mass of melt debris into the coolant below is the principal safety concern, where the possibility exists for fragmentation of such debris into a large surface area for rapid thermal and/or chemical interaction. The 'best estimate' melt conditions assumed in the present evaluation of such energetic thermal and/or chemical interactions for FLHT-5 are assessed from the predicted (Fig. 3) zircaloy melt inventory.

To compare the mass composition and thermal characteristics of the melt debris we make use of Figure 3, which indicates that Nodes 4 and 5 exceed the melting point of α -Zr ($T_{mp} \approx 2200$ K) over the same time period (950-1150 s)

for the FLHT-4 test; versus Nodes 4 and 5 for $t = 500-1200$ s, Nodes 3 and 5 for $t = 1000-1700$ s, and Nodes 5, 6, and 7 for $t = 1500-2500$ s for the FLHT-5 test. Thus, simultaneous melting of at most two nodes was predicted for the FLHT-4 test, versus at most three simultaneous nodes for the FLHT-5 experiment. Thus, the inventory of melt debris in FLHT-5 may exceed that of FLHT-4 by about 50-percent. Using the same procedure outlined in Ref. b for determination of a conservative inventory of Zr/UO₂ melt debris for assessment of thermal and chemical interaction potential, the FLHT-4 mass inventory of Zr/UO₂ melt debris (cladding, liner, plus dissolved fuel) is simply scaled by 50-percent for the FLHT-5 test, where the following best estimate/conservative definition of molten corium^c (fuel + zircaloy) mass inventory are used in for safety evaluation purposes:

INVENTORY OF Zr/UO₂ MELT DEBRIS FOR SAFETY ANALYSIS

	<u>FLHT-4 Estimate</u>	<u>FLHT-5 Estimate</u>
Number of Simultaneous Molten Nodes	2	3
Total Molten Corium Mass (clad, liner, dissolved UO ₂)	= 2856 + 949 ≈ 3800 g	5700 g
Effective Corium Density	= 8.10 g/cm ³	Same
Effective Corium Volume	= 475 cm ³	704 cm ³
Effective Corium Melt Temp.	= 2400 K	2500 K

Note that the effective assumed corium melt temperature is somewhat higher for FLHT-5, i.e., 2500 K. The effect of a somewhat higher inventory of melt debris and higher effective temperature for the FLHT-5 test, on energetic interaction potential is assessed next.

In the above FLHT-5 melt debris estimate, it was assumed that no more than three nodes exist in a molten state over the same time period. In reality much of the melt debris from one node would have drained and refroze

c. Corium is a common term to denote a mixture of fuel and structural materials for core meltdown conditions; in this case it denotes a mixture of α -Zr(O) and UO₂.

at a lower elevation before the onset of melting of an adjacent node. Thus, the assumption of 3 nodes at simultaneous melting for the FLHT-5 test is quite conservative. An estimate of a characteristic drainage time of melt debris (t_d) can be assessed by consideration of the drainage configuration presented in Figure 4. Nusselt-type film drainage is assumed, where a continuous film of molten-Zr liquid adhering to a fuel rod stub flows downward under the action of gravity. If the flow is laminar and caused by gravity alone (no upward force at the surface due to high steam velocity), the drainage mass flow rate and associated t_d can be expressed as:⁶

$$m_d(\text{g/s}) = \frac{(\rho^2 \delta^3 g)}{3\mu} (\pi D)$$

$$t_d(\text{s}) = m_0/m_d$$

where μ is the viscosity of the liquid film, δ is the film thickness, ρ is the liquid density, g is the acceleration due to gravity (980 cm/s^2), m_0 is the mass of material subject to drainage, and D is the diameter of the surface to which the liquid film adheres. For molten-Zr the viscosity and density are

$$\mu = 15 \text{ centipoise} = 0.15 \text{ g/cm}^5$$

$$\rho = 6.49 \text{ g/cm}^3$$

while δ is taken as the maximum film thickness, where equals half the distance between rod stubs

$$\delta = 0.5 (\text{Pitch} - \text{Rod OD}) = 1.275 \text{ cm} - 0.963 \text{ cm} = 0.156 \text{ cm}$$

Thus, m_d is estimated to be

$$m_d = \left[\frac{(6.49)^2 (0.156)^3 980}{3(0.15)} \right] (\pi \times 0.963) = 1053 \text{ g/s}$$

The mass of melt in a node (m_0) is:

$$M_0 = 5700 \text{ g/3-nodes} = 1900 \text{ g/node}$$

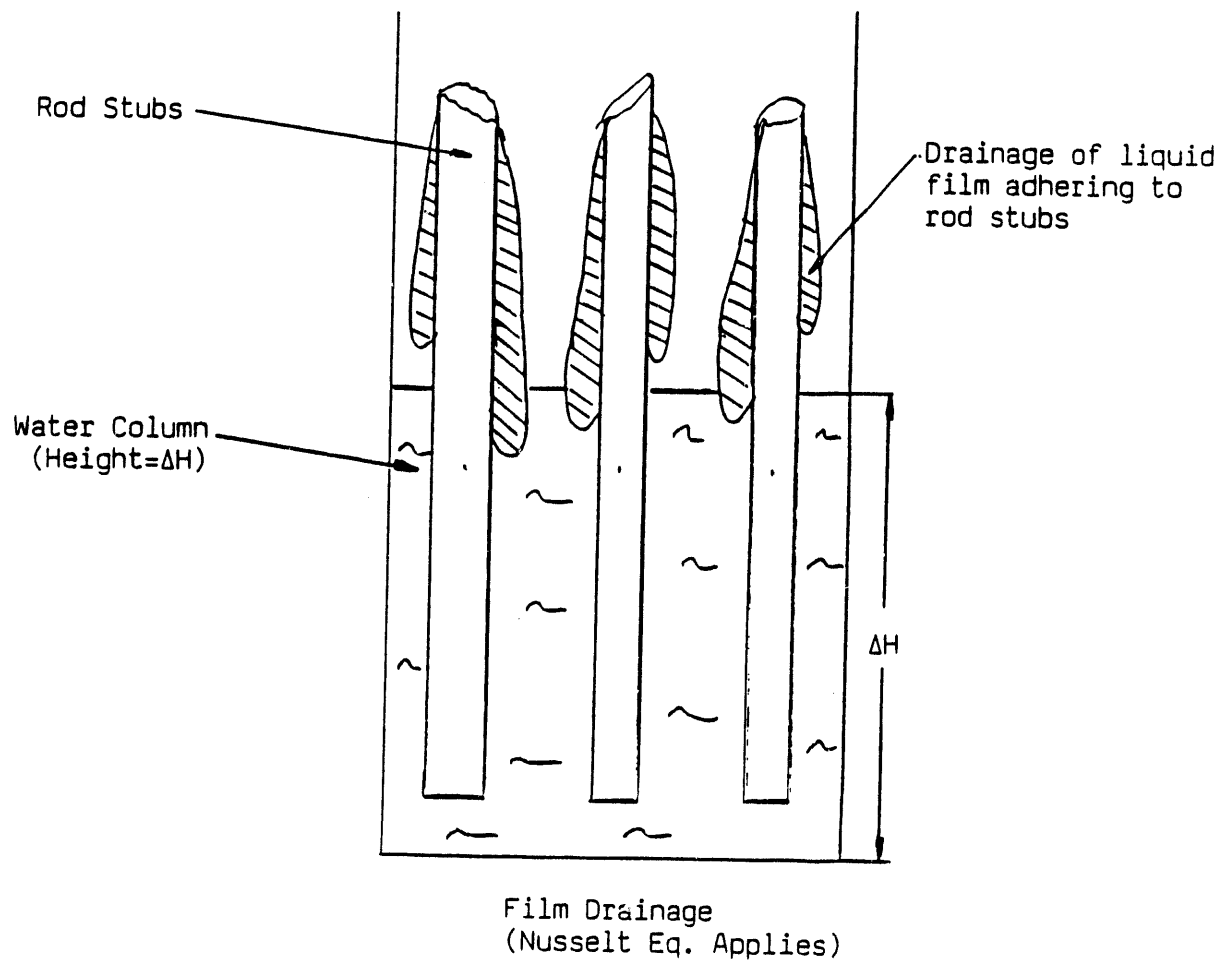


Figure 4. Illustration of filmwise drainage configuration.

Thus, the drainage time of an equivalent of one node of molten zircaloy cladding is

$$t_d = 1900 \text{ g}/1053 \text{ g/s} = 1.8 \text{ sec}$$

Clearly rapid drainage (1.8 sec) of melt debris occurs relative to the time scale at which such melt debris is generated (100's of seconds) on a node-to-node basis. Thus, the assumed FLHT-5 condition of simultaneous melting of 3 nodes is extremely conservative. Nevertheless, for the purpose of this safety assessment, the inventory of melt debris given above (5700 g), for FLHT-5 will be used for assessment of energetic melt-debris/water-coolant interaction potential.

FLHT-5 Steam Explosion Potential:

As discussed in Refs. a and b, the five conditions considered necessary for inducement of energetic steam explosions are:

1. Stable film boiling and coarse intermixing of melt debris and coolant.
2. Destabilization of film boiling by thermal and/or pressure-induced means.
3. Extensive fuel fragmentation and intermixing with liquid coolant, resulting in a large effective heat-transfer area for rapid coherent coolant vaporization.
4. Intimate liquid-liquid contact between molten debris and coolant.
5. Sufficient system constraint resulting in shock pressurization.

Lack of attainment of any one of these five conditions, would be sufficient to preclude the possibility for explosive steam formation. In Ref. b, analysis indicated that conditions 2, 4, and 5 would not be satisfied for the FLHT-4

test conditions; thus, indicating a nil probability for inducement of an energetic steam explosion. Since the phenomena associated with these criteria are independent of temperature and molten mass inventory conditions, a similar conclusion applies to the FLHT-5 test.

It is interesting to note that the only experiments or accidents involving melting of nuclear fuel rods which lead to energetic "steam explosions" were for reactivity excursions (i.e., SL-1 accident, BORAX and SPERT Tests) and the recent Chernobyl accident. In these events rapid reactivity insertion lead to sudden fuel melting and partial vaporization, resulting in forced fuel fragmentation and dispersal into coolant, which provided the initial conditions for fine-scale fuel fragmentation and intermixing with coolant necessary for explosive steam formation. Such reactivity excursion conditions are not applicable to the FLHT test conditions. Larger inventories of molten debris and higher temperatures due not necessarily constitute an increased probability for inducement of energetic steam explosions. Rather satisfaction of favorable initial conditions is of overriding importance. On one hand laboratory experiments using relatively small quantities (e.g. several hundred grams) of melt debris have been "triggered" to explosive conditions, while larger mass fuel meltdown events (e.g. the TMI-2 accident; where upwards of 20 metric tons of melt debris migrated to the water filled lower plenum with benign quenching) have not resulted in energetic explosive interactions. Larger inventories of fuel debris at higher temperatures would increase the stored thermal energy of the system, but it is the rapid conversion of this thermal energy into mechanical work which is of importance to the inducement of explosive events. Rapid fine-scale debris fragmentation, intermixing with coolant, and system constraint are not directly dependent on the total thermal energy of the system but rather are governed by external or system conditions (i.e. as an externally applied pressure pulse or mixing geometry). In sum higher temperatures and larger inventory of melt debris expected in the FLHT-5 test does not in itself increase the probability for inducement of an energetic explosions.

FLHT-5 Steam Spike Potential:

A "steam spike" involves vapor generation on a time scale which is longer than the acoustic relaxation time of the system. Consequently no shock wave is generated (as in steam explosions), but depending upon system venting characteristics overpressurization can develop if the steam generation rate substantially exceeds the capacity for steam removal. Therefore, the principal question of interest is whether the FLHT-venting system can accommodate all expected and off-normal steam production rates. The venting capacity is largely governed by system dimensional characteristics, while steam production is governed by debris/coolant heat transfer properties.

As discussed in Ref. b, the steam removal capacity of the FLHT effluent control and off-gasing system is the same for tests FLHT-2, 4, and 5, since the off-gasing system dimensions and set pressure for actuation of the pressure relief valve are the same for all three tests. Calculations for isentropic compressible flow indicate that once the critical pressure ratio is reached a choked flow condition will occur, where increased upstream pressurization results in no further increase in mass flow rate. The choked flow conditions for the FLHT system pressure of 185 psi, were estimated in Refs. a and b to be:

$$P_1 = \text{upstream pressure} = 340 \text{ psi (23.5 bar)}$$

$$\dot{m}_0 \text{ (choked)} = 350 \text{ g/s cm}^2$$

For high temperature testing, the effluent discharge circuit shown in Figure 5 is via Path-A or Path-B, both of which have an equivalent nominal flow area dictated by their in-line series control valves, with a fully-opened flow area of $\approx 0.0765 \text{ in.}^2$. Should overpressurization in excess of approximately 25 psi occur, Path-C is likewise activated to act in parallel with Paths-A or B. For pressure relief considerations of this safety analysis, the off-gasing capacity is thus dictated by the flow area of Path-A or B in conjunction with Path-C; i.e.:

C.16

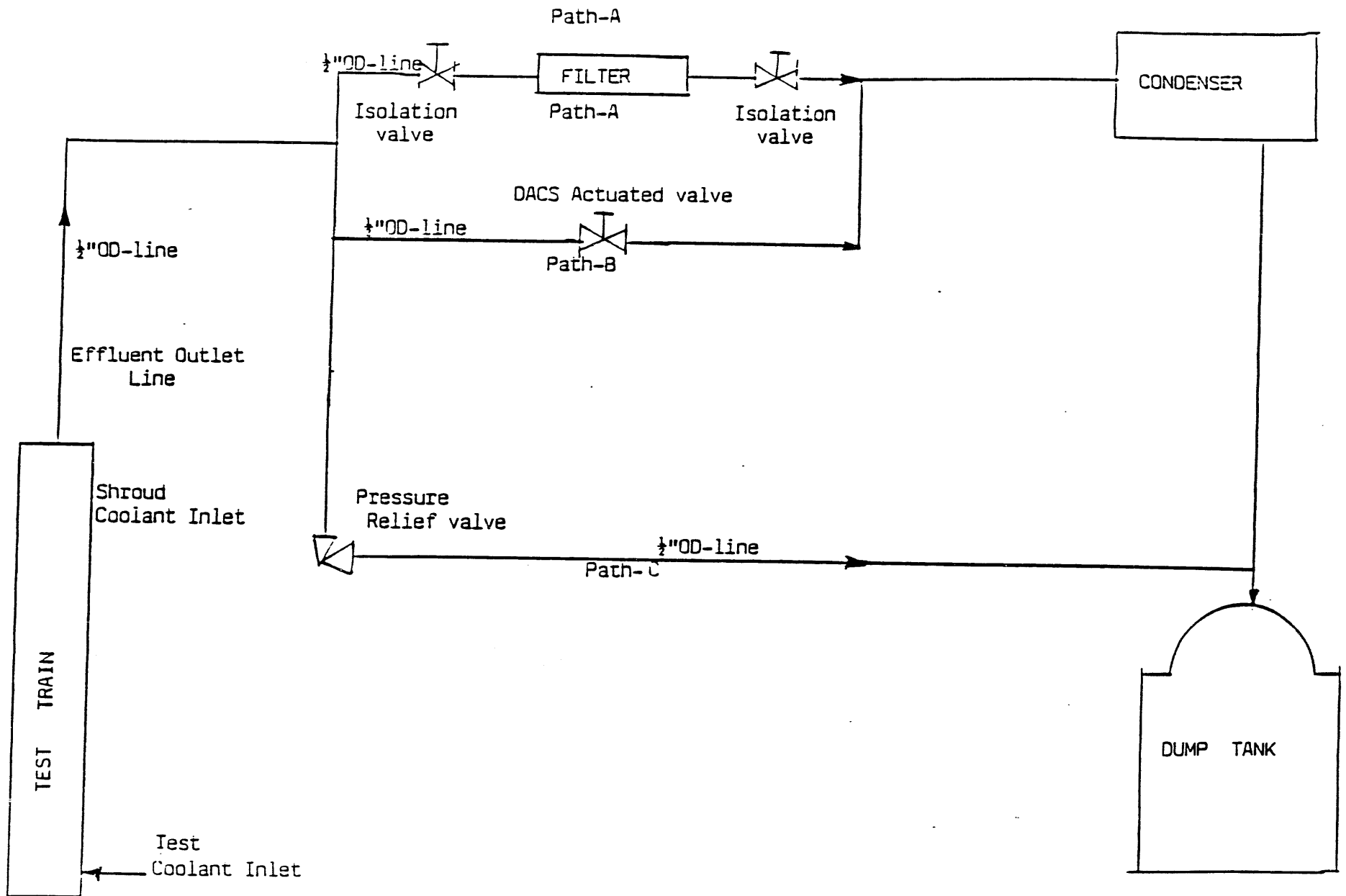


Figure 5. Illustration of effluent multi-path flow control system.

Safety Analysis Flow Area:

$$\begin{aligned} &= \text{Path-A/B} + \text{Path-C} \\ &= 0.0765 \text{ in.}^2 + 0.11 \text{ in.}^2 \\ &= 0.1865 \text{ in.}^2 (1.203 \text{ cm}^2) \end{aligned}$$

This effective vent flow area is the same as previously used in the FLHT-2^a and FLHT-4^b safety reports and also for FLHT-5. Thus, the mass flow capacity of the system is:

$$\dot{m}_0 \text{ (choked)} = 350 \text{ g/cm}^2\text{s} (1.2 \text{ cm}^2) = 421 \text{ g/s}$$

This system dimension governed steam venting capacity is the same for all tests and is compared to the expected steam production rate for FLHT-5.

In the FLHT-4 safety report the maximum steam production was assessed based upon the critical heat flux (CHF) for pool boiling. For all the FLHT tests, the residual water in the lower regions of the test section is expected to be near saturation; thus, one can make use of CHF correlation for saturated pool boiling as formulated by Kutateladze:

$$(q/A)_{\text{CHF,sat}} = 0.14 h_{fg} (\rho_g)^{0.5} [g\sigma_1 (\rho_f - \rho_g)]^{0.25} (\text{cal/cm}^2\text{s})$$

where h_{fg} is the latent heat of vaporization and ρ is density. As can be seen the debris temperature is not controlling but rather the thermodynamic properties of the coolant. A higher debris temperature therefore has little effect on steaming rate, since CHF is the maximum heat flux.

Knowing the critical heat flux, the mass rate of steam production (\dot{m}_v) is estimated as follows:

$$\dot{m}_v = (q/A)_{\text{CHF,sat}} (A_H/h_g)$$

where

m_v = mass rate of steam production, g/cm

A_H = heater surface area, cm^2

h_g = vapor enthalpy, cal/g

In order to assess m_v , the surface heat transfer area (A_H) must be specified. Assuming falldown of a coherent plug of corium melt through a bed of rod stubs in the lower intact region of the test bundle, the heater area can be approximated as cross-sectional flow area of the bundle:

$$A_H \approx 2.3 \text{ in.}^2 = 0.016 \text{ ft}^2 = 14.84 \text{ cm}^2$$

Here again it can be seen that amount of molten material has little impact on steam production, but rather the effective heat-transfer surface area. The assumption of debris particulation equivalent to the open flow area of the bundle seems reasonable, which is the same of all FLHT tests. The calculated steaming rate due to debris quenching was estimated in the FLHT-4 report^b to be 1.65 g/s, which when combined with the nominal FLHT-5 makeup flow of 10 lb/hr (1.26 g/s) gives a 2.9 g/s steam production rate. This is compared to an estimated 422 g/s steam flow rate for choking of the FLHT effluent collection system. The fact that the choked mass flow rate is approximately 145 times greater than the predicted debris/coolant plus normal steaming rate ($m_v = 2.9 \text{ g/s}$), is indicative of a more than adequate off-gasing capacity of the FLHT effluent control system. Thus, irrespective of debris temperatures and mass inventory of molten fuel rod material, adequate steam venting is assured. Thus, the conclusion reached is nil potential for steam spiking for the FLHT-5 experiment.

FLHT-5 Energetic Chemical Reaction Potential

With respect to energetic chemical reactions the primary concern relates to the mass of molten zircaloy, oxidation state, and quenching/fragmentation conditions in with water. An increased mass of molten metallic-zircaloy and higher temperatures (reaction kinetics increases exponentially with

temperature) would tend to increase the potential for a more energetic chemical reaction. However, test conduct largely determines molten zircaloy characteristics, that is that amount of zircaloy predicted to be in a relatively unoxidized state at the time of fuel rod disintegration.

Table 2 compares the predicted residual amounts of alpha plus beta metallic zircaloy clad thickness layers for the FLHT-4 and 5 tests, the nominal clad thickness being 0.061 cm. As indicated a higher degree of oxidation of still intact cladding is predicted for the FLHT-5 test compared to FLHT-4. Thus, the potential for an energetic chemical reaction between unoxidized metallic zircaloy melt debris and water is less, on a mass inventory basis of metallic zircaloy, for the FLHT-5 test than for FLHT-4.

Summary

A comparison of test conduct and expected test conditions for the FLHT-4 experiment and FLHT-5 test indicate only limited additional zircaloy melting and fuel dissolution potential for FLHT-5. An assessment of FLHT-5 test conditions indicates that the necessary criteria for inducement of an energetic "steam explosion" are not satisfied, similar to the conclusions drawn for the FLHT-4 test. Likewise, the steam removal capacity of the FLHT effluent control system is more than sufficient to prevent significant "steam spiking" in all tests. It is therefore concluded that energetic debris/coolant thermal interactions would be relatively benign and not pose a threat to the integrity of the reactor pressure tube (RPT) for the FLHT-5 test. A similar conclusion was drawn in Ref. b for FLHT-4.

Consideration of the exothermic molten-Zr/water chemical reaction, indicates that only for highly fragmented/rapid intermixing configurations and significant system constraint conditions, would explosive chemical reactions occur. Analysis indicates that such fragmentation/constraint requirements would not be satisfied for the FLHT 4 and 5 test conditions. Since the predicted amount of metallic-Zr is less for FLHT-5 than for FLHT-4 (on a mass inventory basis), the potential for an energetic chemical reaction between unoxidized metallic zircaloy melt debris and water for FLHT-5 would be no

TABLE 2

SCDAP CALCULATED ALPHA PLUS BETA
ZIRCALOY THICKNESS AS A FUNCTION
OF TRANSIENT TEST TIME FOR THE
FLHT-4 EXPERIMENT (Boiloff=1.9 g/s)

alpha-Zr(O) + .beta-Zr : Thickness (cm)

Time (Seconds)	Node 1..	Node 2	Node 3	Node 4	Node 5	Node 6	Node 7
375	.061	.061	.060	.059	.055	.060	.061
550	.061	.061	.060	.059	.038	.059	.061
650	.061	.061	.060	.058	.037	.058	.061
750	.061	.061	.060	.056	.036	.057	.061
825	.061	.061	.060	.054	.034	.055	.061
850	.061	.061	.060	.054	.033	.054	.061
875	.061	.061	.060	.053	.033	.054	.061
950	.061	.061	.060	.052	.032	.054	.061
1050	.061	.061	.060	.048	.031	.054	.061
1100	.061	.061	.060	.001*	.031	.054	.060
1150	.061	.061	.060	.001	.030	.054	.060
1175	0.061	0.061	0.060	0.001	0.015	0.054	0.060
1200	0.061	0.061	0.060	0.001	0.001*	0.001*	0.001*

*Oxide Layer Breached

TRUMP CALCULATED ALPHA PLUS BETA ZIRCALOY THICKNESS AS A
FUNCTION OF TRANSIENT TEST TIME FOR THE FLHT-5 EXPERIMENT
(Boiloff = 1.26 g/s)

Time (Seconds)	Node 1	Node 2	Node 3	Node 4	Node 5	Node 6	Node 7
162	0.061	0.061	0.061	0.061	0.061	0.061	0.061
314	0.061	0.061	0.061	0.061	0.061	0.061	0.061
526	0.061	0.061	0.061	0.058	0.045	0.059	0.061
814	0.061	0.061	0.057	0.0	0.037	0.059	0.061
1132	0.061	0.061	0.013	0.0	0.037	0.059	0.061
1383	0.061	0.061	0.0	0.0	0.006*	0.059	0.061
1644	0.061	0.061	0.0	0.0	0.0	0.040	0.061
1938	0.061	0.061	0.0	0.0	0.0	0.0	0.061
2130	0.061	0.061	0.0	0.0	0.0	0.0	0.045
2385	0.061	0.061	0.0	0.0	0.0	0.0	0.0

*Oxide Layer Breached

greater than for FLHT-4. In Ref. b analyses are presented for the FLHT-4 test indicating nil potential for an energetic Zr-water chemical reaction. The same conclusion is reached with respect to the FLHT-5 test conditions.

If you have further questions or require additional analysis not previously presented in Refs. a and b, please feel free to call me at my offices.

Sincerely,

A handwritten signature in cursive script that reads "August Cronenberg".

August Cronenberg, Ph.D.

amw

DISTRIBUTION

No. of
Copies

OFFSITE

- 2 DOE/Office of Scientific and Technical Information
- 2 U.S. Nuclear Regulatory Commission
Office of Nuclear Regulatory Research
Washington, D.C. 20555
ATTN: T. J. Walker, NLN344
R. W. Wright, NLN344

ONSITE

DOE Richland Operations Office
D. C. Langstaff

- 9 Pacific Northwest Laboratory
F. E. Panisko, P8-34
G. L. Tingey, P8-34
Publishing Coordination
Technical Report Files (5)
NRC Project Office

**DATE
FILMED**

1 / 3 / 94

END

